

Microbial Dynamics in Natural Aquifers

Dissertation

der Mathematisch-Naturwissenschaftlichen Fakultät
der Eberhard Karls Universität Tübingen
zur Erlangung des Grades eines
Doktors der Naturwissenschaften
(Dr. rer. nat.)

vorgelegt von
M.Sc. Bijendra Man Bajracharya
aus Kathmandu
Nepal

Tübingen
2016

Gedruckt mit Genehmigung der Mathematisch-Naturwissenschaftlichen Fakultät der Eberhard Karls Universität Tübingen.

Tag der mündlichen Qualifikation:	28.04.2016
Dekan:	Prof. Dr. Wolfgang Rosenstiel
1. Berichterstatter:	Prof. Dr.-Ing. Olaf Arie Cirpka
2. Berichterstatter:	Prof. Dr. Philippe Van Cappellen
3. Berichterstatter:	Dr. Chuanhe Lu

Abstract

Microorganisms in groundwater form ecosystems that can transform chemical compounds. Quantitatively understanding microbial dynamics in soils and groundwater is thus essential for pollutant dynamics and biogeochemistry in the subsurface. This dissertation addresses three factors influencing microbial dynamics in aquifers and soils, namely:

- (1) the influence of grazing on bacteria in eutrophic aquifers, posing the question whether the carrying capacity of bacteria, which has been observed in aquifers, is controlled by higher trophic levels of the groundwater ecosystem;
- (2) the influence of bioenergetic constraints on bacteria in oligotrophic aquifers posing the question how the energy supply controls the dynamics of microorganisms; and
- (3) the influence of fluctuating redox conditions on overall biogeochemical turnover, posing the question whether alteration of oxic and anoxic conditions benefits the efficiency of the microbial community in the degradation of natural complex substrates.

To address the first question, I developed a numerical model simulating a groundwater ecosystem with three trophic levels: a growth substrate, bacteria, and grazers (signifying bacterivorous protozoa, flagellates, ciliates, or bacteriophages). The model is first tested for well-mixed conditions, representing retentostats, and is then coupled to transport to obtain a 1-D bioreactive transport model. In the model, the bacterial population increases, fluctuates, and finally plateaus at a steady-state concentration, which is independent of the substrate concentration. Increasing the substrate exclusively increase the steady-state grazer concentration. When coupled to transport, the same steady-state bacteria concentration is reached over a substantial length of the domain. The simulation results demonstrate that grazing can be a controlling factor in determining the carrying capacity of bacteria in aquifers. I present closed-form expressions for steady-state concentrations in both well-mixed and transport-affected regimes.

To address the second question, I developed a bioenergetic model to simulate the survival of bacteria under energy-limiting conditions. The bacteria allocate the gained catabolic energy to growth, maintenance and the production of extracellular hydrolytic enzymes. The fraction of excess energy spent on hydrolytic enzyme production versus the fraction spent on growth is related to the coverage of the particulate organic matter by hydrolytic enzymes. Additionally, the catabolic energy flux governs the activation and deactivation of the microorganisms. The growth of steady state active microorganisms is balanced with the inactivation rate, which itself is balanced with the maintenance-energy requirement of the dormant microorganisms. Within the bioenergetics framework, kinetic rate laws are expressed in thermodynamic terms. The activity of microorganisms is constrained by thermodynamics, and the behavior of the microorganisms is determined by maximum catabolic energy use. I successfully use this conceptual model to illustrate the degradation of cellulose in an anaerobic environment via cellulolytic fermenting bacteria and sulfate reducing bacteria. I show that thermodynamic feedbacks are particularly important for the fermenting bacteria, which require utilization of their metabolic products by other bacteria to gain energy from fermentation.

To address the third question, I conducted an experiment to observe the effect of alternating redox conditions on carbon turnover in organic-rich soil suspensions. The results are compared with the static (oxic and anoxic) redox environments. The results demonstrate that redox fluctuations initiate various microbial processes including fermentation, aerobic and anaerobic degradation, most likely performed by different bacteria within a very diverse community. Under oscillating redox conditions, the system always remains far from thermodynamic equilibrium thereby supplying labile organic carbon substrates for microbial energy-gain and growth. Carbon turnover is higher under fluctuating than under the anoxic conditions, and there is a high potential to degrade even more carbon than that under static oxic condition.

Kurzfassung

Mikroorganismen im Grundwasser bilden Ökosysteme die chemische Substanzen transformieren können. Ein quantitatives Verständnis der mikrobiellen Dynamik in Böden und Grundwasserleitern ist deshalb essentiell für die Schadstoffdynamik und Biogeochemie des Untergrundes. Die vorliegende Dissertation befasst sich mit drei Faktoren, die die mikrobielle Dynamik in Grundwasserleitern und Böden beeinflusst, nämlich:

(1) den Einfluss des Grazings von Bakterien in eutrophen Grundwasserleitern, was zu der Frage führt, ob die Kapazität für Bakterien, die in Grundwasserleitern beobachtet wurde, durch höhere trophische Ebenen des Grundwasserökosystems kontrolliert wird;

(2) den Einfluss bioenergetischer Beschränkungen auf Bakterien in oligotrophen Grundwasserleitern, was zu der Frage führt, wie die Energieversorgung der Mikroorganismen ihre Dynamik kontrolliert; sowie

(3) den Einfluss fluktuierender Redoxbedingungen auf den biogeochemischen Gesamtumsatz, was zu der Frage führt, ob abwechselnde oxische und anoxische Bedingungen die Effizienz der mikrobiellen Gemeinschaft im Abbau natürlicher komplexer Substrate erhöht.

Um die erste Frage zu beantworten, habe ich ein numerisches Modell entwickelt, das ein Grundwasserökosystem mit drei trophischen Ebenen simuliert: ein Wachstumssubstrat, Bakterien und Grazer (z.B. bacterivore Protozoen, Flagellaten, Ziliaten oder Bacteriophagen). Das Modell wurde zunächst für gut durchmischte Systeme getestet, die Chemostaten und/oder Retentostaten repräsentieren, und wurde dann mit Transportprozessen gekoppelt, um ein eindimensionales bioreaktives Transportmodell zu erhalten. Im Modell nimmt die Bakterienpopulation zu, fluktuiert und erreicht schließlich eine stationäre Konzentration, die von der Substratkonzentration unabhängig ist. Eine Erhöhung der Substratzufuhr führt lediglich zu einer Erhöhung der Grazer-Konzentration. In der Kopplung zum Transport ergibt sich die gleiche stationäre Bakterienkonzentration über eine beträchtliche Länge des Gebietes. Die Simulationsergebnisse demonstrieren, dass Grazing einen bestimmenden Faktor für die Kapazität von Bakterien in Grundwasserleitern darstellen können. Ich präsentiere geschlossene Lösungen

für die stationären Konzentrationen sowohl für gut durchmischten als auch für Transport-beeinflussten Systeme.

Um die zweite Frage zu beantworten, habe ich ein bioenergetisch Modell entwickelt, das den Metabolismus von gemischten Bakterienpopulationen unter Energie-limitierenden Bedingungen simuliert. Die Bakterien teilen die gewonnene katabolische Energie dem Wachstum, dem Erhalt und der Produktion extrazellulärer hydrolytischer Enzyme zu. der Anteil der überschüssigen Energie, der auf die Produktion hydrolytischer Enzyme verwendet wird, versus dem Anteil, der in Wachstum investiert wird, hängt davon ab, wie stark der partikuläre organische Kohlenstoff mit hydrolytischen Enzymen belegt ist. Darüber hinaus steuert der katabolische Energiefluss die Aktivierung und Deaktivierung der Mikroorganismen. Das Wachstum der aktiven Mikroorganismen wird durch Inaktivierungsrate ausgeglichen, welche den Energiebedarf für die Erhaltung der ruhenden Mikroorganismen ausgleicht. Innerhalb des bioenergetischen Rahmens werden kinetische Ratengesetze in thermodynamischen Termen ausgedrückt. Die Aktivität der Mikroorganismen ist durch die Thermodynamik beschränkt und das Verhalten der Mikroorganismen wird durch den maximale Verwendung der katabolischen Energie bestimmt. Ich habe das konzeptionelle Modell erfolgreich auf den anaeroben Abbau von Zellulose durch Zellulose-verwendene Fermentierer und Sulfatreduzierer angewendet. Ich konnte zeigen, dass thermodynamische Rückkopplungen besonders wichtig sind für die fermentierenden Bakterien sind, die darauf angewiesen sind, dass andere Bakterien ihre metabolischen Produkte verbrauchen, damit sie selbst aus der Fermentation Energie gewinnen können.

Um die erste Frage zu beantworten, habe ich Experimente durchgeführt, in denen ich die Wirkung wechselnder Redoxbedingungen auf den Kohlenstoffumsatz in Bodenlösungen mit hohem Gehalt an organischem Kohlenstoff untersuchte. Die Ergebnisse wurden mit statischen (oxischen und anoxische) Redox Milieus verglichen. Die Ergebnisse zeigen, dass Redoxschwankungen zahlreiche mikrobielle Prozesse initiieren, darunter Fermentation, aerober und anaerober Abbau, die aller Wahrscheinlichkeit nach von unterschiedlichen Bakterien in einer sehr diversen Gemeinschaft durchgeführt werden. Unter oszillierenden Redoxbedingungen wird das System ständig vom thermodynamischen Gleichgewicht ferngehalten und liefert dadurch

labile organische Substrate für die mikrobieller Energieverwertung und Wachstum. Der Kohlenstoffumsatz ist größer unter fluktuierenden als unter statisch anoxischen Bedingungen und es besteht ein hohes Potential, dass der Abbau sogar größer ist als unter statischen oxischen Bedingungen.

Acknowledgements

I wish to express my sincere heartfelt gratitude to several people who has contributed immensely towards the successful completion of this work. The first and foremost is Prof. Dr.-Ing. Olaf Arie Cirpka, who gave me the opportunity to work closely and learn from him throughout my Ph.D. The short journey, I have taken in the field of research, begun with reading one of his paper (Cirpka et al., 2006) during my master studies. I vividly remember not being able to contend my excitement, the day when I was selected as one the Ph.D. candidates in his group. His bombardment of creative ideas, encouragements and constructive comments made this journey successful. Because of him, I have truly come to understand the commitment and diligence required to complete this work. I also owe my deepest gratitude to Prof. Dr. Philippe Van Cappellen for his invaluable support and advice throughout this research. I am honored that I got the opportunity to work under his guidance. I am really thankful for the freedom to explore the field of bioenergetics and the patience that he maintained during my mistakes. His critical feedback, advice and motivating guidance have helped me to visualize the grandeur picture of my research. There is also not enough word to thank Dr. Chuanhe Lu properly. He has been a mentor as well as a good friend in this journey of mine. He is the one who I will go to find the answer of the dumbest questions that I can come up with. His open-door policy along with his under his continuous guidance, support and inspiration made this journey possible.

I would like to personally thank my research group ‘Integrated Hydrosystem Modelling’ (Alexandra, Alicia, Anneli, Atefeh, Carolin, Chang, Claus, Diane, Evgenii, Gianna, Jeremy, Jürnjakob, Karim, Maximiliane, Matthias, Marvin, Michael, Reynold, Shangua, Stephan, Yan, and Zhongwen). You guys have been friend and family to me during my stay here. You are the first people whom I come to for advice, personal or work related. The nerdy long discussion on our research with chilled beers is a memory that I would never forget. The awesome memorial trips from Paris, Switzerland to all the way to North America will always remind of you guyz. I must also acknowledge all the staffs of Department of Geoscience for their kind cooperation and providing technical support during this study. Special thanks to the Ecohydrology Research

Group – University of Waterloo (especially to Christina, Chris, Fereidoun, Igor and Ekaterina) for the productive and awesome collaboration work. I really appreciate the support and the confidence that you (Christina, Chris and Fereidoun) had in me that I would be able to carry out the Fluctuating experiment. I am deeply grateful to Ms. Monika Jekelius who helped me with all the paperwork and administrative issues. I can remember numerous occasions where I went seeking her help. I want to express my gratitude to Saroj, Simon and Rachelle for their help in preparation of the manuscript. I cannot remain without thanking “Deutsche Forschungsgemeinschaft via the International Research Training Group (grant GRK 1829)” for granting the fund for this study.

I would as well want to appreciate my parents (Late Moti Man Bajracharya and Nani Hera Bajracharya), other friends and family. My mom has endured the pain of letting me travel half way around the globe to ensure the successful completion of my studies, ensuring that my dreams and passion stay alive. I consider myself very lucky to have the most loving and caring wife ‘Sona Shakya’. She has been my personal cheerleader and best-friend, who left everything behind to be with me. She also felt the same pain and joy as I did for the completion of this work.

Contents

Abstract	i
Kurzfassung	iv
Acknowledgements	vii
List of figures	xiii
List of tables	xiv
1. Introduction	1
1.1 Motivation.....	1
1.2 Identification of research gaps	4
1.3 Objective and structure of the thesis	5
2. State of research	7
2.1 Carrying capacity	7
2.1.1 Temperature and moisture content	8
2.1.2 Resource availability	9
2.1.3 Habitat space.....	9
2.1.4 Interspecies bacterial competition	9
2.1.5 Grazing	10
2.2 Bioenergetics.....	11
2.2.1 Gibbs energy and yield of bacteria in natural environments	12
2.2.2 Dormancy	13
2.2.3 Maintenance energy	15
2.2.4 Previous bioenergetic models	17
2.3 Particulate organic matter: Cellulose	20
2.3.1 Degradation of cellulose	22
2.4 Governing equations for bio-reactive transport	26
2.4.1 Groundwater flow	27

2.4.2	Solute transport.....	27
2.4.3	Bio-reactive transport model	28
2.4.4	Initial and boundary conditions	28
2.4.5	Numerical solution.....	29
3.	Substrate-bacteria-grazer interactions	30
3.1	Introduction.....	30
3.2	Governing equations and mathematical analysis	35
3.2.1	Dynamic retentostat model	36
3.2.2	One-dimensional bio-reactive transport model	40
3.2.3	Approximate steady-state concentration distributions for one-dimensional bio-reactive transport in the presence of grazers.....	42
3.2.4	Linearized stability analysis of the one-dimensional bio-reactive transport model	43
3.3	Model applications.....	44
3.3.1	Retentostat model	44
3.3.2	One-dimensional bio-reactive transport model	47
3.4	Conclusions.....	53
4.	Anaerobic degradation of particulate organic matter: a bioenergetic approach	55
4.1	Introduction.....	55
4.2	Model overview and governing equations.....	58
4.2.1	POM hydrolysis	58
4.2.2	Respiration.....	60
4.2.3	Energy balance of active cells	60
4.2.4	Dormancy	62
4.2.5	Energy balance of dormant cells.....	63
4.2.6	Conservation equations for biomass and hydrolytic enzymes.....	64

4.3	Anaerobic cellulose degradation.....	65
4.3.1	Reaction system.....	65
4.3.2	Parameter values.....	68
4.4	Simulation results and discussion.....	70
4.4.1	Model simulation.....	70
4.4.2	Accounting for bioenergetics.....	79
4.4.3	Sulfate perturbation starting at steady-state.....	83
4.5	Conclusions and future works.....	85
5.	Soil organic matter degradation by microbes in fluctuating vs static redox condition.....	88
5.1	Introduction.....	88
5.2	Materials and methods.....	91
5.2.1	Soil sampling and characterization.....	91
5.2.2	Experiment design and redox oscillation sequence.....	91
5.2.3	Aqueous chemistry analyses.....	92
5.2.4	Greenhouse gas analyses.....	92
5.2.5	Specific ultra violet absorbance analysis.....	93
5.2.6	Solid analyses.....	93
5.3	Results.....	93
5.3.1	pH and redox potential.....	94
5.3.2	Carbon pool.....	95
5.3.3	Electron acceptors.....	99
5.4	Discussion.....	101
5.4.1	Dynamics of pH and Eh.....	101

5.4.2	Transformation of aqueous carbon	102
5.4.3	DOC and aromaticity	104
5.4.4	Electron acceptors, greenhouse gases and microbial activity.....	105
5.4.5	Solid carbon pool and microbial activity.....	106
5.5	Conclusions and future works.....	106
6.	General conclusions and outlook.....	110
6.1	Conclusions.....	110
6.2	Outlook and future perspectives	112
	Appendix to chapter 5	115
A1.	Field site characterization	115
A1.1	Soil preparation:.....	115
A2.	Experimental procedures	116
A2.1	Preliminary experiment	116
A2.2	Reactors setup.....	116
A2.3	Sampling procedure	117
A3.	Figures.....	118
A3.1	Short chain fatty acids	118
A4.	Tables.....	119
7.	Bibliography	121

List of figures

Figure 2.1: Continuum of particulate and dissolved organic carbon in natural waters	21
Figure 2.2: Degradation of cellulose.....	23
Figure 3.1: Schematic of transport processes in the model developed.....	34
Figure 3.2: Time series of concentrations.....	46
Figure 3.3: Transient results of the 1-D bio-reactive transport model.....	49
Figure 3.4: Stability analysis of the one-dimensional bio-reactive transport model.	51
Figure 4.1: Schematic diagram of the energy and carbon flow in a POM fermenter.	59
Figure 4.2: Community dynamics of cellulolytic fermenting microorganisms and sulfate-reducing bacteria for complete cellulose degradation in an anaerobic environment.....	68
Figure 4.3: Simulated time series of concentrations. A: electron-donors, B: hydrolytic enzymes, C: active bacteria, D: dormant bacteria.....	76
Figure 4.4: Simulated energy generation and consumption per unit carbon in the biomass..	77
Figure 4.5: Energy distribution at steady-state conditions.....	80
Figure 4.6: Bacterial yield.....	81
Figure 4.7: Comparison of Bacterial population.....	82
Figure 4.8: Concentration response to a change in sulfate concentration.....	84
Figure 4.9: Concentration response to a change in sulfate concentration with static Gibbs energy calculated at initial concentration..	85
Figure 5.1: Time series of A: pH and B: Eh.	94
Figure 5.2: Dissolved carbons.....	97
Figure 5.3: Greenhouse gases	98
Figure 5.4: Electron Acceptors	100
Figure A.1: Short chain fatty acids	118

List of tables

Table 3.1: Parameters values used in the simulations.....	44
Table 4.1: Parameter values used in the simulations for bioenergetic model.....	71
Table 4.2: Initial concentration used in the simulation for bioenergetic model	74
Table 5.1: Solid phase total organic carbon.....	99
Table A.1: Comparison of artificial and actual groundwater	119
Table A.2: CHNS analysis of soil suspension	119
Table A.3: Sampling Table	120

1. Introduction

1.1 Motivation

Essential biochemical cycling of carbon, sulfur, and nitrogen in the earth surface and sub-surface are regulated by microbes, where the products of one cycle is utilized by the next cycle (Madsen, 2011). Microorganisms gain their energy from and grow on catalysing reactions of reduced and oxidised substrates. The by-products of such reactions may be consumed by other organisms. Microbes play a vital role in the flow of nutrients through various biotic and abiotic components during the biogeochemical cycle. These processes maintain the balance of the biosphere (Falkowski et al., 2008)

Most natural aquifers are oligotrophic in nature, deprived of nutrients and exhibit low microbial concentrations (Whitman et al., 1998). Aquifers comprise numerous and complex habitats for various microbial communities (Griebler and Lueders, 2009). They are resource-limited ecosystems in which organic matter (OM) is efficiently mineralized by microbial communities which are then predated by grazers (Foulquier et al., 2011). These aquifers are major sources of drinking water. Moreover, the dynamics of intrinsic microbial transformations also affect water quality, and ubiquitous microbes also play a significant role in the degradation of natural organic matter and contaminants, the emission of greenhouse gases (GHG), among other processes. Hence, the systematic analysis of groundwater microbes have been performed for several decades (Griebler and Lueders, 2009). Ironically, understanding microbial dynamics has always been a challenge because the interactions between the various functional groups of organisms and their environment have insufficiently been understood.

It is no surprise that numerous models as well as experiments have been built up to represent these complicated systems. Most models of microbial dynamics are based on Monod type growth expressions, which account for potentially rate-limiting substrates only by the fraction of reactive enzymes bound to reactants, whereas other factors, such as the

concentration dependence of the associated energy gain, are neglected (Vallino et al., 1996). The availability of energy substrates, electron acceptors and nutrients, as well as physical and geochemical variables, affect the microbial dynamics as well as the molecular diversity of microbial communities greatly (Boyd et al., 2007; Stolpovsky et al., 2011). Therefore, to fully comprehend biogeochemical changes, the environmental influence on microbial interactions, transport and transformation needs to be understood.

When the energy substrates permeate into natural aquifers either via natural processes (e.g. infiltration) or under anthropogenic influences (e.g. fertilization), the microbial population grow and reach a maximum concentration, known as 'Carrying Capacity'. The population won't grow further and maintains a steady-state concentration. Bio-reactive transport models account this maximum bacterial capacity term to cap excessive microbial growth close to substrate-injection regions. The factors controlling this carrying capacity, however, are not fully understood. Several competing hypotheses on the control of the carrying capacity have been formulated. It could be space limitation (Egli, 2010; Morita, 1988), limited resources availability (Ayuso et al., 2010), interspecies competition (Hibbing et al., 2010) and kinetic mass-transfer limitations (Cirpka, 2010), to name only a few. However, the impact of grazing on bacterial population has not been properly delineated yet, although there are several studies showing that grazing controls the bacterial population (Acea and Alexander, 1988; Habte and Alexander, 1977).

The energy substrate is also one of the limiting factors in natural aquifers that limit bacterial growth. The natural aquifers, mostly oligotrophic in nature, comprise a spectrum of condensed organic matter characterised by low energy content. Only a small fraction of the organic matter (OM) is bioavailable which is generated by chemical or enzymatic hydrolysis of natural organic matter (NOM) (Egli, 2010). Despite the limited energy catalyzed from this small assimilable organic carbon concentration, the microbial populations maintain their presence in the entire biosphere. Quantitative models of NOM degradation are essential to understand the chemical state and evolution of the near-surface environment, and to predict the biogeochemical consequences of ongoing local and global changes. The complex nature of these organic matter represents a major obstacle to the development of such models (LaRowe and Cappellen, 2011). Moreover, only a fraction of the microbial population is

active at any given time, and the microbes are able to switch to dormant or active states with changing environmental conditions (Stolpovsky et al., 2011). The efficient distribution of the generated energy is vital for microbial communities' survival. The microbes also respond to nutrient limitation with a higher metabolic flexibility and lower maintenance needs compared to cultures growing under nutrient-rich conditions (Egli, 2010). Conventional models incorporating key microbial processes are often developed using data collected in nutrient-rich growth media and are not able to represent the conditions of typical natural aquifers.

Microorganisms, which survive in naturally energy-limited environments, have led to new developments in modelling biogeochemical reactions. Thermodynamic constraints are especially relevant under low-energy conditions (Dale et al., 2006; Jin and Bethke, 2003, 2005; LaRowe and Cappellen, 2011; LaRowe et al., 2012). These constraints have only recently been considered in bio-reactive modelling. The total energy generated determines the microbial communities' transformation kinetics including microbial growth, enzyme production, maintenance energy (ME), microbial dormancy, and decay. However, these related issues are poorly understood and incorporated in numerical models. Therefore, a bioenergetics model that determines how energy is being transferred and distributed is required. Bioenergetics help detecting possible pathways without requiring a comprehensive knowledge of the underlying mechanisms (Demirel and Sandler, 2002). The bacterial doubling time (DT) could vary within few minutes to decades depending upon the environmental conditions. Only few studies have been conducted for DT of bacteria in groundwater systems. For example the DT is in order of days in contaminated sandy aquifers and it could be months or even years in natural aquifer (Chapelle, 2000). The models including thermodynamic constraints are also capable of exhibiting this wide range of growth rate coefficients.

Except the energy/carbon substrate, the static (aerobic/ anaerobic) and alternating redox conditions influence bacterial growth to a great extent. Naturally, the redox state in near-surface aquifers changes with the environment conditions. Under oscillating conditions (that is, alternating oxic and anoxic conditions), the system is perpetually far from thermodynamic

equilibrium resulting in maximum opportunities for microbial growth and hence, enhance organic substrate depletion (Parsons et al., 2013). This may also reduce the accumulation of toxic intermediates or dead-end products (Aller, 1994; Gerritse et al., 1990). The experiments on fluctuating groundwater level column operated by Rezanezhad et al. (2014) demonstrated that organic carbon degradation is enhanced where the sediment alternates between saturated anoxic conditions and unsaturated oxic conditions. However, there is no convincing evidence on enhancing carbon release or OM mineralization yet. Before developing models on these environments, more experiments to delineate these differences are crucial to comprehend the influence of oscillating condition on carbon cycling. This study will understand the processes producing and preserving these diversity and dynamics, detect the environmental factor which plays impact on the microbial populations, check the influence of redox conditions on the biochemical evolution, and eventually lead to a better parameterization of bio-reactive transport models at the catchment scale.

1.2 Identification of research gaps

In accordance to the context explained in the previous section, I have identified three major aspects of environmental change in natural aquifers.

- 1) In a favorable environment, (with high input of energy substrates) the microbial populations are supposed to grow tremendously. However, this is not observed. The microbial communities grow up to only a certain maximum concentration. What is the controlling factor?
- 2) In an unfavorable environment, (where energy-supply is limited) the microbial populations do not die out completely. Instead, microorganisms maintain their presence in almost all drastic environments. How do the microorganisms survive under these harsh conditions?
- 3) The natural aquifers may subject to the oxic, anoxic or alternating redox conditions. This could be favorable or unfavorable depending upon the microbial communities. The microbial communities' dynamics change with respect to the change in redox

condition. How do the microbial communities respond to these different redox conditions? Moreover, what would be the impact on carbon turnover?

1.3 Objective and structure of the thesis

Numerous environmental factors, such as temperature, pH, energy substrate, soil moisture condition and redox condition etc., exhibit significant influence on the microbial dynamics and the carbon cycle (Schmidt et al., 2011; Waksman and Gerretsen, 1931). This thesis will address three vital issues of environmental change in the natural aquifer, illustrated in the previous section. With this study, I present a detailed analysis to enhance our knowledge to solve these issues:

Chapter 3: The carrying capacity is the maximum biomass that can be supported by the aquifer. While the concept is simple and can easily be incorporated into microbial growth models, e.g. as a logistic-growth term, the nature of this controlling factor has not been entirely understood. This study will help to outline the current level of understanding of the carrying capacity and also will give insight into other factors affecting the carrying capacity. In this work, a model is developed to demonstrate that “grazing” of the bacteria could be possible factor controlling the bacterial population. Moreover, this model, by means of mathematics, explains the possible top-down control of the microbial population (that is, protozoa, bacteriophage viruses), contrary to the popular belief of bottom-up control (that is, by a limited energy supply).

Chapter 4: This chapter proposes a conceptual bioenergetics model to depict the microbial survival dynamics in an oligotrophic aquifer. The model shows the energy distribution of the bacteria to growth, maintenance and hydrolytic enzymes production. The energy gained also determines the fraction of active and dormant populations of microbes, as well as the decay of the bacteria. Then, the model is applied to the degradation of cellulose in an anaerobic environment with two microbial communities (cellulolytic fermenting bacteria and sulfate reducing bacteria). The model reproduces results that are consistent to observations in natural aquifers.

Chapter 5: An experiment is conducted to understand and distinguish the microbial dynamics and carbon turnover under different redox conditions. Three identical 1L bioreactors are prepared using a carbonate-buffered artificial groundwater solution matching the aqueous chemistry of the field site. Static oxic (O-reactor) and anoxic (R-reactor) and oscillating redox conditions (F-reactor) are maintained for 28 days. The bioreactors were sampled at regular intervals and analyzed for various chemical concentrations and microbial activities including greenhouse gases (CO₂, CH₄ and N₂O), anions, low molecular weight organic acids, DIC, DOC and soil enzymatic activities. The fluctuating redox conditions keep the system away from thermodynamic equilibrium by replenishing important pools of electron donors (e.g. acetate- via fermentation) and acceptors such as Mn⁴⁺ and sulfate. These results demonstrate that the fluctuating condition have the potential to degrade similar concentration of DOC as under oxidizing condition. Only in the F-reactor we can perceive clear synergy between aerobic and anaerobic/fermenting processes to deplete the labile carbon at total rates that are definitely faster than those observed in reducing reactor. One of the most remarkable results is the change in total OM in all bioreactors. Both the O- and the R-reactor show decrease in OM whereas we observe the apparent increase of OM in F-reactor. This is possibility due to the increase in biomass, which also indicates the presence of autotrophic microorganisms. Ironically, within this research period, I have not been able to confirm this hypothesis. In the near future, sample collected for microbial ecological analysis will be examined to confirm this hypothesis.

2. State of research

The following literature review is sub-divided into four different sections addressing important aspects of this dissertation:

- a. the carrying capacity of the subsurface, that is the capability to maintain a maximum biomass, which is discussed under the aspects of potential nutrient, energy, and space limitations and under the aspect of grazing;
- b. the governing equations for bio-reactive transport in groundwater;
- c. the basic concepts of bioenergetics; and
- d. the degradation of macromolecular carbon in different environments.

2.1 Carrying capacity

The carrying capacity is defined by del Monte-Luna et al. (2004) as ‘the limit of growth or development of each and all hierarchical levels of biological integration, beginning with the population, and shaped by processes and interdependent relationships between finite resources and the consumers of those resources.’ The carrying capacity of an environment is the maximum population (density) that the environment can sustain at steady state (McArthur, 2006). It depends on the relationship between the populations and their resources. Initially, microbial populations usually grow slowly; enter an exponential growth phase, and then level off when the carrying capacity of that species has been reached. Fluctuations of the population density around the carrying capacity may be caused by fluctuating environmental conditions, but most bacterial communities adapt to such variations (Battin et al., 2007; Keymer et al., 2006; McArthur, 2006). The concept of the carrying capacity has frequently been criticized because of its elusive interpretation. While postulating the existence of a carrying capacity to explain observations of limited population densities is straightforward, it is less clear which factors control the carrying capacity, and how it could be predicted.

Bio-reactive models may account for the carrying capacity of microbial biomass as maximum biomass concentration (Stolpovsky et al., 2012; Yukalov et al., 2012). However, the effectiveness of such models is contingent on the adequate information about the studied environmental system and the accurate understanding of the main factors that affect microbial population. In aquifers, the carrying capacity is usually believed to depend on different factors such as the availability of food sources, other macro or micronutrients, space for growth, number of sites for suitable reproduction, temperature, and moisture, among others. Anthropogenic influences may significantly affect the carrying capacity. Remus-Emsermann et al. (2012) described the carrying capacity as a ‘sum of many local carrying capacities’.

A simple example is the effect of pH changes on the bacterial communities. Adding nitrogen as ammonium sometimes lowers the soil pH, and bacterial growth can negatively be affected by low pH values (Baath, 1998). pH variations may cause drastic shifts in the relative numbers of different species in a heterogeneous population as it affects specific growth rates (De Vries and Shade, 2013; Horiuchi et al., 2002). It may also induce metabolic shifts of bacteria as seen by the shift in fermentative patterns in lactic acid bacteria (Yu et al., 2007). pH also influences the DOC dissolution (Grybos et al., 2009)

In the following, I have outlined the most important factors affecting the carrying capacity of the microbial biomass without claiming completeness.

2.1.1 Temperature and moisture content

Temperature and water content can affect the carrying capacity considerably and are important factors for bacterial growth in soil (Smith et al., 1997). Low soil temperatures result in slower reaction rates, and frozen soils limit diffusion of substrates thus resulting in lower bacterial activities (Steinweg et al., 2013). Diffusion of enzymes, substrates and the reaction products are affected by the soil moisture content, since there is a limitation of substrate and enzyme diffusion (Stark and Firestone, 1995). The rate of enzyme production and activity including turnover rates are influenced by temperature and moisture (Wallenstein and Weintraub, 2008), and thus can be affected by climate change (Sowerby et al., 2005; Steinweg et al., 2013; Trasar-Cepeda et al., 2007). This will affect the allocation of

resources for enzymes production and the population growth. Temperature causes maintenance costs and high nutrient demand (Joergensen et al., 1990). Carbon cycling processes are also sensitive to minor changes in temperature which could result in a large release of soil carbon back to the atmosphere (Classen et al., 2015).

2.1.2 Resource availability

Food availability in any habitat is a predominant factor for the survival of the species. Normally the carbon/energy source, nutrients, and micro-nutrients are the key factors determining the carrying capacity. The common nutrients for the cells are carbon, nitrogen, sulfur, phosphorus, calcium, magnesium, potassium, iron, oxygen, and additional trace elements. They play vital roles in cellular and metabolic processes, hence; change the carrying capacity of the aquifer. Lack of carbon has been assumed to be the most common limiting factor for bacterial growth in soil, although limitations by other nutrients, e.g. nitrogen and phosphorus have also been observed (Demoling et al., 2007). At low growth rates, more carbon is used for maintenance, leaving less carbon available for growth and biomass production (Demoling et al., 2007). Nutrient deficiencies cause bacterial inability to reproduce and cap the growth of bacteria (Hardin, 1968).

2.1.3 Habitat space

The carrying capacity also relates to the size and number of microbial populations accommodated in the available physical space. In these communities, bacteria compete with their neighbors for space and resources (Hibbing et al., 2010). A high number of bacterial colonies in an environment forces the organisms to share the space which results in overall decrease of growth (Remus-Emsermann et al., 2012).

2.1.4 Interspecies bacterial competition

Microorganisms do not exist isolated in the ecosystem. They share the common habitat with other microorganisms to form a complex ecological web. Such interactions could be positive, negative, or neutral (Faust and Raes, 2012). Depending upon the type of interaction, the

carrying capacity of the ecosystem can change. Antimicrobial production, space competition, predation, and even a swift of growth rate are believed to be a way of obtaining nutrients by one organism at the expense of another (Oehmen et al., 2007). Several species produce adhesions or receptors that bind to specific surface features to increase the chance of winning the competition (Rickard et al., 2003). Different bacterial communities may collaborate to build a biofilm, which provide antibiotic resistance. Such a positive relation is known as mutualism (Rodriguez-Martinez and Pascual, 2006). Syntrophy is another positive interaction in which two different species exchange products for the benefit of both (Woyke et al., 2006). In symbiotic relationship microbes cross-feed on compounds that are produced by other community members as in cellulose degradation (Leschine, 1995). In amensalism, the product of one community harms the other without affecting the producer (e.g, lowering the surrounding pH). Finally, loss-loss relationships are also found among some organisms in which two species with similar niches exclude each other (Gauze, 1934).

2.1.5 Grazing

In a predation-prey relation, one organism benefits from preying on another. An example is the predation of bacteria by bacteriophages or protozoa. Here, predation reduces the size of bacterial population (Wright et al., 1995). Protozoan grazing is believed to be a significant factor controlling the abundance of bacteria in soils (Acea and Alexander, 1988; Habte and Alexander, 1977). Protozoan predation requires a sufficiently large pore size (larger than the size of the protozoa) and water availability (Vargas and Hattori, 1986). Pore throats with sizes of 3 to 6 μm reduces predation by excluding protozoa (Wright et al., 1995). In these aquifers, bacteriovorous viruses may control the bacterial population. While viruses are not predators in a classical sense (they can't metabolize bacterial biomass because they lack an own metabolism in the first place), their effect on the bacterial biomass is identical (viruses infect bacteria, making them produce new viruses rather than reproducing themselves, and finally kill the bacteria). Thus, they can constrain bacterial communities in aquifers (Jürgens et al., 2008; Khatri et al., 2012).

2.2 Bioenergetics

Bioenergetics is the quantitative study of energy conservation and conversion processes in and between living organisms and their environment. It describes the biochemical and metabolic pathways through which the cell ultimately obtains energy. The laws of thermodynamics are applied to microbial biochemistry to see how energy is transferred. Thermodynamics helps identifying possible pathways without requiring a detailed knowledge of the underlying reaction mechanisms (Demirel and Sandler, 2002). It is especially practical for understanding the biogeochemistry of the sub-surface. However, there are still research gaps in representing a sub-surface system via approaches in which the microbial dynamics is expressed in terms of Gibbs energy production.

The study of bioenergetics on microorganisms is of huge interest for the production of biofuel, biogas and understanding microbial dynamics with numerical model. It also helps us to understand the flow of energy in the biosphere.

Energy formation is one of the vital components of metabolism. In order to survive, the microorganisms are able to harness energy from various sources and channel it into biological work. They require energy for maintaining their physiological state, synthesizing cellular components, motility, nutrient uptake, maintaining their membrane potential, among others. The energy is also used to handle environmental influences such as desiccation, osmotic pressure, toxicity and predation (LaRowe and Amend, 2015a).

The generated catabolic energy of redox reactions is stored in the form of adenosine triphosphate (ATP) which is a common molecule for storing energy and driving cellular energy-requiring processes (Hoehler, 2004). ATP is used as an intracellular energy source by all living organisms. ATP is also called the universal “currency” of chemical energy although other high-energy molecules also occur in cells (Mempin et al., 2013). Microorganisms generate ATP through the mechanism called chemiosmosis in which a proton concentration gradient and an electric potential across the membrane, collectively termed the proton-motive force, drive the ATP synthesis. Chemiosmosis can occur only in sealed, membrane limited

compartments that are impermeable to H^+ . The proton-motive force is generated by the stepwise transport of electrons from higher to lower energy states across the membrane, separating the charge across the membrane (Lodish et al., 2000). The terminal phosphate bonds of ATP are relatively weak. This bond breaks down to adenosine monophosphate (AMP) or adenosine diphosphate (ADP) and phosphate which then dissolve in water. The hydration results into energy release. ATP-to-ADP conversion is often assigned with a standard free energy (ΔG°) value of -31.8 kJ/mol (Russell and Cook, 1995).

2.2.1 Gibbs energy and yield of bacteria in natural environments

Microbial growth requires energy. However, energy is lacking in nature, and many ecosystems are termed oligotrophic. The mineral matrix usually stores an adequate energy potential, nevertheless the potential must be transferred into a bioavailable form for the cells. For the microbial community to survive, energy must be available at finite minimum levels which can be harnessed supporting basic biochemical integrity and function (Hoehler, 2004). Catabolic actions only occur as long as the thermodynamic state of the reactions is distant enough from the equilibrium state to permit energy conservation by the microbes (Harder, 1997). When bacteria are limited by energy sources, the free energy change of catabolic reactions is generally tightly coupled to the anabolic steps of synthesis of cell, and total energy flux can be divided into growth and maintenance functions (Russell and Cook, 1995).

Despite the fact that the yield of the bacteria is considered to be dynamic with response to the change of environmental conditions, most models still use it as a constant yield coefficient. The wide variations of biomass yields reported for different microbial growth systems can be explained based on thermodynamic reasoning (von Stockar et al., 2006). The number of cells in the environment is linked with the energy consumption by the bacterial community (LaRowe and Amend, 2015a). Yield can't be easily interpreted in accurate bioenergetics or physiological terms unless considerable circumspection (Russell and Cook, 1995). There are four major factors that affect the yield determination (Russell and Cook, 1995): (1) estimation of ATP production (2) energy source utilization for carbon (3) cell composition changes and (4) maintenance energy. Moreover, energy spilling is the common feature of growth with an excess of energy and an imbalance between anabolism and catabolism.

Energy spilling may allow bacteria to accelerate their processes of cell synthesis and may also have the potential to protect the bacteria from toxic substances (Russell and Cook, 1995). In oligotrophic environments, the cells avoid any energy-spilling reactions (Van Walsum and Lynd, 1998).

Numerous studies have been dedicated to investigate the relationship between the energy gained by a microbial population and its yield (Roden and Jin, 2011; VanBriesen, 2002). However, these yield values are determined in the lab under favorable conditions for bacteria (Hoehler and Jørgensen, 2013). In these studies, the bacteria yield is observed to depend linearly on the catabolic energy generation (Hernandez and Johnson, 1967; Jin and Roden, 2011), while prediction of yield for lower-energy systems is still challenging (Roden and Jin, 2011). In nature, most energy is spent on maintenance and producing enzymes (Morita, 1990, 1988; Russell and Cook, 1995). If the catabolic energy production is low, most energy source will be used for maintenance. Growth under ideal conditions seldom happens in nature, mainly due to the lack of bioavailable energy substrates. Along with the bioavailable energy, other physical and geochemical factors also affect the rate of microbial growth. The delineation of energy needed for growth or the initiation of the starvation state still needs to be clarified (Morita, 1988). Additionally, it is necessary to study how the microbial growth is limited by nutrients rather than energy. Under such conditions, bacteria may spill energy in reactions which can't be categorized into maintenance or growth (Russell and Cook, 1995).

In order to comprehend the rates of biogeochemical processes in the sub-surface, a quantitative relationship between microbial population, their catalysis rate, and energy supply and demand has been developed (LaRowe and Amend, 2015b).

2.2.2 Dormancy

A transition of bacterial cells from an active to an inactive state due to environment change is known as dormancy, which is one of the most effective bacterial survival strategies (Jones and Lennon, 2010; Lennon and Jones, 2011). The factors affecting dormancy include energy substrate, nutrients, toxic or inhibiting chemicals, geochemical and physical variables etc.

Dormant cells display neither characteristic of living cells nor of dead cells, they simply enter a state of low metabolic activity where they do not undergo cell division (Mellage et al., 2015). The dormant bacteria represents a seed which can determine and maintain the bacterial community in the future (Lennon and Jones, 2011). However, not all bacteria switch to dormancy under unfavorable conditions (Konopka, 2000).

Only a fraction of the microbial population is active in an aquifer at any given time. However, microbial growth is a result of increasing the number of active cells only (Morita, 1988). Depending on the environmental conditions, active microorganisms may switch to inactive state or vice versa. Within a given microbial community, only a small portion of the population may grow while the others are in dormant state or in starvation survival state. Usually, this irregular growth, is due to the deficiency of available energy substrates for several physiological types of bacteria in the environment and less because of other environmental factors (Morita, 1988).

It is quite common in modelling to treat the decay of microorganisms by a first-order term with constant decay coefficient which is independent on the mentioned variables and environment condition. This constant decay term, however, cannot explain the long term survival of microorganisms in oligotrophic environments. The dormancy of bacteria may explain this phenomenon. When net growth is not favorable due to depletion of the energy substrate, the cells often use endogenous materials as an energy source (Morita, 1990; Russell and Cook, 1995). The cells reduce the metabolic activity to a minimum which confirm the long term survival of inactive cells. The intracellular potassium concentration may help to distinguish the active and starving cells. Growing cells have a potassium concentration that is at least two-fold larger than that of starving cells (Russell and Cook, 1995).

The bacteria switching to dormancy go through the starvation-survival process. This starvation-survival process has been illustrated by Morita (1990). When the cells have not sufficient environmental or cellular energy-yielding substrates for maintenance, metabolic arrest of the cells occurs. This metabolic arrest permits organisms to survive over extremely long time. However, the energy yielding mechanisms remain intact in starving cells. Starving

cells utilize all their enzymes except those required for obtaining energy from the environment. When the conditions are favorable, the cellular enzymes are synthesized again. Drastic changes occur in the lipid, an integral part of the cell membrane content, during starvation.

Although dormancy is considered as good survival strategy, this may not hold true for all cases. Transiting to different states, both active and inactive, requires certain energy. Rejuvenation requires an adequate amount of available substrate which is usually higher than the amount needed for maintenance of active cells (Stolpovsky et al., 2011). The inactive fraction usually contains a percentage of cells that are incapable of reactivating. The ability to switch between an active and inactive state could also explain lag times in microbial response to changing substrate concentrations (Stolpovsky et al., 2011). The longer the starvation, the longer the lag phases (Morita, 1990). Moreover, dormancy could only be advantageous when the starving periods exceed a certain time (Konopka, 2000). Model simulation predicted that the dormancy is only successful when the starving period is 54 times longer than the minimum generation time. Dormancy under low stress does not provide any benefit, and may decrease the chances of survival population and vice versa for high stress (Bär et al., 2002). Additionally, the dormant bacteria can also be highly sensitive to other disturbances.

2.2.3 Maintenance energy

The maintenance energy is a certain minimum of energy intake to maintain molecular and cellular integrity and functioning (Hoehler, 2004). The maintenance energy also comprises of the rate of energy expenditure required to fix damaged cells, to keep their physiological state (e.g., cell motility, osmoregulation etc.), and also to adapt to extreme conditions (Van Bodegom, 2007). The maintenance energy requirement defines the minimum necessary flux of substrate across the cell membrane, and thereby determines the magnitude of the required concentration gradient (Hoehler, 2004). This threshold for growth is also referred to as 'critical' Gibbs free energy (Harder, 1997). In some studies, maintenance energy is also described by a negative growth rate constant (Russell and Cook, 1995). In summary, the

maintenance is the energy required to keep the microorganism viable and ready to take advantage of opportunity (LaRowe and Amend, 2015a). In a given environment, the maximum microorganism communities are achieved when all the energy conserved is spent entirely on maintenance (Harder, 1997).

Only some portion of the energy gained by catabolism can be used for growth. Bacteria also expend energy on functions that are not directly growth related (Russell and Cook, 1995). In oligotrophic aquifers, a significant portion of catabolic energy is used for maintenance energy. ME is sensitive to a range of environmental parameters which may vary significantly in the subsurface (Hoehler, 2004; Russell and Cook, 1995). Therefore, the proper maintenance energy measurement is elusive and often questioned (Hoehler, 2004; Morita, 1988; Van Bodegom, 2007). The relative energy spent for maintenance at high growth rate is lower than that at lower growth yields. The maintenance values derived from pure culture conditions are higher than those from natural ecosystems. Additionally, the values obtained in culture experiments normally exceed, by orders of magnitude, the levels that can be reasonably supported by geochemical fluxes in natural systems (Anderson and Domsch, 1985; Hoehler, 2004). Morita (1988) therefore refute the application of maintenance values calculated in the lab to natural ecosystems. According to this research, the ME of lab cultures was at least by three orders of magnitude higher than that studied in agricultural or forest soils.

Therefore, Hoehler (2004) described different levels of ME requirement depending upon the environment. The study suggested that the microbes living in an eutrophic environment have maintenance value that are likely 3–6 orders of magnitude higher than in energy-limited natural systems. In term of ATP, the maintenance value ranges between 0.02 to 40 mmoles ATP · (g dry biomass)⁻¹ h⁻¹ depending upon the bacterial species and the environment (Stouthamer and Bettenhausen, 1973). Tijhuis et al. (1993) also compiled numerous data of chemostat studies, and calculated an average ME value for anaerobic microorganisms of 127 J (g dry biomass)⁻¹ · h⁻¹ at 298 K. This study, based on Arrhenius equations, calculated the maintenance energy as species independent.

One of the common mathematical expression for the calculation of yield considering the maintenance requirement was proposed by Tijhuis et al. (1993):

$$\frac{1}{Y} = \frac{1}{Y_{max}} + \frac{ME}{\mu} \quad 2.1$$

where Y is the actual yield of the bacteria, Y_{max} is the maximum possible biomass yield under given conditions, and μ is the maximum rate of bacterial growth.

Temperature is considered as one of the most important factors which can change the ME of the cell. The breakdown rate of biochemical molecules increases with temperature (Hoehler, 2004; Tijhuis et al., 1993). Higher temperature leads to rapid breakdown of biomolecules, thereby increasing the energy input for ME to fix the damage. One of common mathematical expressions is presented below:

$$ME = A \cdot e^{-\frac{Ea}{RT}} \quad 2.2$$

where, Ea is the activation energy, R is the universal gas constant, T is the absolute temperature, and A is an empirically derived constant (Harder, 1997).

2.2.4 Previous bioenergetic models

There are only few studies using bioenergetics concept to simulate microbial dynamics. However, new studies are dedicated to develop bioenergetic models. Most of these models are based on some combination of thermodynamic, stoichiometric, and kinetic principles (Payn et al., 2014). In the following, I discuss some important models that considered thermodynamic constraints.

Van Walsum and Lynd (1998) developed a model that distributed the energy gained by cellulolytic fermentative microorganisms between growth and extracellular hydrolytic enzymes production. The model includes anaerobic cellulose fermentation based on the ethanol fermentation of yeast. A bioenergetic model was developed for the fermentation of glucose by Haughney and Nauman (1990). This model uses energy balances to determine which pathways are utilized by the substrate and to predict substrate consumption, biomass

growth, and the product distribution. However, the fermentation of glucose using mixed cultures of bacteria is still challenging on the industrial scale. For this, an in-depth knowledge of fermentation including metabolic and biochemical principles is necessary. Therefore, González-Cabaleiro et al. (2015) presented a model based on metabolic energy to accurately predict the changes in product spectrum with pH. Additionally, Cueto-Rojas et al. (2015) used the concept of thermodynamics to choose the right substrate for the production of different compounds including biofuels, amino acid and alcohols etc. under anaerobic conditions.

Demirel and Sandler (2002) reviewed the role of thermodynamics in understanding the coupling between chemical reactions and the transport of substances in bioenergetics. The study explained the use of non-equilibrium thermodynamics in bioenergetics and membrane transport to describe the energy conversion and coupling between chemical reaction and diffusional flows. The formulation of linear non-equilibrium thermodynamics could also be a tool to represent the key processes of coupled phenomena of transport and chemical reactions.

Jin and Bethke (2005) outlined two sets of parameters that need to be defined in the rate law; one related to thermodynamics constraints and another appeared in kinetic terms.

$$r = \mu_{\max} \cdot B \cdot F_K \cdot F_T \quad 2.3$$

where, r is the rate of the energy-yielding redox reaction; μ_{\max} stands for the maximum rate of reaction per unit biomass; B indicates the active biomass concentration; and F_K and F_T are two non-dimensional functions that vary between 0 and 1.

The kinetic limitation F_K is represented by a Monod-type term. The bioenergetic term, F_T , expresses growth limitation depending on the available Gibbs energy for a particular pathway (ΔG), which includes the minimum energy required by microorganisms to synthesize ATP under conditions of active microbial growth (Jin and Bethke, 2005). The function introduced by Jin and Bethke (2005) incorporates an energetic barrier term and relates to the Gibbs energy required to synthesize ATP which effectively sets a minimum energy threshold that must be available for microorganisms to catalyze reactions. As a result, though this model

can be applied in low energy environments, there is a cut-off below which it is no longer applicable. This limitation ensures that a particular microbially-mediated reaction can only proceed if the bioenergetic driving force is thermodynamically spontaneous, regardless of the kinetic driving force.

However, turnover times for super slow growing yet active bacteria are thousands years. These active microorganisms should catalyze chemical reactions at some finite rate for generation of energy. However, the utilization of energy is too slow for models considering F_T , which depend on the ΔG_{ATP} term. Therefore, LaRowe et al. (2012) presented a new formulation based on the comparison of the amount of energy available from any redox reaction with the energy required to maintain the membrane potential ($\Delta\Psi$); a proxy for the minimum amount of energy required by an active microorganism. It states that the concentrations of ions inside and outside the cell must be distinct and maintained. The established electrical potential gradient is a fundamental descriptive component of active cells. The dominant thermodynamic driving force behind ATP production in most species is $\Delta\Psi$. This new model can represent the lowest levels of metabolic activity, which are not implemented in current formulations, and can be incorporated into quantitative models of microbial activity.

Payn et al. (2014) also combined thermodynamics and kinetics to model aquatic microbial metabolism and growth. This model applies fundamental ecological theory to simulate the impact of various potential metabolic reactions on ecological biogeochemistry. LaRowe and Amend (2014) developed an innovative geochemical modelling of redox reaction energetics to understand the growth, active bacterial population, diversity, and populations in deep sea sediments. This bioenergetic model can be used to predict microbial activities in any environment where the geochemistry is well characterized, even if microbiology data have not been collected.

Most of these models essentially proposed that microorganism require a minimum energy from the catabolic reactions. This concept is merged with the kinetic models that signifies reaction rate. Hence, LaRowe and Amend (2015b) developed a bioenergetic model that

considered microbial activities as a rate with which energy should be made available and consumed. It shows the relationship between the power consumption and the bacterial population in the environment through the energy based yield coefficient. This model also takes into account the constraints of environmental influences on biomolecule synthesis. The models developed in this study are used to demonstrate the relationship between catabolic reaction rates, Gibbs energy of reaction, maintenance energy, biomass yield coefficients, microbial population sizes and doubling/replacement times. LaRowe and Amend (2015a) applied this bioenergetics model in marine sediment to quantify the power that the bacteria use in ultra-low energy environments. Moreover, the study also shows a clear link between power consumption and the bacterial population.

Nowadays, there is the possibility of calculating the energy required to synthesize numerous biomolecules in different environments (Amend et al., 2013). There are uncertainties associated with these calculations according to environmental stresses. Moreover, the energetic cost of all these steps, the timescale over which it is required by the microbes and the responses of these to environmental stresses are still not achievable. The quantification of bioavailable Gibbs energy is still possible if there is sufficient geochemical data available (LaRowe and Amend, 2015a and references inside).

Nevertheless, the bioenergetics models should produce results that are representative of the real environment. The bioenergetic model developed in this study shows an efficient wholesome approach of distribution of energy by the bacterial communities and also the effect on the microbial community themselves. This is not the focus of any of these previous studies. The developed model uses ideas from few of these previous models (Heijnen and Dijken, 1992; Jin and Bethke, 2002, 2005, 2003; LaRowe et al., 2012; Stolpovsky et al., 2011; Tjihuis et al., 1993; Van Walsum and Lynd, 1998).

2.3 Particulate organic matter: Cellulose

Total organic matter (TOM) consists of particulate organic matter (POM) and dissolved organic matter (DOM). The organic carbon (OC) comprises almost half of the OM (Kaplan and Newbold, 1995). POC is the OC with particle sizes of less than 2 mm and larger than

0.45 μm and DOC is the organic carbon suspended in water which is defined by the standardized pore-size of filters of 0.45 μm (Thurman, 1985). Figure 2.1 illustrates the continuum of POC and DOC and the type of organic particles and molecules in sediments.

The POM is poorly soluble and too large to enter cell membranes. The hydrolysis of POM results in oligo- and mono-meric carbon substrates which are sources of energy and food for the microorganisms. Cellulose is the most abundant form of POM in the earth surface and the enzymatic hydrolysis of the cellulose is a key step in global carbon cycle (Wilson, 2011). In this thesis, cellulose is used as an example to understand the degradation of POM via bioenergetics model.

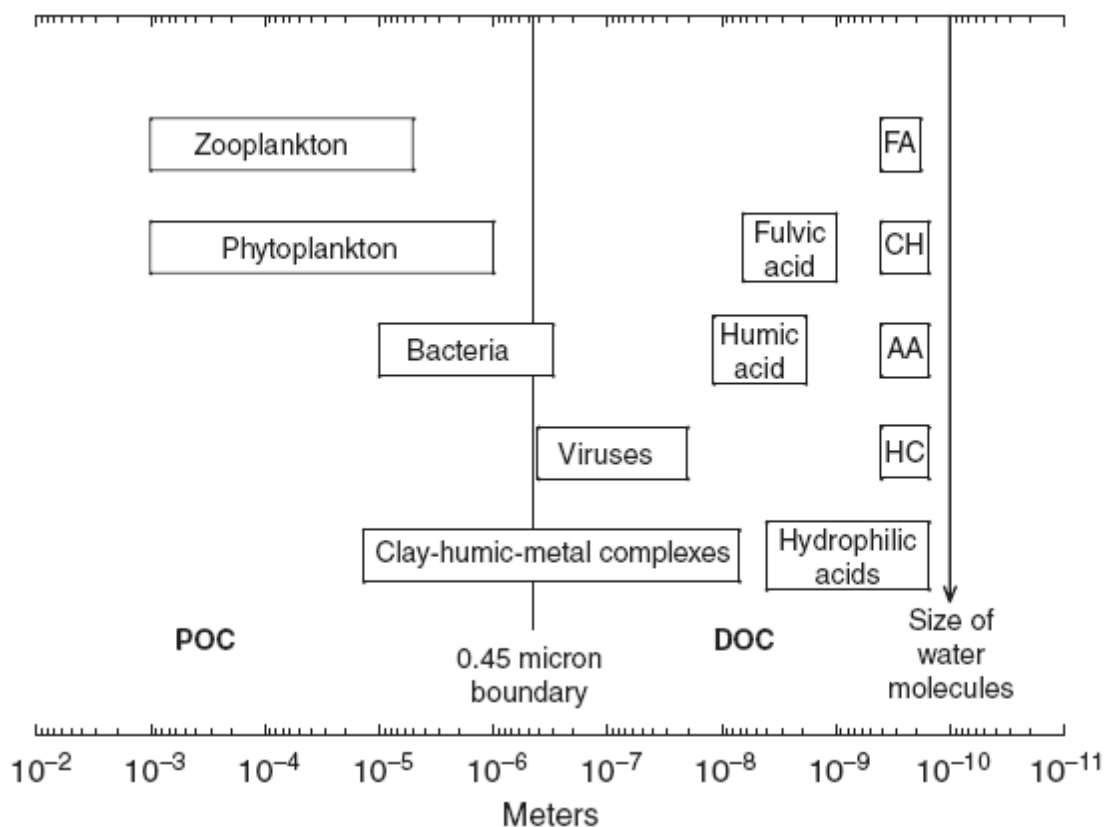


Figure 2.1: Continuum of particulate and dissolved organic carbon in natural waters (where, FA-Fatty Acids; CH-Carbohydrates; AA-Amino Acids; HC-Hydrocarbons). Source: Thurman, 1985

2.3.1 Degradation of cellulose

Cellulose is a homopolymer consisting of glucose units joined by β -1,4 glycosidic bond (Béguin and Aubert, 1994). Although cellulose is abundant in nature, only a small fraction of microorganisms is able to degrade it. This is due to its insolubility and crystalline regions in which the neighbouring molecules have strong interactions, such as hydrogen bonds and hydrophobic stacking (Brown, 1996). Cellulolytic microorganisms, primarily fungi and bacteria, are responsible for the degradation of cellulose in soil, although some insects and molluscs produce their own cellulases and degrade cellulose (Wilson, 2008).

Cellulolytic bacteria, cellulases and source of cellulose are very diverse in nature; hence, the precise degradation of cellulose in any environment is still ambiguous (Wilson, 2011). Figure 2.2 elucidates the general pathways of cellulose degradation. This figure also illustrates the processes involved and energy generating steps in both aerobic and anaerobic environments. Most bacteria produce extracellular hydrolytic enzymes, cellulases, as the cellulose cannot be transported across the cell membrane. The products of the cellulases such as cellobiose, glucose, and other soluble sugars are taken into the cell where the oligomers are metabolized further by cellobiose phosphorylase or by β -glucosidase to form glucose (Coughlan, 1991; Wilson, 2008).

In both aerobic and anaerobic environments, the first step of cellulose degradation is the hydrolysis of cellulose into monomers. Some microorganisms use the free cellulose mechanism in which they secrete a set of individual cellulases, most of which contain carbohydrate binding domain (CBM) (Wilson, 2011); while other bacteria use cellulosomes, large extracellular multi-enzyme complexes composed of several cellulases (Desvaux et al., 2001; Wilson, 2008). The cellulosomes are usually bound to the external surface of the microorganism. The enzyme complex also helps the bacteria to attach to the cellulose. Only few of the enzymes in cellulosomes contain a CBM (Wilson, 2008). The cellulase system consists of three main types of enzymes: (a) endoglucanases, which break non-covalent bonds; (b) exoglucanases (cellobiohydrolases), which act on the existing or endoglucanase-generated chain ends to split cellobiose units from cellulose; and (c) β -glucosidase, which hydrolyse cellobiose and low-molecular-weight cellodextrins to yield glucose molecules

(Pérez et al., 2002). Cellobiose hydrolysis by β -glucosidase prevents the accumulation of cellobiose, which is an inhibitor of exoglucanase activity (Jurtshuk, 1996).

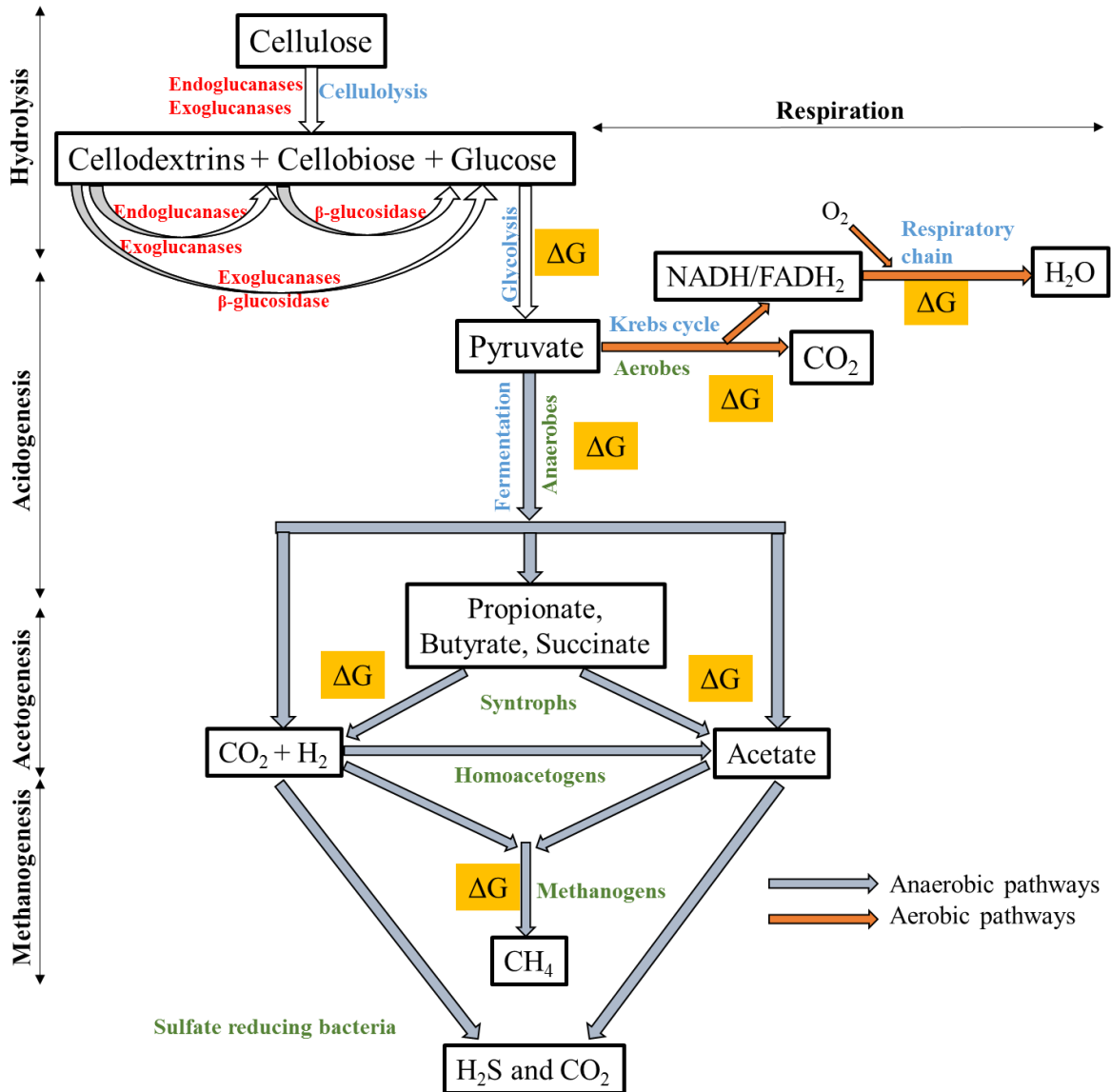


Figure 2.2: Degradation of cellulose. ΔG represent the energy generated during the degradation. The microorganism and microbial processes are represented by green and blue letters respectively. The hydrolysis steps and hydrolytic enzymes are denoted by red letters.

In oxic environments, aerobic microorganisms utilize glucose via glycolysis and Krebs cycle to gain catabolic energy. Two pyruvate molecules are created from a single glucose molecule

through glycolysis, with the release of two ATPs. The Krebs cycle is the oxidative process in respiration by which pyruvate is completely decarboxylated to CO₂ generating additional ATPs and NADH/FADH₂. These high-energy compounds (NADH and FADH₂) are utilized in an electron transport chain (respiratory chain) to produce more energy through oxidative phosphorylation, where oxygen is the terminal electron acceptor (Jurtshuk, 1996).

Complete oxidation of glucose by aerobes can be represented by the following equation:



This complete process of glycolysis, Krebs cycle and electron transport chain produces approximately 38 ATPs (that is, 380,000 calories) from a single glucose molecule (Jurtshuk, 1996).

About 5-10 % of cellulose in nature is degraded under anaerobic conditions (Leschine, 1995). Anaerobic degradation is a multi-step process of serial and parallel reactions. The metabolic versatility of anaerobes expresses itself in their ability to perform various fermentation and respiration reactions, employing several electron acceptors (e.g. carbon dioxide, inorganic sulphur compounds, and inorganic nitrogen compounds) instead of oxygen.

Under anaerobic condition, cellulolytic fermentative microorganisms do not degrade cellulose completely; other types of microorganisms operate in combination with them in order to completely oxidize organic matter in anoxic sediments (Lovley and Chapelle, 1995). During fermentation, the oxidation of the organic compounds is incomplete, but this process yields sufficient energy for microbial growth (Jurtshuk, 1996). Many facultative anaerobes also perform fermentation under anaerobic conditions or can use alternative terminal electron acceptors for respiration depending on the environmental conditions (Botheju et al., 2010). Fermentation does not utilize an electrochemical gradient as that in electron transport chain. Instead, the microorganism performs internally balanced redox reactions to produce energy regardless of the external environment (Konhauser, 2007). Fermentative organisms use NADH and other cofactors to produce many different reduced metabolic by-products, often including hydrogen gas (H₂). Hydrogen gas is also produced in many types of fermentation

reactions (mixed acid fermentation, butyric acid fermentation, butanol fermentation), and the electron acceptor NAD^+ is regenerated from NADH which is utilized again during glycolysis (Jurtshuk, 1996).

Anaerobic respiration uses electron acceptors other than oxygen such as sulfate (SO_4^{2-}), nitrate (NO_3^-), sulphur (S), or fumarate etc. This process still uses a respiratory electron transport chain. However, these terminal electron acceptors have smaller reduction potentials compared to oxygen and generate less energy per oxidized molecule. Anaerobic utilization of soluble sugar starts from glycolysis producing pyruvate which then enters the Krebs cycle. The rest of the energy is obtained via electron transport chains using different electron acceptors. Therefore, cellulose is completely oxidized via microbial food-chain processes by anaerobic communities (Leschine, 1995).

The degradation via anaerobic process, including fermentation and respiration, to mineralize cellulose can be categorized into four major processes (Lovley and Chapelle, 1995).

- 1) Hydrolysis
- 2) Acidogenesis
- 3) Acetogenesis
- 4) Methanogenesis

The first step is hydrolysis of the cellulose into simpler OM, such as glucose. This soluble OM can pass through the cell walls of the bacteria. It is now fermented by the same cellulolytic bacteria or acid forming bacteria, yielding CO_2 , H_2 , and organic acids (e.g. formate, lactic, acetate, propionate and butyrate etc.), and alcohols (Leschine, 1995). This step is called acidogenesis. The simple organic end products formed from this incomplete biologic oxidation process also serve as electron-donors for other anaerobic microorganisms. The third step is called acetogenesis where the product of acidification is converted into acetic acid, carbon dioxide and hydrogen, respectively. Syntrophic bacteria play a key role in the conversion to CH_4 and CO_2 . They usually grow in the presence of H_2 -consuming organisms through interspecies H_2 transfer (Leschine, 1995). The combination of these three steps is also known as acid fermentation (Haandel and Lubbe, 2012). In the final step, the

products of acid fermentation (mainly acetate) are also converted to CO_2 , H_2 and CH_4 (Christensen et al., 2000; Leschine, 1995; Lovley and Chapelle, 1995). H_2 is also an energy source for methanogens and sulfate reducing bacteria, which keep the concentration of H_2 low to produce methane. Methanogens are usually present along with fermentative bacteria. This interaction is considered to be syntrophic because the methanogens, which rely on the fermenters for H_2 save the fermenters from toxicity produced due to the accumulation of hydrogen. Again, homoacetogens use H_2 to reduce CO_2 forming acetate (Leschine, 1995; Pérez et al., 2002). When methanogens were used as the H_2 -consuming organisms, a shift in fermentation pattern to form more acetate and less electron sink products was observed (Marvin-Sikkema et al., 1990). Very little amount of H_2 escape into the atmosphere since it is immediately consumed by methanogens or homoacetogens (Jurtshuk, 1996). In alternate pathways, if sulfate is present in the environment, the sulfate reducer will consume the hydrogen and acetate to form sulfide, outcompeting the methanogens (Leschine, 1995).

In every four consecutive steps, the catabolic reactions generate energy. The free energy released in the reactions is partially used for synthesis of the anaerobic bacterial populations (Haandel and Lubbe, 2012).

2.4 Governing equations for bio-reactive transport

The governing equations presented here illustrate groundwater flow, substrate transport and microbial degradation of the substrate in the subsurface. In this dissertation only one-dimensional steady-state flow in fully saturated porous media is considered.

In modeling porous media, usually conservation laws for solute mass and fluids are formulated for a representative elementary volume (REV). All parameters are averaged over the REV. The exact pore structure of the medium is lost and the medium is considered a continuum.

2.4.1 Groundwater flow

Groundwater flows from areas of higher potential (typically expressed as hydraulic head) to areas of lower potential. This is expressed in Darcy's law:

$$\mathbf{q} = -\mathbf{K}\nabla h \quad 2.4$$

in which \mathbf{q} [LT^{-1}] is the specific discharge vector, that is, the volume transferred per bulk cross-sectional area, \mathbf{K} [LT^{-1}] is the hydraulic conductivity tensor, a symmetric positive definite matrix, h [L] is the hydraulic head, and ∇ is the nabla operator. Darcy's law is substituted into the continuity equation, stating that the divergence of \mathbf{q} is zero under steady-state conditions in systems without internal sources or sinks, to form the groundwater-flow equation.

2.4.2 Solute transport

Groundwater flow causes the redistribution of solute mass. Solutes are transported in porous media with the flow of ground water (advection), and by molecular diffusion and mechanical dispersion. The conservative transport of a dissolved, non-sorbing solute can be described by the advection-dispersion equation:

$$\frac{\partial c}{\partial t} + \nabla \cdot (\mathbf{v}c) - \nabla \cdot (\mathbf{D}\nabla c) = 0 \quad 2.5$$

where c [ML^{-3}] is the concentration of the solute, $\mathbf{v} = \mathbf{q}/n$ [LT^{-1}] is the seepage velocity with n [-] denoting porosity, and \mathbf{D} [L^2T^{-1}] is the dispersion tensor. The negative sign implies that the dispersive solute flux is oriented from higher concentration area to the lower one.

For this study, only 1-D flow and transport are considered. Then the advection-dispersion equation becomes:

$$\frac{\partial c}{\partial t} + v \cdot \frac{\partial c}{\partial x} - D \cdot \frac{\partial^2 c}{\partial x^2} = 0 \quad 2.6$$

in which x [L] is the spatial coordinate and D [L^2T^{-1}] is the dispersion coefficient of the porous medium.

2.4.3 Bio-reactive transport model

Let's now consider a reactive substrate with concentration c_s [ML^{-3}]. Then, the advection-dispersion equation is amended by a reactive source/sink term:

$$\frac{\partial c_s}{\partial t} + v \cdot \frac{\partial c_s}{\partial x} - D \cdot \frac{\partial^2 c_s}{\partial x^2} = -r_s \quad 2.7$$

where r_s [$ML^{-3} T^{-1}$] is the net reaction rate of the substrate, which may be the sum of several individual reaction rates. Typically, the reaction rates are assumed to depend uniquely on the concentrations of the reactants and of the biomass. A typical kinetic law to predict reaction rates is the Michaelis-Menten law, also denoted Monod law if the reaction is proportional to biomass growth:

$$r_s = \frac{\mu^{max}}{Y} \cdot \frac{c}{K+c} \cdot c_{bac} \quad 2.8$$

where μ^{max} [T^{-1}] is the maximum specific growth rate of the bacteria, Y [$M_{bac} M^{-1}$] is the bacterial yield, c_{bac} [$M_{bac}L^{-3}$] is the bacterial concentration, and K [ML^{-3}] denotes the half-velocity concentration of the substrate (Monod constant).

The related growth and decay rates of bacterial and grazers required for the bio-reactive transport are explained in detail in chapter 3.

2.4.4 Initial and boundary conditions

The governing partial differential equations have to be supplemented by appropriate initial and boundary conditions. Initial conditions include the hydraulic-head and concentration distributions throughout the domain at the initial time. In steady-state simulations, no initial states are needed. Boundary conditions indicate how an aquifer interacts with the environment outside the model domain. Mathematical boundaries are commonly defined in three categories: Dirichlet (fixed value), Neumann (fixed normal gradient component), and Cauchy (fixed combination of values and normal derivatives).

2.4.5 Numerical solution

The finite volume method is a suitable approach to discretize the spatial domain because it guarantees local mass conservation (Muyinda, 2014). This technique is used in the present thesis. The domain is subdivided in control volumes with grid spacing Δx , and a balance equation is formulated for each control volume. Gradients at the interfaces of two control volumes are approximated by the difference of the values in the two control volumes divided by the grid spacing, whereas concentration values themselves (needed for the evaluation of advective fluxes) are approximated by the values on the upstream side (upwind differentiation). Upon spatial discretization, the system of coupled partial differential equations is converted to a large system of ordinary differential equations, which are nonlinear due to the reactive terms. Rather than applying my own temporal discretization method, I rely on the Gear solver implemented in Matlab as function `ode15s`. This is a variable-order implicit solver based on backward-differentiation formulas that are particularly suited for stiff systems of differential equations.

3. Substrate-bacteria-grazer interactions

The content in this chapter is modified from 'Bajracharya, B., Lu, C., Cirpka, O.A., 2014. Modeling substrate-bacteria-grazer interactions coupled to substrate transport in groundwater. Water Resour. Res. 50, 4149–4162. doi:10.1002/2013WR015173.'

3.1 Introduction

Microbial activity in porous media is of utmost importance for biogeochemical cycling and pollutant turnover in natural aquifers and technical fixed-bed reactors. Common models applied to simulate microbial activity in porous media account for a single or a few types of biomass, each of which catalyzing a specific solute transformation; microbial growth is assumed proportional to the transformation rate; and a first-order biomass decay term represents microbial death. Previous studies have shown that most bacteria in groundwater are attached to the aquifer's sediment and are therefore immobile (Griebler et al., 2001; Griebler and Slezak, 2001), even though expressions for passive transport, motility, attachment, detachment, and straining of microbes have been developed (Corapcioglu and Haridas, 1985; Hill and Häder, 1997; Tufenkji, 2007). The rate laws describing microbial reactions act as sink-source terms in the transport equations of the solutes, typically formulated on the basis of the advection-dispersion equation. A review of bio-reactive transport models is given by Barry et al., (2002).

In many applications of bio-reactive transport to natural attenuation and remediation of contaminated aquifers, microbial activity is controlled by bringing the reacting electron donors and acceptors together. In these set-ups, transverse mixing across plume fringes (e.g., Anneser et al., 2008; Cirpka and Valocchi, 2007; Davis and Sieburth, 1984; Fraser et al., 2008; Prommer et al., 2009; Thornton et al., 2001) and kinetic mass transfer between water and non-aqueous phase liquids or mineral phases (e.g., Schäfer and Therrien, 1995; Watson et al., 2005), rather than the microbial dynamics, often determine the overall reaction rates.

This may be different in many natural groundwater ecosystems. A good counter-example is bank filtration and hyporheic exchange (e.g., Doussan et al., 1997; Grünheid et al., 2005; Marzadri et al., 2012). Here, the organic electron donors and oxygen as the most important electron acceptor are typically mixed within the streams, but their transformation is limited by the low bacterial density in the flowing water. Once the stream water enters the stream bed, it is exposed to microbial biomass attached to the sediments. That is, the system behaves like a continuously fed fixed-bed reactor. A second example of microbial reactions in groundwater that are not controlled by mixing of the substrates is the operation of mixing wells in active bioremediation (e.g., Hyndman et al., 2000; Mccarty et al., 1998; Phanikumar et al., 2005). Here, missing substrates are added to groundwater recirculation wells, and the mixture of contaminant and reactants are jointly re-injected into the aquifer via the injection screens of the recirculation wells. Again, a stream tube within the aquifer originating from such an injection screen may be seen as a continuously fed fixed-bed reactor.

Using the models discussed above to simulate continuous injection of a growth substrate into a sand column leads to excessive biomass growth near the inlet, even if the substrate concentration in the inflow is small. This, however, is not observed in the field (Luna et al., 2009; Pedersen and Ekendahl, 1990; Zhou et al., 2012). Various authors have thus introduced a biomass-capacity term penalizing biomass growth beyond a maximum concentration (Stolpovsky et al., 2012; Yukalov et al., 2012; Zhou et al., 2012). One approach to implement the carrying capacity is based on the logistic-growth equation used in theoretical ecology:

$$\frac{dc_{bac}}{dt} = \mu_{bac} \cdot c_{bac} \cdot \left(1 - \frac{c_{bac}}{c_{bac}^{\max}}\right), \quad 3.1$$

in which c_{bac} [$M_{bac}L^{-3}$] is the biomass concentration, t [T] is time, μ_{bac} [T^{-1}] is the specific growth rate coefficient, and c_{bac}^{\max} [$M_{bac}L^{-3}$] is the maximum biomass concentration, or carrying capacity. Mathematically similar expressions, such as biomass-inhibition terms, have been used as well (Zysset et al., 1994). It may be noteworthy that the introduction of a carrying capacity is not needed for a set-up in which the macroscopic control of microbial

activity is by physical mixing processes, such as in the case of fringe-controlled biodegradation.

While the concept of a carrying capacity is intriguing, its mechanistic explanation remains unclear. Some authors speculate on space constraints within the porous medium, but bacteria in natural aquifers colonize only a small fraction of the grain surface (Anneser et al., 2010). Other authors assume that kinetic uptake of solutes by the bacteria or diffusive mass transfer within the pore space limits biomass growth (Egli, 2010; Morita, 1988). However, assuming a diffusive length scale of 100 micrometers within a pore, the characteristic time scale of diffusion is on the order of ten seconds, which does not pose a significant kinetic limitation (Cirpka, 2010). Nutrient availability has also been suggested as factor controlling biomass growth (Ayuso et al., 2010) but appears unlikely in natural aquifers unless large substrate loads are to be transformed.

All possible explanations for the occurrence of a carrying capacity discussed above are based on the assumption of a bottom-up control of groundwater ecosystems. That is, the basic supply of substrates or nutrients to the biota limits the overall turnover of the ecosystem. An alternative explanation is based on top-down control, where organisms on a higher trophic level limit the abundance of those on lower levels. In groundwater ecosystems, higher trophic levels include grazers, such as protozoa, and bacteriophages, that is, viruses infecting bacteria. These agents grow on the bacteria, leading to a negative feedback on the bacteria concentration which may limit the turnover of the substrate. The current study explores the possibility of top-down controls in groundwater ecosystems by means of mathematical analysis.

Grazers are quite common in both shallow and deep aquifers (Harvey et al., 1995). The dynamics of substrate-bacteria-grazer interactions have been intensely analyzed for more than three decades (Azam et al., 1983; Butler et al., 1983; Fenchel, 1982). Models to represent these biotic interactions have already been developed (Cao et al., 2008; Khatri et al., 2012; Wright, 1988). A focus has primarily developed around differing aspects of biotic interactions such as the influence of the grazer size on predation (Calbet et al., 2001; Gasol,

1994), the grazing rate (Davis and Sieburth, 1984) and energy flow (Azam et al., 1983), among others.

Environmental concentrations of grazers and bacteriophages suggest that they play a vital role in controlling bacterial growth in aquatic bacterial communities (Davis and Sieburth, 1984; Boras et al., 2009). Viruses also actively act as predators; infect the bacteria and hinder the population of the bacteria (Jürgens et al., 2008; Khatri et al., 2012). Research performed in coastal environment showed that both viruses and grazers are responsible for substantial bacterial mortality (Harvey et al., 1995). Viral lysis, along with grazing can be a cause of mortality in aquatic bacterial communities and the supremacy of those two processes vary among ecosystems (Boras et al., 2009). Some studies indicate that viruses are important predators in eutrophic systems, whereas protists play a major role in bacterial losses in oligotrophic water bodies (Boras et al., 2009).

The presence of grazers is found to enhance net bacterial activity by improving the recycling rate of limiting nutrients (Harvey et al., 1995; Tufenkji, 2007). However the role of grazing within bioremediation processes is inadequately understood at this time and rarely incorporated within biodegradation models (Mittal and Rockne, 2012). Only few studies have been directed towards substrate-bacteria-grazers interactions within aquifers as most studies have been applied to marine environments or laboratory experiments. Presently it is unclear whether and how grazers control bacterial biomass within porous media. The impact of grazers on specific bacterial functions, bioremediation and biogeochemical transformations are likely, but have rarely been considered in detail (Jürgens et al., 2008; Mittal and Rockne, 2012). Common bio-reactive transport models couple bacteria-substrate interactions to advective-dispersive transport (Corapcioglu and Haridas, 1985; Regnier et al., 2005), but to the best of our knowledge, bio-reactive transport models including substrates, bacteria, and predators are yet missing.

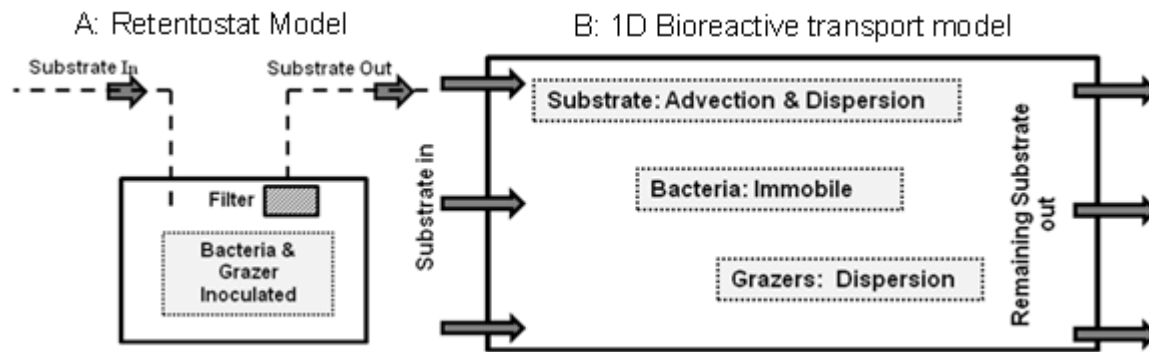


Figure 3.1: Schematic of transport processes in the model developed (A) Retentostat model where the mixed reactor is inoculated with bacteria and grazers while the substrate is injected with the inflow and washed out with the outflow water and a filter is employed to restrain organisms from exiting the reactor with the outflow (B) 1-D model where the substrate is injected with the inflow into the column that is inoculated with bacteria and grazers. Substrate is subject to advection and dispersion whereas bacteria are immobile and grazers are allowed to disperse.

In this study, we present the mathematical analysis of an idealized groundwater ecosystem considering three trophic levels: (1) a dissolved organic substrate, introduced into the system with the inflowing water, (2) a bacteria population growing on the substrate, and (3) a population of grazers growing on the bacteria. Bacteria and grazers also undergo first-order decay. We first analyze a perfectly mixed flow-through system with immobile bacteria and grazers, representing a single retentostat (Figure 3.1 A). We are particularly interested in identifying possible steady states of the system, their stability and dependence on either substrate supply (supporting the hypothesis of bottom-up control) or grazing (supporting top-down control). We subsequently extend the analysis to one-dimensional porous media in which, in addition to the reactive processes, the substrate undergoes advective-dispersive transport, the bacteria are considered immobile, and the grazers undergo a combination of random walk and chemotactic movement (Figure 3.1 B). We analyze spatial profiles of concentrations at steady state, their stability and their dependence on system parameters. In particular, we explore whether constant bacterial concentrations occur without explicit introduction of a maximum biomass concentration. The mathematical model of the present

study focuses on grazing, which may be replaced by virus lysis without changing the principal concept.

3.2 Governing equations and mathematical analysis

We simulate microbial dynamics, biotic interactions, and transport in two types of reactors. In order to analyze basic dynamics of the ecological system, we first simulate a continuously fed retentostat considering the concentrations of a growth substrate, a bacterial population, and a grazer population as dynamic state variables. We apply classical expressions for substrate utilization, related bacterial growth, grazing, and biomass decay. The grazers could also be replaced by bacteriophages, that is, viruses infecting the bacteria, without changing the mathematical model. We choose the retentostat as a zero-dimensional model of an aquifer because the largest fraction of microbial biomass is immobile in groundwater systems, and also protozoa are known to be strongly retained in aquifers (Bales et al., 1995; Harvey et al., 1995).

In the second system, we couple one-dimensional advective-dispersive solute transport to the ecological expressions. The growing substrate is continuously injected into the system with water flow. As frequently done in bio-reactive transport models, the bacteria are considered immobile, whereas we allow for a random walk of the grazers by applying a Fickian diffusion term, combined with chemotactic movement towards the food source. Conceptually, this is similar to considering many retentostats in series. If grazers were to be replaced by bacteriophages, retarded advection of this component may be needed, but the latter is beyond the scope of the current analysis.

In order to keep our models simple, we do not account for additional organisms or substrates, we neglect transport of bacteria, kinetics of solute uptake by the bacteria, and sorption of the substrate. All coefficients are considered constant in time and uniform in space, and the transport domain is one-dimensional. Most important of all, we do not predefine carrying capacities of bacteria and grazers. This implies that asymptotic concentrations of the

organisms approached in the system at late times naturally result from the dynamic expressions applied in the model.

3.2.1 Dynamic retentostat model

The idealized retentostat is a perfectly mixed flow-through bioreactor in which a growing substrate is continuously introduced into the system by the inflow and washed out via the outflow. Inside the reactor, bacteria utilize the substrate for growth. Our model setup also includes grazers which exclusively grow on the bacteria. In contrast to the substrate, the cells of living bacteria and grazers are not washed out of the reactor. In our model, substrate utilization is described by Monod kinetics, whereas grazing is described by a second-order grazing law as applied in the classical Lotka-Volterra model:

$$r_{sub} = \frac{\mu_{bac}^{max}}{Y_{bac}} \cdot \frac{c_{sub}}{c_{sub} + K_{sub}} \cdot c_{bac}, \quad 3.2$$

$$r_{graz} = k \cdot c_{bac} \cdot c_{graz}, \quad 3.3$$

in which r_{sub} [$M_{sub}L^{-3} T^{-1}$] and r_{graz} [$M_{bac}L^{-3} T^{-1}$] are reaction rates of substrate utilization and grazing, μ_{bac}^{max} [T^{-1}] is the maximum specific growth rate of the bacteria, K_{sub} [$M_{sub}L^{-3}$] denotes the corresponding half-velocity concentration of the substrate (Monod constant), Y_{bac} [$M_{bac}M_{sub}^{-1}$] is the bacterial yield, k [$L^3M_{graz}^{-1} T^{-1}$] is the second-order grazing rate coefficient, whereas c_{sub} [$M_{sub}L^{-3}$], c_{bac} [$M_{bac}L^{-3}$], and c_{graz} [$M_{graz}L^{-3}$] are the concentrations of substrate, bacteria, and grazers, respectively. For the ease of computation, all concentrations are expressed in units of milligram carbon per liter of water.

In order to account for loss of organic carbon due to respiration, we consider the bacterial yield Y_{bac} and the grazer yield Y_{graz} [$M_{graz}M_{bac}^{-1}$], quantifying the fraction of food organic carbon incorporated into the biomass of the grazing organism.

The substrate concentration is affected by injection with the inflow, loss by the outflow, and substrate utilization leading to the following ordinary differential equation:

$$\frac{dc_{sub}}{dt} = \frac{1}{\tau}(c_{in} - c_{sub}) - r_{sub}, \quad 3.4$$

in which t [T] is time, c_{in} [$M_{sub}L^{-3}$] denotes the substrate concentration in the inflow, $\tau = V/Q$ [T] is the residence time of the reactor with the reactor volume V [L^3] and the volumetric flow rate Q [L^3T^{-1}].

The bacteria concentration is affected by bacteria growth due to substrate utilization, loss due to grazing, and first-order decay, whereas the grazer concentration increases due to grazing and decreases due to first-order decay:

$$\frac{dc_{bac}}{dt} = r_{sub} \cdot Y_{bac} - r_{graz} - \mu_{bac}^{dec} \cdot c_{bac}, \quad 3.5$$

$$\frac{dc_{graz}}{dt} = r_{graz} \cdot Y_{graz} - \mu_{graz}^{dec} \cdot c_{graz}, \quad 3.6$$

in which μ_{bac}^{dec} [T^{-1}] and μ_{graz}^{dec} [T^{-1}] are the first-order decay rate coefficients of bacteria and grazers, respectively.

3.2.1.1 Possible steady-state concentrations of the retentostat model

At steady state, the rates of change of all concentrations are zero. Substituting Eqs. (3.2 & 3.3) into Eqs. (3.4-3.6), setting the resulting expressions to zero, and rearranging terms yields three possible steady-state solutions. In the trivial steady state, all biota are extinct and the substrate concentration equals the inflow concentration. In a second steady state, the grazers are extinct, and bacterial growth is balanced by first-order decay. Here, we consider only the steady-state solution in which all three concentrations, denoted c_{sub}^{∞} , c_{bac}^{∞} , and c_{graz}^{∞} , are non-zero:

$$c_{bac}^{\infty} = \frac{\mu_{graz}^{dec}}{k \cdot Y_{graz}}, \quad 3.7$$

$$c_{sub}^{\infty} = \frac{1}{2} \left(c_{in} - K_{sub} - \tau \cdot \frac{\mu_{bac}^{\max}}{Y_{bac}} c_{bac}^{\infty} + \sqrt{\left(c_{in} - K_{sub} - \tau \cdot \frac{\mu_{bac}^{\max}}{Y_{bac}} c_{bac}^{\infty} \right)^2 + 4K_{sub} \cdot c_{in}} \right), \quad 3.8$$

$$c_{graz}^{\infty} = \frac{1}{k} \cdot \left(\frac{c_{sub}^{\infty}}{K_{sub} + c_{sub}^{\infty}} \cdot \mu_{bac}^{\max} - \mu_{bac}^{dec} \right). \quad 3.9$$

Eq. (3.7) implies that, in the presence of grazers, the steady-state bacteria concentration c_{bac}^{∞} does neither depend on the inflow concentration c_{in} of the substrate, nor on parameters related to substrate-bacteria interactions. c_{bac}^{∞} is purely defined by the grazer dynamics.

A brief analysis reveals that very small values of the steady-state substrate concentration c_{sub}^{∞} , e.g. caused by small values of c_{in} , may lead to negative values of the steady-state grazer concentration c_{graz}^{∞} , implying that under such conditions this particular steady state cannot be reached, that is, the grazers become extinct. In such a case, a steady state is possible in which the substrate concentration is independent of c_{in} and reflects only parameters of the bacterial dynamics (equations not shown). If this substrate steady-state concentration is smaller than c_{in} , the corresponding steady-state bacteria concentration renders negative, implying that this steady state is not reached either, and the biota-free steady-state solution remains the only possible solution.

3.2.1.2 Linearized stability analysis of the retentostat model

While the steady state derived in the previous section is a valid fix point of the dynamic system, it is not yet clear whether it is actually approached by the system under constant conditions. A common approach to analyze the stability of a fix point is to linearize the system of ordinary differential equations about the proposed steady-state solution (Khatri et al., 2012):

$$\frac{dc}{dt} \approx \mathbf{J}(\mathbf{c} - \mathbf{c}^{\infty}), \quad 3.10$$

in which $\mathbf{c}=[c_{sub}, c_{bac}, c_{graz}]^T$ is the column vector of concentrations, and \mathbf{J} is the Jacobian matrix defined as:

$$\mathbf{J}_{ij} = \left. \frac{\partial}{\partial c_j} \left(\frac{\partial c_i}{\partial t} \right) \right|_{\mathbf{c} = \mathbf{c}^\infty}, \quad 3.11$$

that is, the 3×3 matrix of the partial derivatives of all rates of concentration changes with respect to all concentrations, derived about the steady state. Deriving \mathbf{J} about the steady-state solution with non-zero grazer concentration, we obtain:

$$\mathbf{J} = \begin{bmatrix} -\frac{1}{\tau} \frac{\mu_{bac}^{\max}}{Y_{bac}} \cdot \frac{K_{sub}}{(K_{sub} + c_{sub}^\infty)^2} \cdot c_{bac}^\infty & -\frac{\mu_{bac}^{\max}}{Y_{bac}} \cdot \frac{c_{sub}^\infty}{K_{sub} + c_{sub}^\infty} & 0 \\ \mu_{bac}^{\max} \cdot \frac{K_{sub}}{(K_{sub} + c_{sub}^\infty)^2} \cdot c_{bac}^\infty & 0 & -k \cdot c_{bac}^\infty \\ 0 & k \cdot Y_{graz} \cdot c_{graz}^\infty & 0 \end{bmatrix}. \quad 3.12$$

The analytical solution for the linearized problem of Eq. (3.10) is:

$$\mathbf{c}(t) \approx \mathbf{V} \begin{bmatrix} \exp(\lambda_1 t) & 0 & 0 \\ 0 & \exp(\lambda_2 t) & 0 \\ 0 & 0 & \exp(\lambda_3 t) \end{bmatrix} \mathbf{V}^{-1} (\mathbf{c}(0) - \mathbf{c}^\infty) + \mathbf{c}^\infty, \quad 3.13$$

in which λ_i is the i -th eigenvalue of the Jacobian \mathbf{J} , and \mathbf{V} is the matrix of corresponding eigenvectors. A positive real component in any of the three eigenvalues would indicate that a small deviation of the concentrations from the fix-point solution is magnified, revealing that the system is incapable of achieving the fix point. This characterizes a linearly unstable system. By contrast, if the real components of all eigenvalues are negative, exponential relaxation occurs towards the fix point, so that this steady state can be approached by the system (Khatri et al., 2012).

Non-zero imaginary components of the eigenvalues imply oscillations of the system close to the fix point. Since the solution in the time domain is real, complex eigenvalues are

accompanied with complex conjugate values, and also the corresponding complex eigenvectors are complex conjugates of each other. Complex eigenvalues with a negative real part reveal decaying oscillations, with the concentrations approaching the fixed steady-state in an alternating manner. For these cases, the time period T_i of oscillations [T] and half-life $t_{1/2,i}$ [T] of their amplitudes are computed by:

$$T_i = 2\pi / \text{Im}(\lambda_i), \quad 3.14$$

$$t_{1/2,i} = -\ln(2) / \text{Re}(\lambda_i). \quad 3.15$$

3.2.2 One-dimensional bio-reactive transport model

We now consider bio-reactive transport in a one-dimensional saturated porous medium such as a one-dimensional aquifer or a fixed-bed reactor. The solute undergoes advective-dispersive transport and consumption by bacterial activity:

$$\frac{\partial c_{sub}}{\partial t} + v \cdot \frac{\partial c_{sub}}{\partial x} - D_{sub} \cdot \frac{\partial^2 c_{sub}}{\partial x^2} = -\frac{\mu_{bac}^{max}}{Y_{bac}} \cdot \frac{c_{sub}}{c_{sub} + K_{sub}} \cdot c_{bac}, \quad 3.16$$

in which x [L] is the spatial coordinate, v [LT^{-1}] denotes the seepage velocity, and D_{sub} [L^2T^{-1}] is the dispersion coefficient of the substrate. The governing equation for the bacteria, considered immobile, is identical to the one used for the retentostat:

$$\frac{dc_{bac}}{dt} = \left(\mu_{bac}^{max} \cdot \frac{c_{sub}}{c_{sub} + K_{sub}} - \mu_{bac}^{dec} - k \cdot c_{graz} \right) \cdot c_{bac}, \quad 3.17$$

whereas we assume that random movement of the grazers can be described by Fickian diffusion, which is coupled to the reactions of the retentostat. The diffusion coefficient of the grazers decreases with increasing bacteria concentration, resulting in a “chemotactic” movement of the grazers towards higher bacteria concentrations.

$$\frac{\partial c_{graz}}{\partial t} - \frac{\partial}{\partial x} \left(D_{graz} \frac{\partial c_{graz}}{\partial x} \right) = \left(k \cdot Y_{graz} \cdot c_{bac} - \mu_{graz}^{dec} \right) \cdot c_{graz}, \quad 3.18$$

$$D_{graz} = \min\left(D_{graz}^{\max}\left(1 - \frac{c_{bac}}{c_{bac}^{noD_{graz}}}\right), 0\right), \quad 3.19$$

in which D_{graz} [L^2T^{-1}] is the “diffusion” coefficient of the grazers, quantifying their random movement. It is known that grazers usually migrate by random walk combined with chemotaxis (Fenchel, 2004; Machemer, 2001). Grazers can actually congregate at food source within a few minutes from distance up to few centimeters in an aquatic medium (Fenchel and Blackburn, 1999). This is implemented in the model by linearly reducing D_{graz} from its maximum value D_{graz}^{\max} [L^2T^{-1}] with the bacteria concentration. At a maximum bacteria concentration $c_{bac}^{noD_{graz}}$ [$M_{bac}L^{-3}$] for grazer diffusion, the random movement of the grazers is assumed zero. By making the random movement of the grazers dependent on the food supply, chemotaxis is possible without the need of actively sensing concentration gradients.

As boundary conditions, we assume a known flux concentration c_{in} of the substrate at the inlet ($x=0$), and vanishing first derivatives for c_{sub} at $x=L$ and for c_{graz} at both boundaries, in which L [L] is the length of the domain:

$$\begin{aligned} v c_{sub} - D_{sub} \frac{\partial c_{sub}}{\partial x} = v \cdot c_{in}, \quad \frac{\partial c_{graz}}{\partial x} = 0 \text{ at } x = 0, \\ \frac{\partial c_{sub}}{\partial x} = \frac{\partial c_{graz}}{\partial x} = 0 \text{ at } x = L. \end{aligned} \quad 3.20$$

We solve Eqs. (3.16-3.20) by applying the Finite Volume Method with grid spacing Δx for spatial discretization, using upwind differentiation for advection, and solving the resulting large system of non-linear ordinary differential equations with the Gear solver implemented in Matlab as function `ode15s`.

3.2.3 Approximate steady-state concentration distributions for one-dimensional bio-reactive transport in the presence of grazers

We approximate the steady-state concentration distributions in the one-dimensional advective-dispersive-reactive system by neglecting the dispersive terms in Eqs. (3.16 & 3.18) and setting the time derivatives of the concentrations to zero:

$$0 = (k \cdot Y_{graz} \cdot c_{bac}^{\infty} - \mu_{graz}^{dec}) \cdot c_{graz}, \quad 3.21$$

$$\frac{dc_{sub}^{\infty}}{dx} = -\frac{\mu_{bac}^{\max}}{v \cdot Y_{bac}} \cdot \frac{c_{sub}^{\infty}}{c_{sub}^{\infty} + K_{sub}} \cdot c_{bac}^{\infty}, \quad 3.22$$

$$0 = \left(\mu_{bac}^{\max} \cdot \frac{c_{sub}^{\infty}}{c_{sub}^{\infty} + K_{sub}} - \mu_{bac}^{dec} - k \cdot c_{graz}^{\infty} \right) \cdot c_{bac}^{\infty}. \quad 3.23$$

Then, as long as grazers are sustained, the steady-state bacteria and grazer concentrations follow the corresponding expressions of Eqs. (3.7 & 3.9), whereas the steady-state substrate concentration is (see Simmons et al., 1995):

$$c_{sub}^{\infty}(x) = K_{sub} \cdot W \left(\frac{c_{in}}{K_{sub}} \exp \left(\frac{c_{in}}{K_{sub}} - \frac{\mu_{bac}^{\max} \cdot c_{bac}^{\infty} \cdot x}{v \cdot Y_{bac} \cdot K_{sub}} \right) \right), \quad 3.24$$

in which $W(a)$ is Lambert's W -function with argument a , meeting $a = W(a) \exp(W(a))$.

The steady-state concentration profiles of Eqs. (3.24, 3.7 & 3.9) for $c_{sub}^{\infty}(x)$, $c_{bac}^{\infty}(x)$, and $c_{graz}^{\infty}(x)$ are valid until $c_{graz}^{\infty}(x)$ according to Eq. (3.9) becomes zero. We denote the distance at which this occurs x_{graz} [L]. Substituting Eq. (3.9) into $c_{graz}^{\infty}(x_{graz}) = 0$ and solving for $c_{sub}^{\infty}(x_{graz})$ yields:

$$c_{sub}^{\infty}(x_{graz}) = \frac{\mu_{bac}^{dec}}{\mu_{bac}^{\max} - \mu_{bac}^{dec}} \cdot K_{sub}, \quad 3.25$$

which may be substituted into Eq. (3.24), to compute the distance x_{graz} over which grazers are sustained:

$$x_{graz} = \frac{v \cdot Y_{bac} \cdot K_{sub} \cdot k \cdot Y_{graz}}{\mu_{bac}^{max} \cdot \mu_{graz}^{dec}} \left(\frac{c_{in}}{K_{sub}} - \frac{\mu_{bac}^{dec}}{\mu_{bac}^{max} - \mu_{bac}^{dec}} + \ln \left(\frac{c_{in}}{K_{sub}} \cdot \frac{(\mu_{bac}^{max} - \mu_{bac}^{dec})}{\mu_{bac}^{dec}} \right) \right), \quad 3.26$$

in which we have considered that Lambert's W -function is defined by its inverse. For $x > x_{graz}$, the steady-state substrate concentration $c_{sub}^{\infty}(x)$ is too small to sustain grazers. Our experience from the numerical analysis is that downstream of this point the trivial solution, in which the last valid solution of the steady-state solute concentration $c_{sub}^{\infty}(x_{graz})$ remains constant and both the bacteria and grazer concentrations are zero, is the most realistic analytical approximation.

Because the steady-state bacteria concentration $c_{bac}^{\infty}(x)$ according to Eq. (3.7) does neither depend on the substrate concentration $c_{sub}^{\infty}(x)$ nor on parameters related to substrate-bacteria interactions, the approximate steady-state spatial profile of the bacteria biomass $c_{bac}^{\infty}(x)$ is constant for $x \leq x_{graz}$.

3.2.4 Linearized stability analysis of the one-dimensional bio-reactive transport model

The stability analysis of the retentostat system, expressed in Eqs. (3.10, 3.11, 3.13-3.15), can also be applied to the spatially discretized bio-reactive transport equations. For this purpose, we compute the Jacobian matrix \mathbf{J} by direct numerical differentiation of the system of ordinary differential equations resulting from spatial discretization of the bio-reactive transport equations. The sensitivities are derived about the spatial concentration distribution at the end of the simulated time period where steady state has almost been achieved. We are particularly interested in verifying that all real components of the eigenvalues of \mathbf{J} are negative. We also consider the smallest absolute real component of complex eigenvalues representing the slowest decaying oscillatory signal component, for which we compute the corresponding time period T_i , half-life $t_{1/2,i}$, and the related contributions of the substrate,

bacteria, and grazer concentrations to the corresponding eigenvector. This information describes which oscillations remain the longest in the system, the temporal frequency of the oscillations, and how quickly they vanish.

3.3 Model applications

3.3.1 Retentostat model

In the first model, we consider a single retentostat of 1L volume. The volumetric flux Q is 1 mL/min with an inflow concentration c_{in} of 1 mg C L⁻¹. The initial concentrations of the substrate, bacteria, and grazers are 0 mg C L⁻¹, 0.01 mg C L⁻¹, and 0.01 mg C L⁻¹, respectively. The simulations are performed until steady-state is reached, which is about 50 days.

Table 3.1: Parameters values used in the simulations.

Parameters	Description	Values	Units	Reference
c_{sub}	Initial substrate concentration	0.00	[mg C L ⁻¹]	
c_{bac}	Initial bacteria concentration	0.01	[mg C L ⁻¹]	
c_{graz}	Initial grazer concentration	0.01	[mg C L ⁻¹]	
K_{sub}	Half-velocity concentration of the substrate (Monod constant)	0.1	[mg C L ⁻¹]	(Owens and Legan, 1987)
μ_{bac}^{max}	Maximum specific growth rate of the bacteria	1×10^{-4}	[s ⁻¹]	(Reardon et al., 2002)
c_{in}	Substrate concentration in the inflow	1.0	[mg C L ⁻¹]	
k	Second-order grazing rate coefficient	1×10^{-4}	[L Mg C S ⁻¹]	
Y_{bac}	Bacterial yield	0.3	[mg C mg ⁻¹ C ⁻¹]	(Reardon et al., 2002)
Y_{graz}	Grazer yield	0.2	[mg C mg ⁻¹ C ⁻¹]	(Wright, 1988)
μ_{bac}^{dec}	First-order decay rate coefficient of bacteria	1×10^{-5}	[s ⁻¹]	(Corapcioglu and Haridas, 1985)

μ_{graz}^{dec}	First-order decay rate coefficient of grazers	2×10^{-6}	$[s^{-1}]$	(Wright, 1988)
r_{sub}	Reaction rates of substrate utilization	N/A	$[mg\ C\ L^{-1}\ s^{-1}]$	
r_{graz}	Reaction rates of grazing	N/A	$[mg\ C\ L^{-1}\ s^{-1}]$	
Specific parameters for the one-dimensional column simulation				
D_{sub}	Dispersion coefficient of the substrate	1×10^{-8}	$[m^2\ s^{-1}]$	
D_{graz}^{max}	Diffusion coefficient of the grazers	1×10^{-9}	$[m^2\ s^{-1}]$	(Murray and Jackson, 1992)
$C_{bac}^{noD_{graz}}$	Bacteria concentration at which grazer diffusion becomes zero	5	$[mg\ C\ L^{-1}]$	
v	Seepage velocity of 1-D column	1/86400	$[m\ s^{-1}]$	
Specific parameters for the retentostat simulation				
V	Reactor volume	1×10^{-3}	$[m^3]$	
Q	Volumetric flow rate through the reactor	$\frac{1.67 \times 10^7}{8}$	$[m^3\ s^{-1}]$	

The parameters of Monod and biomass-decay kinetics are unique for specific microorganisms and may depend on temperature, pH, and other environmental condition. Only little is known about the transport behavior of protozoa within the subsurface, as the subsurface microbial transport literature has largely focused on bacteria and viruses (Harvey et al., 1995). More importantly, quantitative investigations on the death of bacteria and grazers are scarce. Thus, the parameter values listed in Table 3.1 are based on previous studies, intelligent guesses, and have been selected after testing the models with various parameter combinations. We have chosen a value of the second-order grazing rate coefficient (k) that gives a steady state bacterial concentration similar to observations found in natural aquifers. This value of k is $1 \times 10^{-4}\ L\ mg\ C\ s^{-1}$.

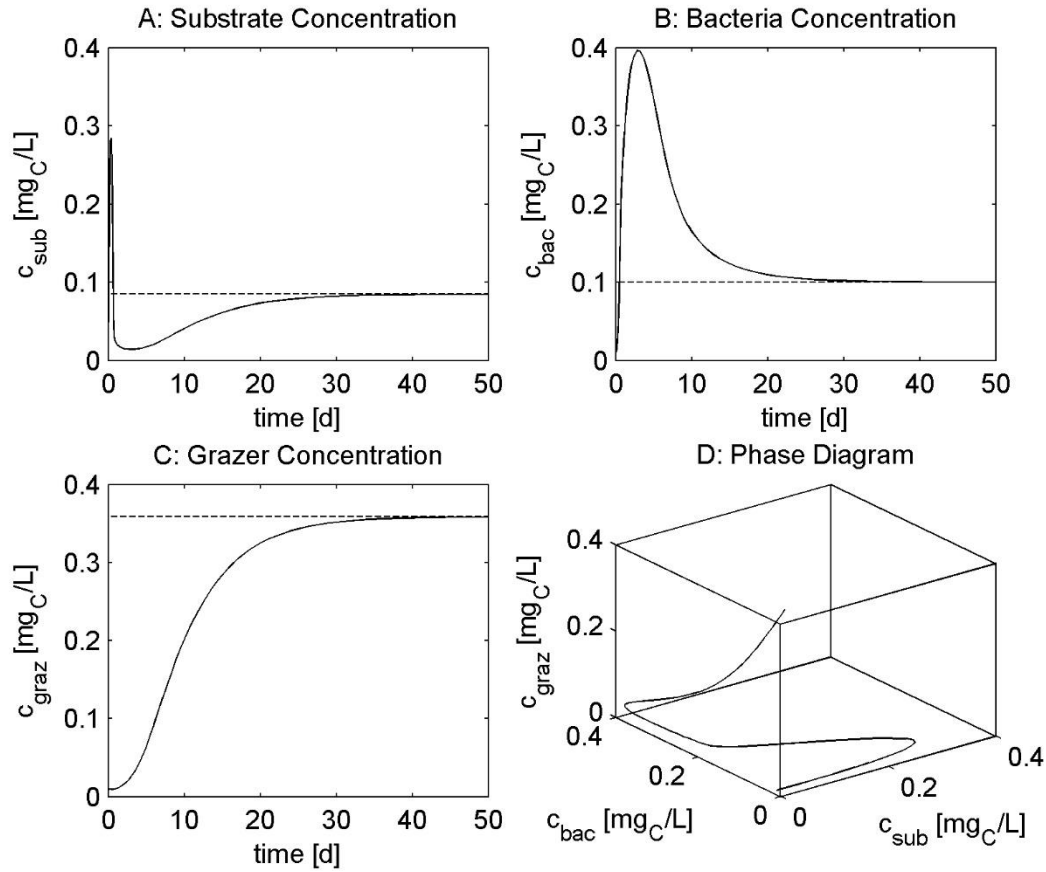


Figure 3.2: Time series of concentrations (A-C) and phase diagram (D) for the retentostat model. All concentrations are in mass carbon per volume of water; parameters according to Table 3.1.

Figure 3.2 shows the simulated time series of all concentrations in the retentostat and a phase diagram. At the very beginning, the substrate concentration increases rapidly reaching its peak at about 9 hours. The presence of the substrate initially facilitates bacteria growth without being affected by the grazers too much. After the first few hours but within the first three days, the increasing substrate consumption by the bacteria leads to a decrease of the substrate concentration which slows down bacterial growth. From the third day on, the bacteria concentration decreases again. The increasing bacteria concentration leads to improved growth conditions for the grazers. With increasing grazer concentrations, the bacteria concentration decreases and thus the substrate concentration increases, which in turn could improve the growth conditions for the bacteria. With the parameters chosen, the

concentrations exponentially approach their steady-state values predicted by Eqs. (3.7-3.9) without apparent oscillations about the asymptotic values. Using different parameter combinations, approaching steady-state may be subject to dampened oscillations.

As discussed above, the steady-state bacteria concentration c_{bac}^{∞} depends solely on parameters related to grazing. This is in contrast to the concepts put forward by Wright, (1988) and Billen et al., (1980), who assumed that the steady-state bacterial concentration primarily depends on the ratio of the substrate input to the grazing rate. Our model analysis reveals that the bacteria concentration does not depend on the inflow concentration c_{in} . At steady-state, the bacteria act like a catalyst, transferring organic carbon from the dissolved fraction to higher trophic levels in a linear heterotrophic food chain (Azam et al., 1983; Mittal and Rockne, 2012; Wright, 1988). Increasing the substrate input increases the steady-state grazer concentration sustained by the system.

The stability analysis according to Eqs. (3.10-3.15) yields two complex eigenvalues, $\lambda_{1,2} = (-4.81 \times 10^{-5} \pm 4.57 \times 10^{-5}i) \text{ s}^{-1}$, and one real eigenvalue, $\lambda_3 = -1.59 \times 10^{-6} \text{ s}^{-1}$. All real components are negative, confirming a stable steady-state of non-zero concentrations that is approached by the system. The oscillatory components of perturbations about the steady-state decay fairly quickly with a half-life of 4 hours, which is much shorter than the corresponding time period of oscillations of 1 day and 14 hours. The quick decay of the oscillatory components explains why no oscillations are observable at late times in Figure 3.2. At these late times, the dominant component of deviations from the steady-state is the eigenvector with the real eigenvalue. Translating this eigenvalue to a half-life, results in about 5 days. In Figure 3.2, the exponential approach towards the steady-state solution is visible from about day 7 on.

3.3.2 One-dimensional bio-reactive transport model

The one-dimensional model is simulated for 100 days using the parameter values listed in Table 3.1. The reactive coefficients are identical to those of the retentostat model. The effective flow velocity of 1 meter per day is a typical groundwater value. The substrate dispersion coefficient of $1 \times 10^{-8} \text{ m}^2 \text{ s}^{-1}$ corresponds to a dispersivity of 1 mm, which is a

typical value for a uniform sand column. The maximum diffusion coefficient D_{graz}^{max} of the grazers of $1 \times 10^{-9} \text{ m}^2 \text{ s}^{-1}$ lies in the reported range of 1×10^{-10} to $3 \times 10^{-7} \text{ m}^2 \text{ s}^{-1}$ (Harvey et al., 1995; Kiørboe et al., 2004; Murray and Jackson, 1992). Choosing the bacteria concentration $c_{bac}^{noD_{graz}}$ above which grazer diffusion stops to be 5 mg C L^{-1} is equivalent to a cross-diffusion coefficient of $2 \times 10^{-10} \text{ m}^2 \text{ s}^{-1} \text{ L mg}^{-1} \text{ C}$.

Figure 3.3 A-C shows the concentration distributions of all three components as a function of space and time. At the beginning of the simulation, an unretarded, mainly advective concentration front invades the domain. The presence of the substrate facilitates substantial bacteria growth followed by growth of the grazers. This leads to a combined bacteria-grazer peak traveling through the domain. The presence of grazers diminishes the bacteria population, which again leads to a reduction of the grazer concentration and increment of the substrate concentration. This behavior is repeated several times with decreasing oscillations. From day 50 onwards, the oscillations fluctuate in a more or less regular pattern about the steady-state concentration distribution, which is approached in the asymptotic limit.

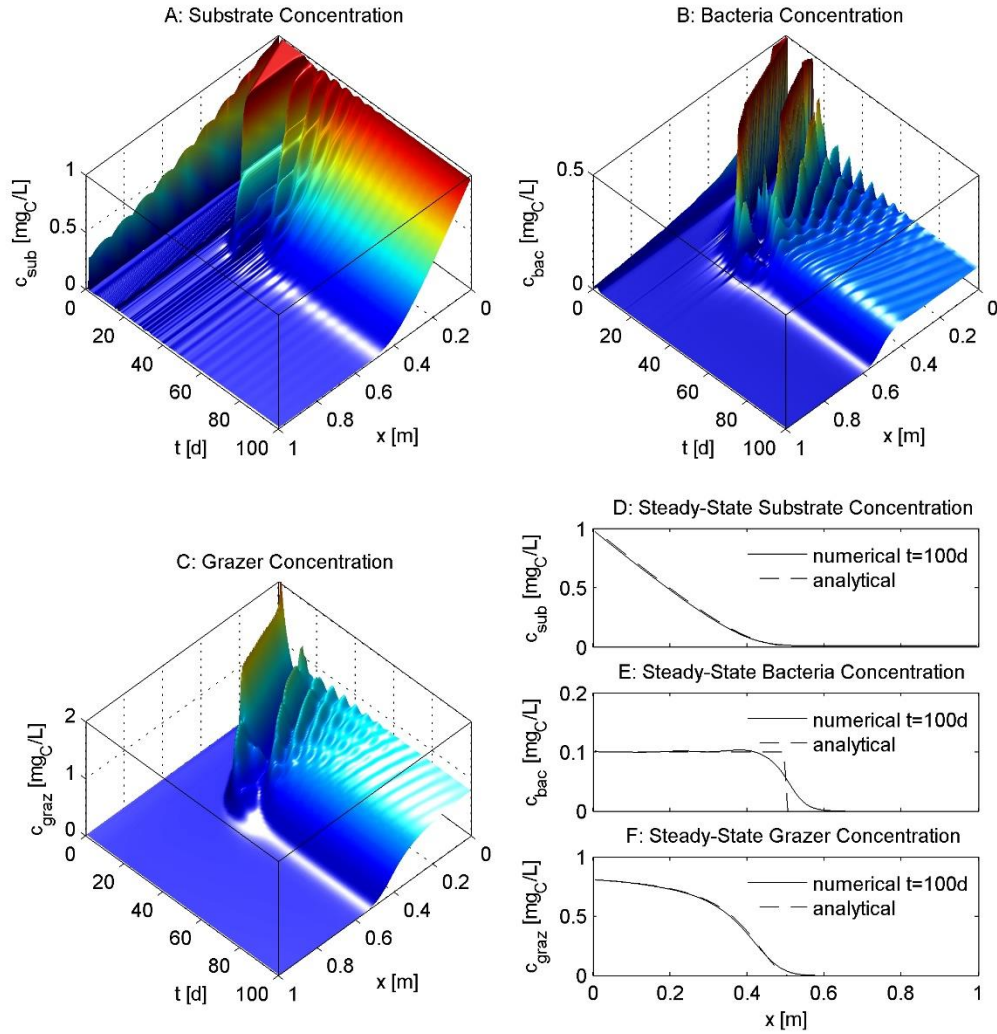


Figure 3.3: Transient results of the 1-D bio-reactive transport model: Concentration of (A) substrate, (B) bacteria, (C) grazers as function of time and space; (D, E & F) comparison of analytical and numerical solution at late times.

Figure 3.3 D-F show length profiles of the concentrations at the end of the simulation after 100 days together with the analytical expressions for strictly advective-reactive transport of Eqs. (3.7, 3.9, 3.24). The simulated steady-state substrate concentration decreases with travel distance until it reaches its asymptotic minimum value of $0.0109 \text{ mg C L}^{-1}$, which confirms

the analytical value of $0.0111 \text{ mg C L}^{-1}$ according to Eq. (3.25). The steady-state substrate profile computed by numerical simulation agrees very well with the analytical expression of Eq. (3.24), even though the latter was derived for transport with zero dispersion.

The numerically simulated results confirm that in the presence of grazers, the system approaches a steady-state in which bacterial growth and predation balance at constant bacteria concentrations, so that the higher turnover of substrate near the inlet supports higher grazer concentrations ($0.807 \text{ mg C L}^{-1}$ at $x = 0 \text{ m}$). The values are monotonically decreasing with decreasing substrate concentrations. The analytical grazer model of Eq. (3.9) in conjunction with the substrate profile according to Eq. (3.24) again agree very well with the numerical steady-state solution, at least over the largest part of the domain. The analytical expression of Eq. (3.26) predicts that at $x_{graz} = 0.50 \text{ m}$, the substrate concentration reaches such a small value that grazers cannot be sustained anymore. The numerical result shows a gradual decrease instead. This can be explained by grazer diffusion which is not accounted for in the analytical expression. Comparative simulations without grazer diffusion (not shown) confirm a much sharper drop of the grazer (and the bacteria) concentrations.

The simulated steady-state bacteria concentration remains constant over the first 0.4 m at a value of almost exactly 0.1 mg C L^{-1} as predicted by the analytical expression of Eq. (3.7), which solely depends on the presence and the parameters of the grazers. While the analytical model predicts a sharp drop of the bacteria concentration at x_{graz} , the numerical profile is smoothed. Interestingly this smoothing is caused by diffusion of the grazers rather than that of the bacteria, and it is much less pronounced for smaller grazer diffusion coefficients. Overall, the independence of the steady-state bacteria concentration on the substrate concentration indicates top-down rather than bottom-up control.

The dispersion coefficients of the grazers and the substrate do not largely impact the shape and length of the steady-state plume, the only substantial difference is whether the plateau bacteria concentration drops sharply (no diffusion/dispersion) or smoothly (large diffusion/dispersion). At late times, the chemotactic component of the grazer diffusion has no influence on the steady-state concentrations, because the steady-state gradient of the bacteria

concentration is zero anyway. However, all dispersion/diffusion terms influence the time needed until steady-state is reached.

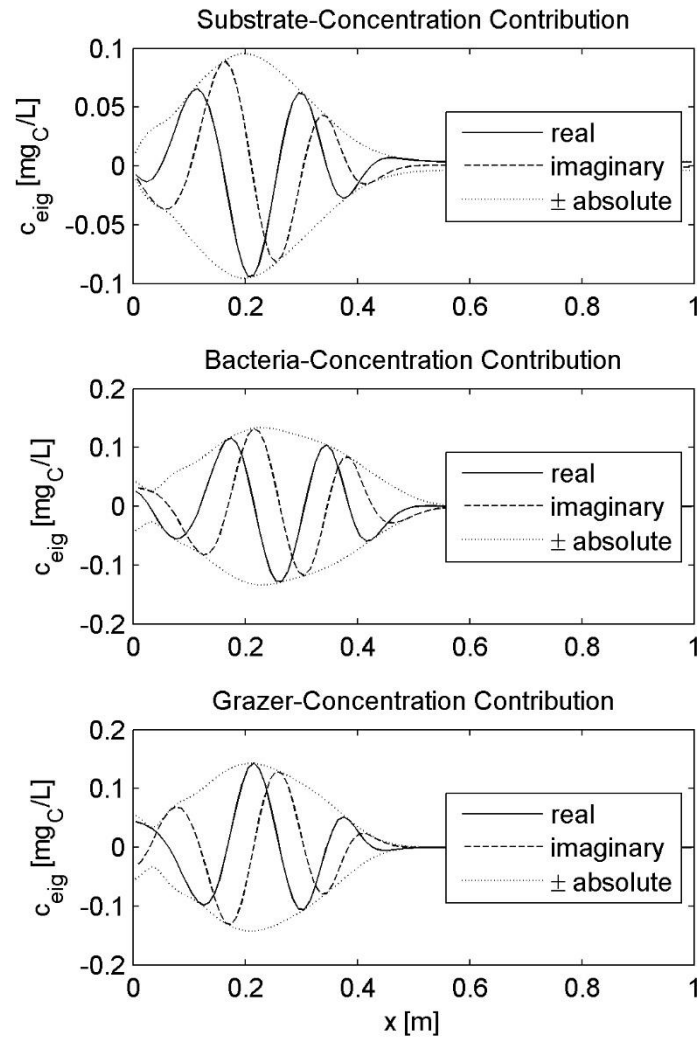


Figure 3.4: Stability analysis of the one-dimensional bio-reactive transport model, compound-specific contributions to the complex eigenvector related to the complex eigenvalue with the largest real component. These contributions define the slowest decaying oscillatory deviations from the steady-state solution.

The overall good agreement between the analytical and numerical expressions for steady-state concentration distributions simplifies the analysis of scenarios by just considering the analytical expressions. For instance, if the injected substrate concentration is increased, the late-time bacteria concentration according to Eq. (3.7) is not affected, but the length x_{graz} over which substantial bacterial biomass can be found will be increased according to Eq. (3.26). The extra input of carbon will lead to a steady-state concentration profile of the substrate according to Eq. (3.24), starting with almost the same spatial gradient and achieving the same asymptotic substrate-concentration value of Eq. (3.25). In qualitative terms, because the bacterial concentration is limited by predation, only a percentage of substrate will be consumed near the inlet. The remaining concentrations will be transported further downstream and thus increase the length over which bacteria and grazers can be found.

The linearized stability analysis about the steady-state solution reveals that all real components of eigenvectors are negative, confirming a stable fix point approached by the system. Figure 3.3 A-C illustrate that initially strong oscillations of concentrations occur which are gradually dampened. The slowest decaying oscillation corresponds to the complex eigenvalue with the largest (i.e., the least negative) real component, which is $\lambda = (-7.28 \times 10^{-7} \pm 1.33 \times 10^{-5}i) \text{ s}^{-1}$. The real component of this eigenvalue indicates a half-life $t_{1/2,i}$ of the oscillatory fluctuations about the steady-state solution of approximately 11 days, whereas the imaginary component indicates a time period of the oscillations of 5 days and 11 hours. Figure 3.4 shows the corresponding compound-specific contributions to the complex eigenvector. These contributions define the slowest decaying oscillatory deviations from the steady-state solution. The profiles actually resemble the waves of concentration fluctuations about steady-state moving slowly in the upstream direction towards the end of the simulations.

We repeated the stability analysis for one-dimensional bio-reactive transport without grazer diffusion. Under these conditions, the oscillations of concentrations persist over a much longer time, and simulation times had to be increased at least tenfold to achieve quasi steady-state. However, the steady-state, now resembling the analytical expressions even better, was reached nonetheless. This behavior was also reflected by the linearized stability analysis about the steady-state solution. All real components of the eigenvalues were negative, and

the complex eigenvalue with the largest real component indicated a half-life of the oscillations about ten times larger than in the reference case, whereas the frequency and eigenvector patterns were rather similar. These findings can be explained by grazer diffusion smoothing sharp gradients of the grazer concentration which dampens the oscillations of all components by feedbacks between the different trophic levels.

3.4 Conclusions

In this study, we have presented a one-dimensional bio-reactive transport model that accounts for substrate-bacteria-grazer interactions using parameters accumulated in a literature survey. One of the key results of this study pertains to the steady-state concentration distribution of the bacteria. The bacterial concentration was found to remain constant throughout a certain length of the model domain while the steady-state concentration of the grazers, and particularly the length over which bacteria and grazers can be found, are positively linked to the substrate inflow. While the inflowing substrate will be consumed by the bacteria, the resulting growth of the bacteria population will eventually be balanced by higher concentration of the grazers. After a time period of oscillatory concentrations, the duration of which is strongly influenced by substrate and grazer diffusion, the ecological community successfully achieves a steady-state with spatially uniform bacteria concentrations. This implies that grazing is a potential explanation for the “maximum biomass” used in reactive transport models, provided that there is enough substrate to sustain bacteria and grazers. Our model results conclude that groundwater ecosystems may rather be top-down than bottom-up controlled. Previous studies also elucidated that grazing exerts a major control on bacterial biomass in oligotrophic ecosystems (Foulquier et al., 2011).

Further studies, in particular experiments, are required in order to confirm our findings. Transport in porous media, and even more so microbial activity, are affected by various environmental factors such as temperature, chemical environment, heterogeneity, properties of cell surfaces, cell motility, size and shape, organism type, and growth phase, among others (Tufenkji, 2007). For some of these components, model expressions exist that may be added

to our model in future studies for a more in-depth view of the dynamic interactions. In the present study, we have presented a simple model in order to understand the elementary functional capacities of a steady-state system and identify its principal controls, without claiming completeness of the system description. Moreover, new methods are needed to improve our capability of measuring microbial activity and interactions. A need also exists for careful observations of long timespan experiments of microbial processes in selected ecosystems in order to assess their quasi steady-state behavior.

4. Anaerobic degradation of particulate organic matter: a bioenergetic approach

4.1 Introduction

To survive, cells need to extract useable energy from their environment. In many subsurface systems, the availability of energy substrates is limited and therefore exert a strong control on the growth and activity of the resident microbial populations. Relatively little research has focused on the allocation of catabolic energy within cells and across different microbial groups in energy-limited environments, such as oligotrophic aquifers or deep-sea sediments (Morita, 1988). In these environments, optimizing catabolic energy use may be critical to microbial survival by suppressing energy spilling reactions (i.e., wasting) and catabolic energy is directed towards anabolic processes (i.e., growth, maintenance, and enzyme production) (Russell and Cook, 1995).

In bioenergetics, catabolic energy yields are calculated without a detailed representation of the biochemical reaction pathways (Demirel and Sandler, 2002). A number of studies have investigated the relationship between catabolic Gibbs energy and microbial growth yields (Roden and Jin, 2011; VanBriesen, 2002). However, growth yields have experimentally been obtained in the laboratory mostly under conditions that favor rapid growth and high metabolic rates (Hoehler and Jørgensen, 2013). Reported empirical relationships between growth yields and Gibbs energy tend to work well for higher-energy yielding catabolic reactions (e.g., aerobic respiration and denitrification), while considerable deviations between predicted and observed growth yields are found for lower-energy yielding pathways (e.g., sulfate respiration and methanogenesis) (Roden and Jin, 2011). Consequently, the applicability of the existing relationships to natural energy-limited environments remains an open question.

In contrast to most laboratory culture studies, microbial growth in natural, oligotrophic aquifers is slow. For example, Phelps et al. (1994) report bacterial doubling times of decades to centuries for an ultra-oligotrophic aquifer. In these environments, one expects microorganisms to devote a majority their catabolic energy production to non-growth functions, including cellular maintenance processes. The maintenance energy (ME) demand is the minimum rate of catabolic energy production needed to ensure survival of the cell (Hoehler, 2004). It includes processes such as DNA repair and osmoregulation. Quantification of ME requirements is a controversial topic, with values varying significantly depending on environmental conditions and measurement methods (Hoehler, 2004; Morita, 1988; Van Bodegom, 2007). Very few studies have addressed the allocation of energy in microbial communities inhabiting oligotrophic systems (Morita, 1988; Van Walsum and Lynd, 1998).

An additional, often over-looked, energy sink in the microbial energy budget is the synthesis and exudation of extracellular hydrolytic enzymes (HE) that initiate the breakdown of macromolecular particulate organic matter (POM). In many subsurface environments, POM is the primary source of energy substrates sustaining microbial communities. We may thus expect subsurface chemoorganotrophic microorganisms to invest a significant portion of their catabolic energy production in the release of HE into their surroundings. Given that POM hydrolysis controls the rate at which direct energy substrates are made available to microorganisms, HE production represents a key process in the subsurface carbon cycle (Wilson, 2011).

The Gibbs energy gain from catabolism has previously been invoked as a regulating factor in the transition of microbial cells from the active to dormant state, and vice versa (Stolpovsky et al., 2011). If the total ME demand of a microbial population exceeds the energy that can be extracted from the environment, active cells respond by entering a reversible state of low metabolic activity and, hence, reduced cellular ME. Dormant cells resuscitate when the potential catabolic energy production under given environmental conditions exceeds the total ME requirement. Thus, under changing environmental conditions, we can expect simultaneous adjustments of new biomass growth, HE production, and the proportions of active and dormant states (Morita, 1988).

Van Walsum and Lynd (1998) proposed a model in which cellulolytic fermentative microorganisms distribute their limited supply of adenosine triphosphate (ATP) between biomass growth and the production of hydrolytic enzymes. The model, however, does not allow cells to respond to energy limitation by going dormant, nor the rationale for different cellulose conversion factors, specific enzymes activities, or the Gibbs' energy generated per mole of glucose are made very clear. Payn et al. (2014) combined thermodynamics and kinetics to model aquatic microbial metabolism, taking into account maintenance requirements and biomass growth, but not HE production and the alternation between active and dormant states. Resat et al. (2012) presented a comprehensive kinetic model based on the concept of optimum cellular resource allocation. While this model includes enzyme production, biomass growth, and dormancy, it requires assigning a large set of adjustable, often poorly constrained and site-specific, parameter values.

In the present study, we build further on the concept that in energy-limited environments the activity and population dynamics of chemoorganotrophic communities is largely regulated by the optimization of catabolic energy use. The proposed bioenergetic approach is applied to the degradation of cellulose, a major constituent of organic detritus derived from terrestrial plants. Microorganisms are known to secrete up to 50% of their protein production as hydrolytic enzymes to degrade cellulose (Wilson, 2011). The model explicitly represents the release of HE in the catabolic energy balance of microorganisms. The abundance of HE controls the rate at which monomers are produced outside the cells. All other biochemical processes, taking place at the surface or inside the cells, are included in the ME requirement of the organisms. The model further represents dormancy and resuscitation to the active state as adaptive responses of microorganisms to fluctuations in the catabolic energy supply (Figure 4.1).

To illustrate the model dynamics, we consider a community consisting of two inter-dependent functional groups: cellulolytic fermenting bacteria (CFB) and strictly anaerobic sulfate reducing bacteria (SRB) (Figure 4.2). The latter are representative of respiratory microorganisms typically found in deeper subsurface with depleted highly energetic terminal

electron acceptors (TEAs), such as oxygen and nitrate, have been exhausted. As a general modeling framework, the catabolic energy optimization approach developed in this paper can be extended to more complex, energy-limited microbial communities by the incorporation of additional functional groups.

4.2 Model overview and governing equations

In natural environments, microbial communities typically comprise both active and dormant cells (Stolpovsky et al., 2011). Depending on the environmental conditions, the fraction of dormant biomass ranges from 20 to 80%, with several studies showing up to 95% of soil microorganisms present in the inactive state (Jones and Lennon, 2010; Lennon and Jones, 2011). Only active microorganisms are capable of growth, while only a subset of these microorganisms release HE that hydrolyze POM into monomers that can be taken up and used as electron donors by microorganisms (Wilson, 2011). Hydrolysis is usually considered as the rate limiting step in degradation of complex POM (Eastman and Ferguson, 1981; Rivers and Emert, 1988; Tiehm et al., 1997). The corresponding model conceptualization is illustrated in the Figure 4.1.

4.2.1 POM hydrolysis

We consider a subsurface environment where the degradation of POM is continuously balanced by the re-supply of hydrolyzable POM. Hence, in what follows, we assign a constant POM concentration which eliminates the need for a separate conservation equation for POM. The HE that hydrolyze POM can be free floating or attach to the external cell surface (Wilson, 2008). We assume that binding of HE to POM obeys a Langmuir adsorption isotherm. If, in addition, we assume that the hydrolysis rate scales linearly with the concentration of the enzyme-POC complexes (Vavilin et al., 2008), the extracellular hydrolysis rate r_{hyd} [mol-C/L/d] (molar carbon per day) follows the classical Michaelis-Menten (or Monod) rate law:

$$r_{hyd} = r_{hyd}^{max} \cdot \frac{[HE]}{[HE] + K_{HE}} \quad 4.1$$

where, r_{hyd}^{max} [mol-C/L/d] is the maximum hydrolysis rate, $[HE]$ [mol-C/L] (Molar concentration) denotes the extracellular hydrolytic enzyme concentration, and K_{HE} [mol-C/L] is the half-saturation constant for POM hydrolysis. r_{hyd}^{max} could be expressed as the product of the concentration of bioavailable POM and a maximum specific hydrolysis rate, but the latter two quantities are poorly constrained variables (see chapter 4.3.2 for detail), so that it makes no sense to separate the two factors making up r_{hyd}^{max} .

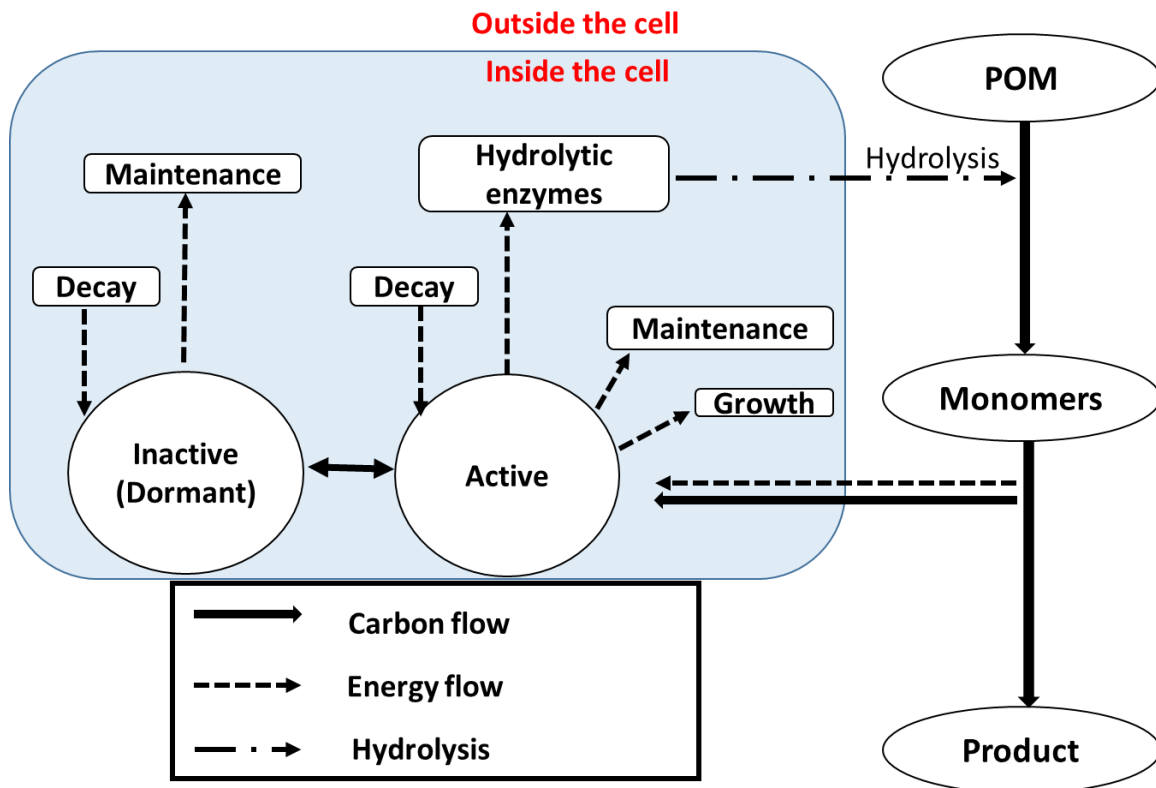


Figure 4.1: Schematic diagram of the energy and carbon flow in a POM fermenter. The circle represents the biomass; ellipses represent organic matter; and rectangles represent the investment or source of energy.

4.2.2 Respiration

Monomers, produced by extracellular hydrolysis and fermentation, are utilized by active cells as direct energy substrates. In the following, we consider the respiration of monomers. The rate of respiration r_{resp} [mol-C/L] is assumed to follow the Monod rate law commonly used to describe substrate utilization by microbial cells:

$$r_{resp} = \mu_{resp}^{max} \cdot X_{ac} \cdot \frac{[S]}{[S]+K_S}, \quad 4.2$$

in which μ_{resp}^{max} [d⁻¹] is the maximum specific respiration rate, X_{ac} [mol-C/L] the active biomass concentration, $[S]$ [mol-C/L] the monomer concentration, and K_S [mol-C/L] the half-saturation constant. Then, the change rate of the monomer concentration is the difference between the hydrolysis and respiration rates:

$$\frac{d[S]}{dt} = r_{hyd} - r_{resp}. \quad 4.3$$

4.2.3 Energy balance of active cells

Energy gained from the respiration of the external monomers is used for cellular maintenance, production of HE, and biomass growth. If the availability of external monomers becomes severely limited, cellular compounds can serve as additional energy substrates. For simplicity, we lump the decrease in biomass that accompanies cell death and the utilization of non-essential energy resources within the cell (i.e., endogenous respiration). The energy balance of the active biomass is then expressed as:

$$-r_{resp} \cdot \Delta G_{resp} = X_{ac} \cdot ME_{ac} + r_{HE} \cdot \Delta G_{HE} + r_{gr} \cdot \Delta G_{gr} + r_{dec}^{ac} \cdot \Delta G_{dec}^{ac}, \quad 4.4$$

where $\Delta G_{resp} < 0$ [kJ/mol-C] is the Gibbs energy of the respiration reaction, $ME_{ac} > 0$ [kJ/mol-C] denotes the maintenance energy rate for active cells, $\Delta G_{HE} > 0$ [kJ/mol-C] is the Gibbs energy of reaction for HE production, $\Delta G_{gr} > 0$ [kJ/mol-C] is the Gibbs energy of biomass synthesis, $\Delta G_{dec}^{ac} < 0$ [kJ/mol-C] denotes the Gibbs energy released during oxidation of cellular components, r_{gr} [mol-C/L/d] is the biomass growth rate, r_{HE} [mol-C/L/d] is the

HE production rate, and r_{dec}^{ac} [mol-C/L/d] is the decay rate for active biomass. All Gibbs energies of reactions in Eq. (4.4) can be calculated using:

$$\Delta G_r = \Delta G^0 + RT \ln Q \quad 4.5$$

where ΔG_r and ΔG^0 [kJ/mol-C] are the actual and standard Gibbs energies of reaction, respectively; T [K] is the absolute temperature, R [kJ/K/mol-C] denotes the universal gas constant, and Q the reaction quotient, that is, the ratio of the product concentrations over the reactant concentrations. The ΔG_r is computed at every time step taking into account the change in reaction quotient.

In the model simulations, the specific maintenance-energy demand (ME_{ac}) for any given microbial group is kept constant. In addition, we assume that, when allocating catabolic energy, cells give priority to fulfilling their maintenance requirements before investing into growth or HE production. If the catabolic energy production is insufficient to supply the maintenance of the entire active biomass, there is neither cell growth nor HE production. Furthermore, biomass decay (cell death plus endogenous respiration) is assumed to make up for the energy shortage. This is expressed mathematically as:

$$\text{If } -r_{resp}\Delta G_{resp} < X_{ac} ME_{ac}$$

then,

$$r_{HE} = 0; \quad r_{gr} = 0;$$

$$r_{dec}^{ac} = -\frac{X_{ac} \cdot ME_{ac} + r_{resp}\Delta G_{resp}}{\Delta G_{dec}^{ac}}. \quad 4.6$$

Conversely, if the catabolic energy supply is greater than the maintenance requirement of the active cell population, excess energy is available for growth and HE production. The release of exoenzymes, including HE, has been shown to respond to changes in environmental conditions, such as temperature, pH, moisture content and dissolved-oxygen concentration (Hall et al., 2014; Sinsabaugh and Follstad Shah, 2012; Sinsabaugh et al., 2008). Microorganisms most likely also adjust the production of exoenzymes to the availability of

the targeted external resources, although the underlying mechanisms remain poorly understood (Lynd et al., 2002; Moorhead et al., 2013; Sinsabaugh and Follstad Shah, 2012). Overall, we expect the biomass-HE-POM system to strive for a balance between maximizing access to the resource and minimizing the wasting of exoenzymes (Wang et al., 2013).

If, for a given availability of POM, the HE concentration is too low, more excess catabolic energy production is diverted into HE production. If the HE concentration is too high, HE production is inhibited and more of the excess energy is invested in biomass growth. Mathematically, this behavior is captured by introducing an inhibition coefficient, K_{HE} [mol-C/L/d] that regulates HE production. Together with the assumption that, in case of excess catabolic energy production, there is no biomass decay, we obtain:

$$\text{If } -r_{resp}\Delta G_{resp} > X_{ac} \cdot ME_{ac}$$

then,

$$r_{dec}^{ac} = 0;$$

$$\frac{r_{HE}\Delta G_{HE}}{r_{HE}\Delta G_{HE} + r_{gr}\Delta G_{gr}} = \frac{K_{HE}}{[HE] + K_{HE}}; \quad 4.7$$

$$r_{gr} = \frac{-r_{resp}\Delta G_{resp} - X_{ac}ME_{ac}}{\Delta G_{gr}} \cdot \frac{[HE]}{[HE] + K_{HE}}; \quad 4.8$$

$$r_{HE} = \frac{-r_{resp}\Delta G_{resp} - X_{ac}ME_{ac}}{\Delta G_{HE}} \cdot \frac{K_{HE}}{[HE] + K_{HE}}. \quad 4.9$$

4.2.4 Dormancy

An important strategy of microorganisms to survive unfavorable conditions is to switch to a dormant state (Stolpovsky et al., 2011). Dormancy creates a microbial seed bank ready to be resuscitated upon the return of more favorable conditions (Lennon and Jones, 2011). In our model, the switching between active and dormant states is controlled by the relative magnitudes of the catabolic energy production and maintenance requirements of the microbial population. When the maintenance energy rate is greater than the catabolic energy production, active cells enter the dormant state. In the opposite case, dormant cells

resuscitate. In the model, this behavior is represented through the following dimensionless switch function:

$$\theta = 0.5 \cdot \left[\tanh \left(\frac{-r_{resp} \Delta G_{resp}}{X_{ac} ME_{ac}} - 1 \right) + 1 \right], \quad 4.10$$

with values ranging between 0 and 1. The deactivation rate r_{deac} [mol-C/L/d] is then calculated as:

$$r_{deac} = k_{deac} \cdot (1 - \theta) \cdot X_{ac}, \quad 4.11$$

in which k_{deac} [1/d] is the deactivation rate coefficient. The activation rate r_{ac} [mol-C/L/d] is obtained from:

$$r_{ac} = k_{ac} \cdot \theta \cdot X_{in}, \quad 4.12$$

where k_{ac} [1/d] is the activation rate coefficient, and X_{in} [mol-C/L/d] is the concentration of the inactive biomass.

Eq. (4.10) yields θ -values approaching zero when the catabolic energy production ($-r_{resp} \Delta G_{resp}$) is small compared to the maintenance energy requirement of the active microbial population ($X_{ac} ME_{ac}$). In contrast, when the catabolic energy gain largely exceeds the maintenance requirement, θ is close to 1, and inactive cells transform into active cells. The use of the switch function θ to simulate the dynamic response of the partitioning between active and dormant cells is similar to that proposed by Stolpovsky et al. (2011), who analyzed data from laboratory experiments in which microorganisms were exposed to a discontinuous supply of substrate and reactivated after periods of starvation.

4.2.5 Energy balance of dormant cells

The dormant microorganisms cannot use external monomeric substrates, grow, or produce HE. However, they still need to invest some energy to maintain their molecular and cellular integrity, albeit at much lower rates than active cells. Dormant cells use endogenous

compounds, such as glycogen or hydroxyalkanoates, as energy substrates, resulting in a reduction of biomass (Lennon and Jones, 2011). The corresponding energy balance is:

$$X_{in} \cdot ME_{in} + r_{dec}^{in} \cdot \Delta G_{dec}^{in} = 0, \quad 4.13$$

resulting in:

$$r_{dec}^{in} = \frac{X_{in} \cdot ME_{in}}{-\Delta G_{dec}^{in}}, \quad 4.14$$

where ME_{in} [kJ/mol-C/d] is the maintenance energy requirement of the inactive biomass, ΔG_{dec}^{in} [kJ/mol-C] is the free energy released by the degradation of cellular constituents, and r_{dec}^{in} is the decay rate of inactive biomass [mol-C/L/d]. Note that, as for the active cells, we use the term decay to include all processes leading to a reduction in the microbial biomass, that is, endogenous respiration, and cell lysis.

4.2.6 Conservation equations for biomass and hydrolytic enzymes

The conservation equations for biomasses of the active and inactive cells, X_{ac} and X_{in} , and the concentration of HE read as:

$$\frac{dX_{ac}}{dt} = r_{gr} + r_{ac} - r_{deac} - r_{dec}^{ac}; \quad 4.15$$

$$\frac{dX_{in}}{dt} = r_{deac} - r_{ac} - r_{dec}^{in}; \quad 4.16$$

$$\frac{d[HE]}{dt} = r_{HE} - k_{dec}^{HE} \cdot [HE], \quad 4.17$$

where k_{dec}^{HE} [d⁻¹] is the rate coefficient for first-order decay of HE. Spatial distributions of the biomasses and HE concentration can, in principle, be computed by coupling Eqs (4.15-4.17) to transport equations, while the response to temporal changes in POM availability could be simulated by adding a conservation equation that accounts for the sources and sinks of POM.

4.3 Anaerobic cellulose degradation

4.3.1 Reaction system

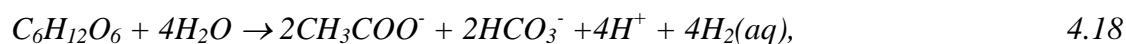
Cellulose is a major refractory compound in terrestrial plant detritus (Béguin and Aubert, 1994; Leschine, 1995; Lynd et al., 2002; Pérez et al., 2002). It is used here as a representative for POM in soil and groundwater environments. Microorganisms use a variety of hydrolytic enzymes to degrade cellulose via a number different pathways, which have yet to be completely characterized (Wilson, 2009, 2011). In anaerobic environments, cellulolytic fermentative microorganisms are able to obtain energy for growth from the degradation of cellulose (Jurtshuk, 1996). Fermentation of glucose, resulting from the hydrolysis of cellulose, produces CO_2 , H_2 , and different combinations of intermediate products such as ethanol, formate, acetate, lactate, and succinate (Leschine, 1995; Lovley and Chapelle, 1995; Christensen et al., 2000). These fermentation products may serve as electron donors to other anaerobic microorganisms. Microbial communities that include cellulolytic fermenters operating in concert with heterotrophic or methanogenic microorganisms can therefore completely oxidize cellulose to CO_2 .

The model microbial community considered here consists of two interacting functional groups: cellulolytic fermenting bacteria (CFB) and sulfate-reducing bacteria (SRB). We assume that only the CFB are able to hydrolyze cellulose, while the SRB depend on the metabolites produced by CFB as their energy source (Wilson, 2008; Wrighton et al., 2014). Synergistic communities of fermenters and SRB have been shown to completely degrade cellulose to carbon dioxide with the production of sulfide, under strictly anaerobic conditions (Leschine, 1995). In the model application, sulfate is used as representative of the terminal electron acceptors (TEAs) found in suboxic and anoxic subsurface sediments. The same approach can be extended to microbial groups using alternative TEAs, such as, ferric iron mineral phases, CO_2 , or organic electron acceptors.

In the model, the dynamics of cellulose degradation by the CFB-SRB community are modulated by the availability of the energy substrates (Eq. 4.2). Hence, we implicitly assume

that the concentration of the TEA or those of essential nutrients (N, P, Fe, micronutrients), as well as other physical-chemical conditions (e.g., pH and temperature) are not limiting the microbial activity. Additional limiting factors can be incorporated in the model by expanding the kinetic expressions presented in chapter 4.2. For example, the dependence of the respiration rate on the TEA abundance can be accounted for by multiplying the right-hand side of Eq.(4.2) by a Monod-type term when calculating the concentration of sulfate (Pallud and Van Cappellen, 2006).

The CFB perform two key tasks: the release of extracellular enzymes, facilitating the hydrolysis of cellulose to glucose, and the fermentation of glucose (Figure 4.2). The mathematical formulations describing the activity of CFB are identical to those developed in chapter 4.2 (Eqs. 4.2-4.17), with glucose as the monomer and replacing the rate of respiration by the rate of fermentation of glucose by the active CFB. In addition, we assume that glucose fermentation produces acetate (CH_3COO^-) and H_2 , intermediates commonly observed during the anaerobic degradation of natural organic matter (Novelli et al., 1988). Acetate is considered to be one of the main carbon and energy substrates fueling respiration in anaerobic sediments (Roden, 2008). Many organic compounds, such as ethanol, lactate, propionate and butyrate, produced as by-products of fermentation processes usually transform into acetate and H_2 before complete oxidation to CO_2 (Leschine, 1995; Lovley and Chapelle, 1995). Hence, the following simplified reaction is used to represent glucose fermentation:



Natural populations of SRB utilize H_2 and a variety of small organic compounds as energy substrates (Plugge et al., 2011). In the model, the latter are collectively represented by acetate. The corresponding reactions are then:



Sulfide, produced by the reduction of sulfate, is assumed to react rapidly with iron containing mineral phases to form insoluble ferrous iron sulfides (Rickard and Luther, 1997), hence avoiding the accumulation of free sulfide to toxic levels (Reis et al., 1992). Similarly, we assume that H_2 concentrations remain low and constant because H_2 produced by fermentation is transferred directly to the H_2 consuming SRB (Novelli et al., 1988). Consequently, losses of H_2S and H_2 to the gas phase are considered to be negligible. By removing H_2 and acetate, the SRB help maintain thermodynamically favorable conditions for the CFB.

According to the stoichiometry of the glucose fermentation reaction (Eq. 4.18), 2/3 of the carbon from glucose goes to acetate and 1/3 to carbon dioxide, while 2/3 moles of H_2 are formed per mole glucose carbon consumed. The conservation equations for acetate and H_2 can then be written as:

$$\frac{d[Ac]}{dt} = \frac{2}{3}r_{ferm} - r_{Ac}, \quad 4.21$$

$$\frac{d[H]}{dt} = \frac{2}{3}r_{ferm} - r_H, \quad 4.22$$

where $[Ac]$ [mol-C/L/d] and $[H]$ [mol-C/L] are the concentrations of acetate and H_2 , r_{ferm} [M/d] is the rate of fermentation (which replaces the respiration rate r_{resp} in Eq. 4.2), and r_{Ac} [mol-C/L/d] and r_H [mol/L/d] are the rates of acetate and H_2 consumption, respectively.

The rates of acetate and hydrogen consumption are calculated by using acetate and H_2 as the substrates and the active SRB biomass in Eq. 4.2. Sulfate is assumed to be present in non-limiting constant concentrations. The equations of chapter 4.2 are applied to the SRB with the only difference that the SRB do not produce HE. Thus, any catabolic energy in excess of the maintenance energy requirement can be invested to growth.

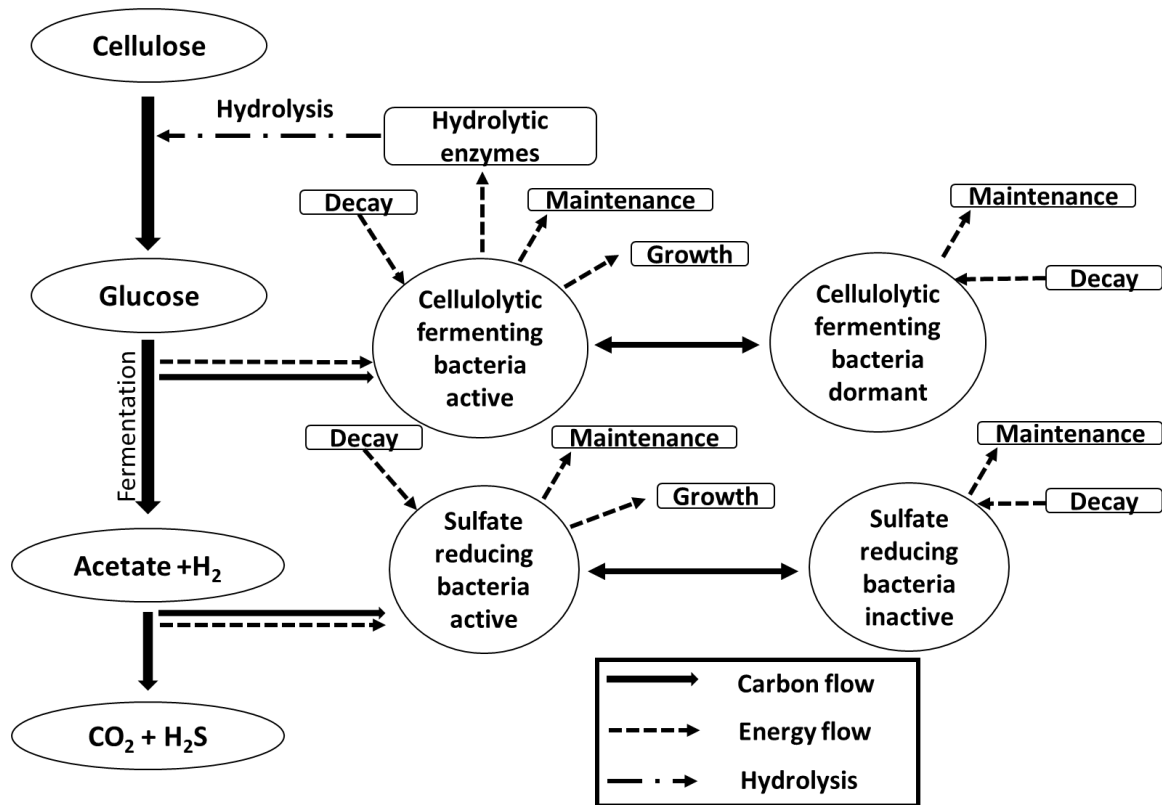


Figure 4.2: Community dynamics of cellulolytic fermenting microorganisms and sulfate-reducing bacteria for complete cellulose degradation in an anaerobic environment.

4.3.2 Parameter values

The parameter values used in the simulations are given in Table 4.1. They are intended to be representative of oligotrophic subsurface environments, although for most of the parameters, variations can be expected from one site to another. Concentration units are expressed per unit of total volume of the porous medium, that is, adding the volumes solid and aqueous phases.

A key parameter controlling the overall POM degradation dynamics is the maximum cellulose hydrolysis rate, r_{hyd}^{max} . Previous studies report a wide range of hydrolysis rates depending on the source of cellulose, soil types, the specific microorganisms and hydrolytic enzymes etc. involved (Bezerra and Dias, 2004; Small et al., 2008). Rate coefficients of POM hydrolysis range widely between 0.2 and 2×10^{-5} per day depending on various

environmental conditions (Roden and Wetzel, 2002; Roden, 2008; Rotter et al., 2008). Additionally, POM concentration also varies widely (Carter et al., 2003; Figueiredo et al., 2010; Handayani et al., 2010; Peter et al., 2012; Roden, 2008; Whitbread, 1995). Even though it is possible to accurately quantify POM concentrations, its bioavailable fraction remains uncertain (Morita, 1988). For example, the cellulose fraction in POM varies significantly about the average value of 26.7% (Wang et al., 2013). Due to the combined uncertainties of bioavailable POM and its maximum hydrolysis rate coefficients, we have introduced the maximum hydrolysis r_{hyd}^{max} which is identical to the turnover rate of carbon from POM to monomers. For this study, an average value is taken from various literature studies (Roden and Wetzel, 2002; Canfield et al. 2005; Roden, 2008; Rotter et al., 2008). The value of 10^{-5} mol-C/L for the half-saturation constant of cellulose hydrolysis, K_{HE} , is largely arbitrary. As Resat et al. (2012) showed in their cellulose degradation simulations, the overall model outcomes are relatively insensitive to the chosen value of K_{HE} , unless extreme values are chosen which also holds true in our simulation.

Other sensitive model parameters include the maintenance energy requirements for active bacteria (ME_{ac}) and the Gibbs energies for biomass growth (ΔG_{gr}) for the different microbial groups. The ME_{ac} -value sets the catabolic energy production threshold that needs to be exceeded to sustain biomass growth. This ME can vary over 5-6 orders of magnitude depending upon the environmental conditions (Hoehler, 2004). For the active SRB and CFB, we use the temperature-dependent empirical formula for anaerobic microorganisms proposed by Tjihuis et al. (1993). As a typical groundwater temperature for Central Europe, we use 10°C. The dormant SRB and CFB are assigned the same value as that derived experimentally for an agricultural soil at 15°C (Anderson and Domsch, 1985). The Gibbs energy of dissipation (i.e. energy for growth) of the microorganisms is calculated by the empirical expression of Heijnen and Dijken (1992) whereby glucose and acetate are used as the carbon sources for the CFB and SRB, respectively.

The initial concentrations are listed in Table 4.2. They were chosen based on concentration values found in natural aquifers, namely of hydrogen sulfide (Detmers et al., 2001); sulfate

(Lovley and Chapelle, 1995); acetate, glucose and hydrogen (Lovley and Chapelle, 1995; Lovley and Phillips, 1989; Novelli et al., 1988). Values of ΔG_{gr} are obtained from the empirical expression of Heijnen and Dijken (1992) with glucose and acetate as carbon sources for the CFB and SRB, respectively. In the simulations shown below, the Gibbs energies of reaction are calculated at each time step by Eq. 4.5 to account for their concentration dependence. As simplifications we assume that the decay of dormant and active biomasses yield the same Gibbs energies, and apply the same activation and deactivation rate coefficients to the different bacterial groups.

4.4 Simulation results and discussion

4.4.1 Model simulation

The system of ordinary differential equations using all concentrations as dynamic state variables was implemented as Matlab function and solved with the Matlab-internal solver `ode15s`. The simulation was run for 600 days until steady-state was reached. During the initial days of simulation, it can be observed that the system undergoes a sudden change in concentrations of electron-donors, hydrolytic enzymes, active and dormant bacteria (Figure 4.3). This indicates that the initial concentrations used in the model simulations deviate from the steady-state approached by the system. Unless extreme initial conditions are considered, the system approaches the same steady-state concentrations regardless of the initial conditions. Figure 4.4 shows simulated time series of energy fluxes of the cellulolytic fermenting bacteria (CFB) and the sulfate-reducing bacteria (SRB) per unit carbon biomass, respectively. Energy generation and distribution are calculated as energy turnover per time per mol-C biomass. Figure 4.5 illustrates the allocation of energy in the form of a pie-chart. Figure 4.6 shows the time series of yield of mol-C biomass per joule gained.

Table 4.1: Parameter values used in the simulations

Parameter	Description	Value	Units	Reference
r_{hyd}^{max}	Maximum hydrolysis rate	1.12×10^{-5}	[mol-C/L/d]	Calculated based on Roden and Wetzel, 2002; Canfield et al. 2005; Roden, 2008; Rotter et al., 2008
μ_{Ac}^{max}	Maximum specific acetate utilization rate by sulfate-reducing bacteria	29.28	[d ⁻¹]	Calculated based on Scheibe et al. (2009)
μ_H^{max}	Maximum specific hydrogen utilization rate by sulfate-reducing bacteria	7.675	[d ⁻¹]	(Khosrovi et al., 1971)
μ_{ferm}^{max}	Maximum specific fermentation rate	5.4	[d ⁻¹]	Calculated based on Scheibe et al. (2009)
$ME_{ac,SRB}$	Maintenance-energy requirement for active sulfate-reducing bacteria	17.76	[kJ/mol-C biomass/d]	(Tijhuis et al. 1993)
$ME_{in,SRB}$	Maintenance-energy requirement for inactive sulfate-reducing bacteria	0.312	[kJ/mol-C biomass/d]	(Anderson and Domsch 1985)
$ME_{in,ferm}$	Maintenance-energy requirement for inactive cellulolytic fermenters	0.312	[kJ/mol-C biomass/d]	(Anderson and Domsch 1985)
$ME_{ac,ferm}$	Maintenance-energy requirement for active cellulolytic fermenters	17.76	[kJ/mol-C biomass/d]	(Tijhuis et al. 1993)
$\Delta G_{gr,SRB}$	Gibbs energy required to form sulfate-reducing bacteria	426	[kJ/mol-C biomass]	Calculated based on the empirical formula using acetate as the C-source (Heijnen and Dijken, 1992)

- Microbial Dynamics in Natural Aquifers -

$\Delta G_{dec,ferm}^{ac}$	Gibbs energy gained from decaying biomass of active fermenters	67	[kJ/mol-C biomass]	(Heijnen and Dijken, 1992)
$\Delta G_{dec,ferm}^{in}$	Gibbs energy gained from decaying biomass of dormant fermenters	67	[kJ/mol-C biomass]	(Heijnen and Dijken, 1992)
$\Delta G_{dec,SRB}^{ac}$	Gibbs energy gained from decaying biomass of active sulfate-reducing bacteria	67	[kJ/mol-C biomass]	(Heijnen and Dijken, 1992)
$\Delta G_{dec,SRB}^{in}$	Gibbs energy gained from decaying biomass of dormant sulfate-reducing bacteria	67	[kJ/mol-C biomass]	(Heijnen and Dijken, 1992)
$\Delta G_{gr,ferm}$	Gibbs energy required to form fermenters	211	[kJ/mol-C biomass]	Calculated based on Heijnen and Dijken (1992)
ΔG_{HE}	Gibbs energy required to form hydrolytic enzymes	50.16	[kJ/mol-C biomass]	Assumed based on Karp (2009)
k_{dec}^{HE}	Decay rate coefficient of hydrolytic enzymes	0.005	[d ⁻¹]	Calculated based on Resat et al. (2012)
K_{HE}	Michaelis-Menten/Monod constant for concentration of hydrolytic enzymes	1×10^{-5}	[mol-C/L]	Back calculated
K_{Ac}	Michaelis-Menten/Monod constant for acetate in sulfate reduction	2×10^{-3}	[mol-C/L]	(Roden, 2008) and reference there within
K_H	Michaelis-Menten/Monod constant for H ₂ in sulfate reduction	1×10^{-5}	[mol-C/L]	(Dale et al., 2006)
K_S	Michaelis-Menten/Monod constant for glucose in fermentation	1.33×10^{-4}	[mol-C/L]	(Kleman and Strohl, 1994)
$k_{deac,ferm}$	Deactivation rate coefficient of fermenters	1.2	[d ⁻¹]	(Stolpovsky et al., 2011)
$k_{deac,SRB}$	Deactivation rate coefficient of sulfate-reducing bacteria	1.2	[d ⁻¹]	(Stolpovsky et al., 2011)
$k_{act,ferm}$	Activation rate coefficient of fermenters	1.2	[d ⁻¹]	(Stolpovsky et al., 2011)

- Microbial Dynamics in Natural Aquifers -

$k_{act,SRB}$	Activation rate coefficient of sulfate-reducing bacteria	1.2	[d ⁻¹]	(Stolpovsky et al., 2011)
---------------	--	-----	--------------------	---------------------------

Table 4.2: Initial concentration used in the simulation

Description	Value	Units
Acetate	1×10^{-5}	[mol-C/L]
Glucose	1×10^{-7}	[mol-C/L]
Hydrogen	1×10^{-9}	[mol/L]
Active cellulolytic fermenting bacteria	1×10^{-6}	[mol-C/L]
Dormant cellulolytic fermenting bacteria	1×10^{-6}	[mol-C/L]
Active sulfate reducer	1×10^{-6}	[mol-C/L]
Dormant sulfate reducer	1×10^{-6}	[mol-C/L]
Temperature	283.15	[K]
Gibbs energy generated by reaction of hydrogen and sulfate at 10°C	-75.02	[kJ/mol-C]
Gibbs energy generated by reaction of acetate and sulfate at 10°C	-84.79	[kJ/mol-C]
Gibbs energy by fermentation of glucose into acetate and hydrogen at 10°C	-39.22	[kJ/mol-C]
Hydrogen sulfide	5.73×10^{-6}	[mol/L] or [M]
Bicarbonate	3.44×10^{-3}	[mol/L] or [M]
H ⁺	1×10^{-7}	[mol/L] or [M]
Sulfate	4.68×10^{-5}	[mol/L] or [M]

4.4.1.1 Initial lag and growth phase

Initial glucose and acetate/hydrogen concentrations are too low to provide the CFB and SRB with sufficient energy for growth. Therefore, at the beginning of the simulation (0 – 2 days), the maintenance-energy requirement for both types of active bacteria is higher than the catabolic energy gained during either fermentation or sulfate reduction and no growth is observed (inset of Figure 4.4). Consequently, the CFB and SRB compensate for the energy gap by using endogenous reserves and the concentration of active biomass decreases while dormant biomass increases (Figure 4.3 C and D). The unfavorable initial conditions (0 – 2 days) also inhibit hydrolytic enzyme production, leading to a decrease in HE concentration due to decay. However, the concentration of hydrolytic enzymes is sufficient to induce immediate POM hydrolysis thereby resulting in a rapid increase in glucose concentration within days followed by an increase in the hydrogen and acetate concentrations, respectively (inset of Figure 4.3 A). The increased concentrations of all dissolved electron donors, result in an increased catabolic energy gain by both types of bacteria (Figure 4.4). After two days, the energy gained from the fermentation of glucose exceeds the maintenance-energy requirement of the CFB, which start growing rapidly and producing hydrolytic enzymes. The SRB take four days longer until growth begins (Figure 4.6). Consequently, the dormant CFB and SRB decrease in the beginning since they start to resuscitate in response to the advantageous conditions.

The same behavior can be observed in the energy turnover shown in Figure 4.4. The increased concentrations of all electron donors, results in the increased catabolic energy gain of both types of bacteria. Within 15 days, the energy gained from the fermentation of glucose far exceeds the maintenance-energy requirement of the CFB, which start growing rapidly. The SRB follow the same pattern for growth. The yield (molar carbon per unit joule) is very high during this period which last two and three weeks, respectively, from the first day of simulation. A high fraction of energy is spent on HE production and growth during this period by CFB compared to the rest of the simulation period (inset of Figure 4.4). The intricate interplay between abundance and activity of the bacteria and solute concentrations leads to non-monotonic concentration time

series, as observed in a peak of dissolved electron donors and hydrolytic enzymes (Figure 4.3 A and B).

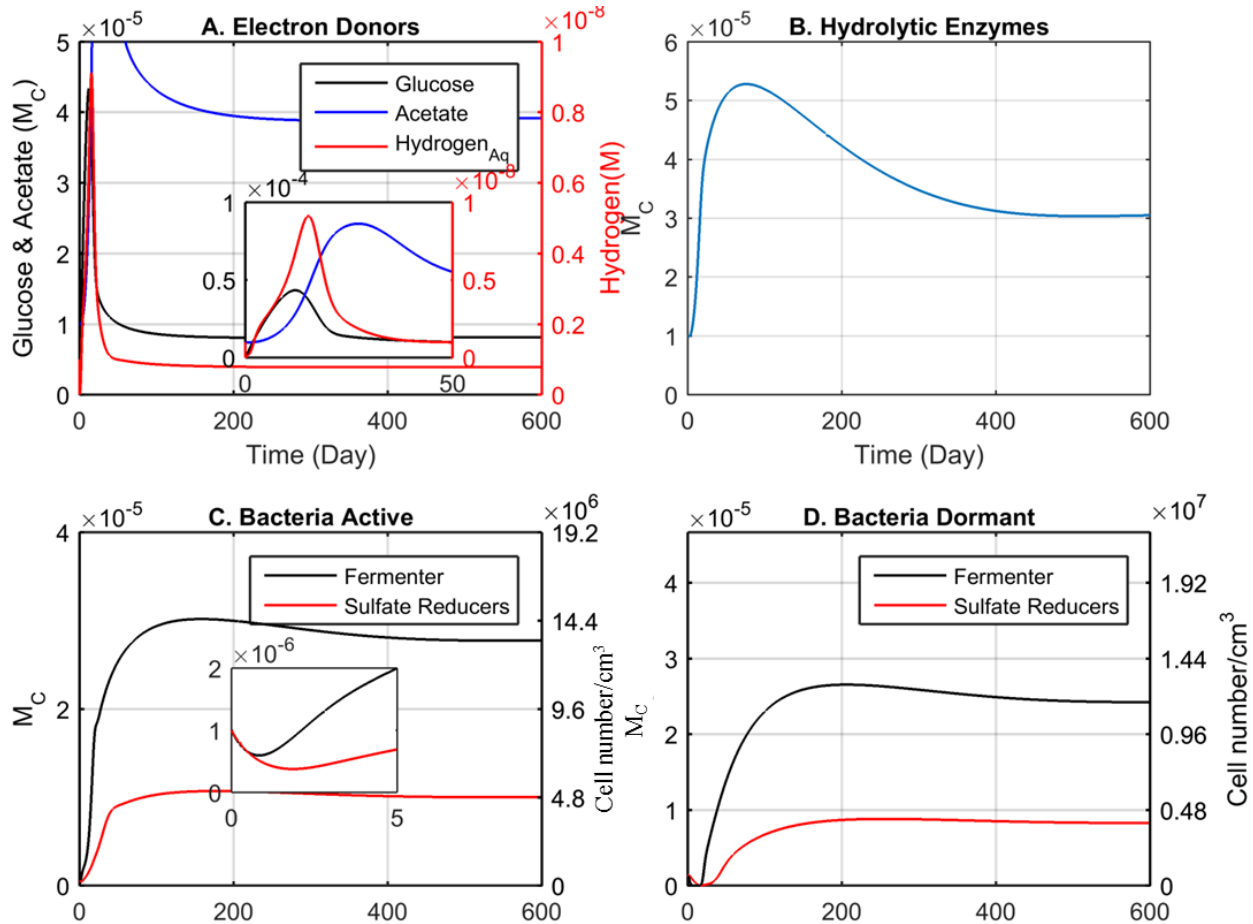


Figure 4.3: Simulated time series of concentrations. A: electron-donors, B: hydrolytic enzymes, C: active bacteria, D: dormant bacteria. All concentrations are in mass carbon per volume except hydrogen which is in mass per unit volume (that is, moles). The inset figures in 'A' and 'C' show the first 100 and 5 days of simulation respectively. Parameters are according to Table 4.1 and Table 4.2.

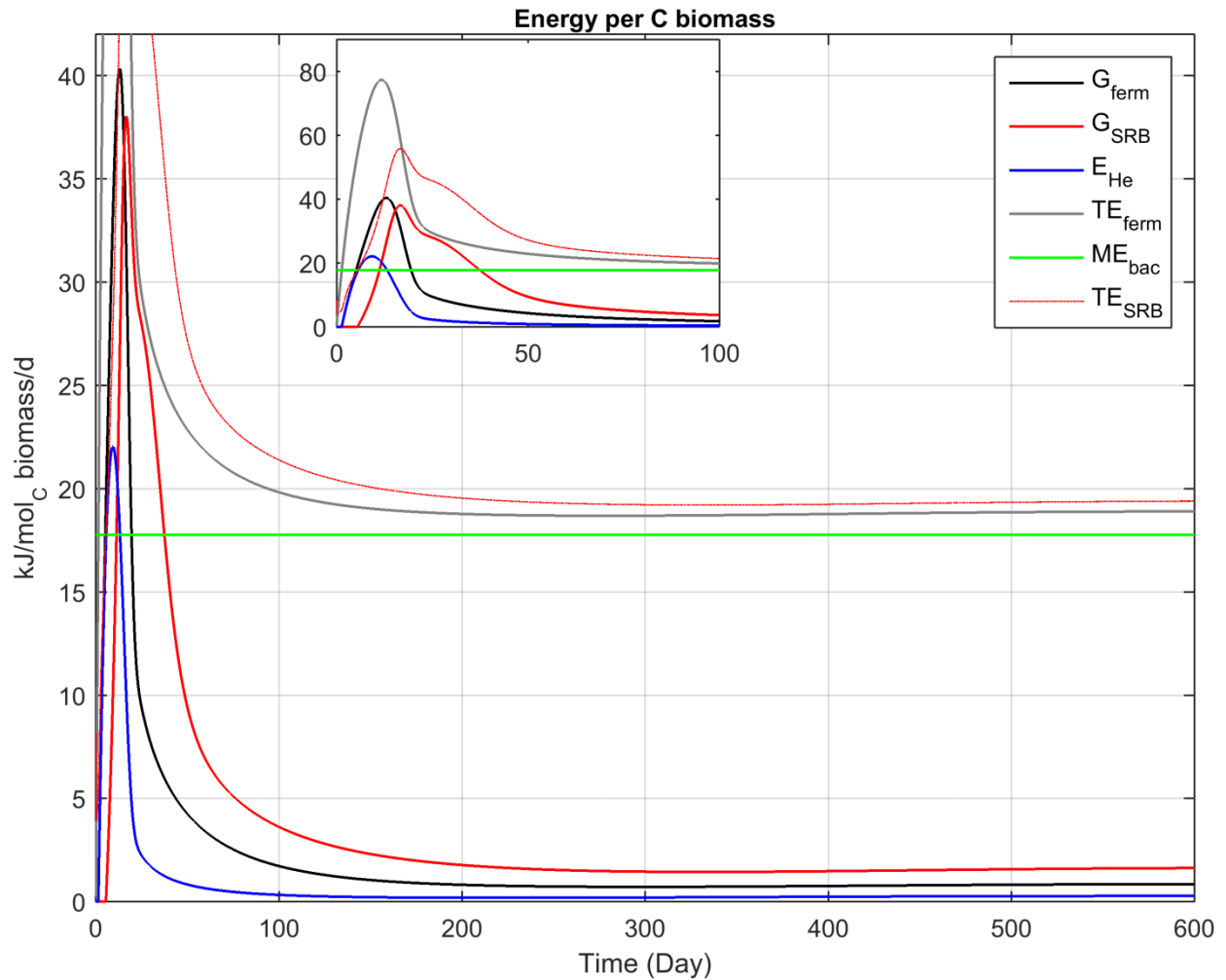


Figure 4.4: Simulated energy generation and consumption per unit carbon in the biomass. The inset figure shows the first 100 days of simulation. For cellulolytic fermenting bacteria and sulfate-reducing bacteria; total energy generated by represented by TE_{ferm} and TE_{SRB} , energy consumed by growth is G_{ferm} and G_{SRB} and energy invest on extracellular hydrolytic enzymes is E_{He} for both figures. Maintenance energy for both cellulolytic fermenting bacteria and sulfate-reducing bacteria are displayed as ME_{bac} . Parameters are according to Table 4.1 and Table 4.2.

4.4.1.2 Approach of steady-state

Within three weeks, glucose and hydrogen concentrations start to decrease because they are used by the larger bacterial population while acetate concentration starts decreasing after five weeks.

The difference between the total energy (TE) and maintenance energy start to decline with increased bacterial concentration and low electron-donor concentration (Figure 4.4) but remarkably both active bacterial concentrations still continue to increase. However, the rate of growth slows down due to the declining energy difference. After approximately 150 days, the difference between total energy supply and maintenance-energy demand becomes practically constant (Figure 4.4). From this moment onward, both bacterial concentrations begin to decrease. Finally, the steady-state concentrations of active and dormant CFB are reached at 2.77×10^{-5} mol-C/L (1.33×10^7 cells/cm³) and 2.42×10^{-5} mol-C/L (1.16×10^7 cells/cm³), respectively. Thus, approximately half of the CFB is active in the steady-state. The SRB follows almost the same growth and decay pattern as CFB with some delay. Under steady-state conditions, the growth of active biomass is balanced by deactivation, and the gain of dormant biomass is balanced by the maintenance-energy requirement of the dormant biomass. The active and dormant SRB plateaus at concentrations of 9.9×10^{-6} mol-C/L (4.75×10^6 cells/cm³) and 8.27×10^{-6} mol-C/L (3.96×10^6 cells/cm³), respectively. Similarly to the fermenters, somewhat more half the sulfate reducers in the steady-state are active. The percentage of active biomass is close to values found in both marine and fresh-water environments (Lennon and Jones, 2011). The total biomass of microorganisms in both physiological states amounts to 7.02×10^{-5} mol-C/L (3.37×10^7 cells/cm³). This is in the high range of the bacterial abundance found in typical porous aquifers (Griebler and Lueders, 2009). The bacterial concentration is found in the range of 10^5 to 10^8 cells/cm³. This may be explained by neglecting natural predators or bacteriophages, in the aquifer which may control the steady-state concentration of the bacteria (Bajracharya et al., 2014).

After three weeks, the difference between total energy generated and ME decreases. As a consequence, less energy can be allocated to growth and hydrolytic enzymes. The concentration of HE steadily increases for almost 80 days, peaks, and decreases to a steady-state value of 3.05×10^{-5} mol-C/L after approximately 550 days. The concentration of glucose eventually plateaus at the steady-state value of 8.16×10^{-6} mol-C/L. The interplay of the two bacteria leads to steady-state concentrations of acetate and dissolved molecular hydrogen of 3.92×10^{-5} mol-C/L and 7.91×10^{-10} M, respectively. These electron-donor concentrations show significant spatiotemporal variation in different natural environments. Our simulation results of hydrogen and acetate concentration lies in the range observed in the literature (Dale et al., 2006; Hoehler et

al., 1998; Lovley and Chapelle, 1995). A similar concentration of glucose has also been observed in anaerobic and marine sediments (Lovley and Phillips, 1989; Dale et al., 2006). We thus consider the simulation results plausible.

The total catabolic energy gained by active CFB at steady-state is 18.9 kJ/mol-C biomass/d (Figure 4.4). According to the simulation, the fermenters invest 94% of the energy produced in maintenance, 5% in growth (which eventually ends up in maintenance of dormant biomass), and the remaining 1% in the production of hydrolytic enzymes (Figure 4.5). The catabolic energy gained by active SRB at steady state is 19.4×10^{-3} kJ/mol-C biomass/d. The SRB spend 92% on the maintenance of active biomass; the remaining 8% is invested in growth, but is funneled to the maintenance of the dormant biomass. These results are consistent with those observed in energy-oligotrophic environments (Del Giorgio and Cole, 1998; Russell, 1986); whereby the bacterial growth efficiency has been reported as low as 1% (Del Giorgio and Cole, 1998). The fastest doubling time for CRB and SRB is approximately 13 and 17 days in our simulation, whereas literature values vary from minutes to millennia (Phelps et al., 1994). Griebler and Lueders, (2009) report a typical doubling time in the range of 1-320 days for natural groundwater. A study on geobacter species in the subsurface mentions a doubling time of approximately 15 days (Mailloux and Fuller, 2003). We conclude that our results are reasonable.

4.4.2 Accounting for bioenergetics

The microbial growth yield varies according to the energy generated from the environment (Heijnen and Dijken, 1992). Most kinetic models use constant growth yields for the conversion of substrates to biomass. By contrast, Roden and Jin, (2011) assumed a linear relationship between bacterial growth yields and the Gibbs energy generated, concluding that the growth yield should be modeled dynamically based on the Gibbs energy generated rather than taken as static value from literature. Our model implicitly results in a dynamic growth yield because the catabolic Gibbs energy gained by the bacteria changes over the course of the simulation. Figure 4.6 shows the simulated growth yield per unit energy generated as function of time. To the best of our knowledge, this is the first model to illustrate a dynamic growth yield based on bioenergetics. The total-energy gain of the fermenters is higher than that of the sulfate reducers

during the initial 20 days of simulation (Figure 4.4). However, this energy is divided into producing hydrolytic enzymes and growth. Due to this division, the yield of SRB becomes higher than CFB on the 7th day (Figure 4.6). At steady-state, the yield of CFB and SRB is 0.2×10^{-3} and 0.22×10^{-3} mol-C/J respectively.

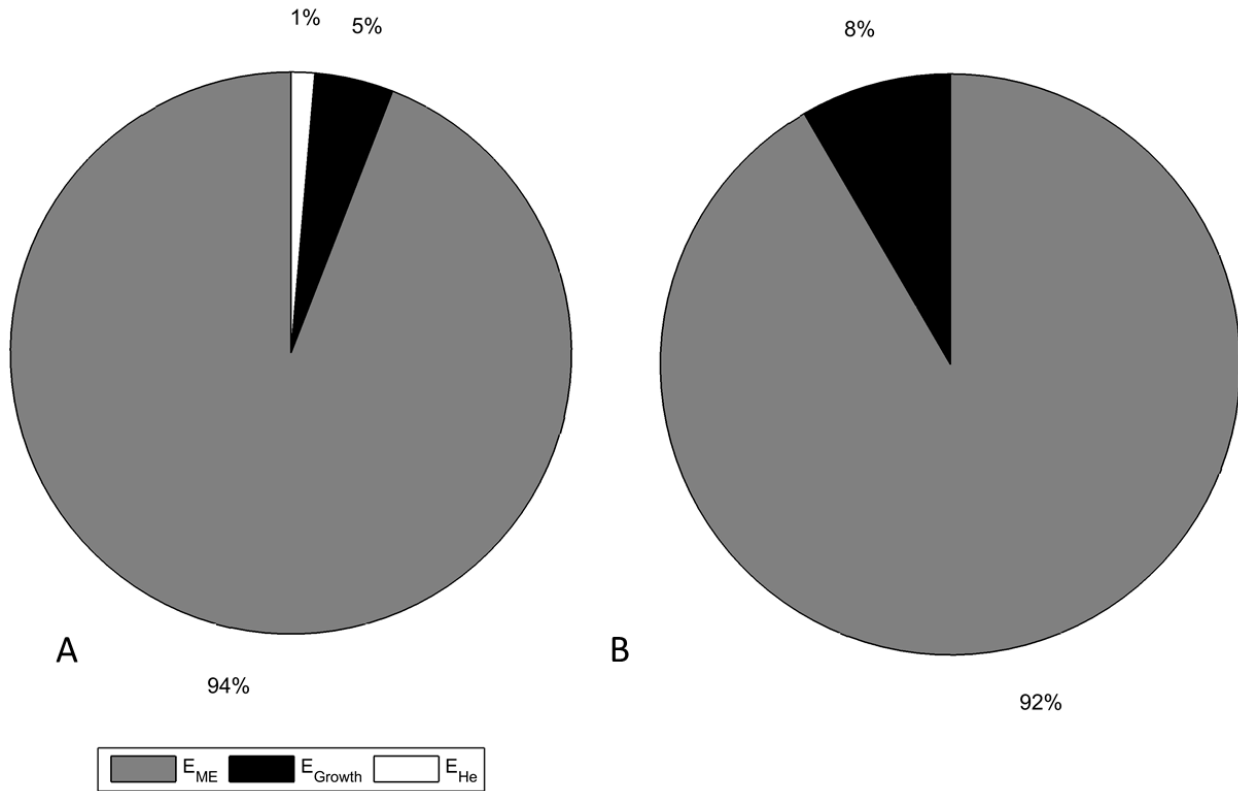


Figure 4.5: Energy distribution at steady-state conditions A: Cellulolytic fermenting bacteria, B: Sulfate reducing bacteria.

It is also noteworthy that the energy per unit carbon biomass of the SRB is higher than that of the CFB under steady-state conditions (Figure 4.4). Despite larger energy generation, the steady-state yield (Figure 4.6) and concentration of the SRB (Figure 4.4) is smaller than those of the CFB (0.2 and 0.22 C mol/J respectively). This is due to the fact that more energy is necessary to form SRB than CFB.

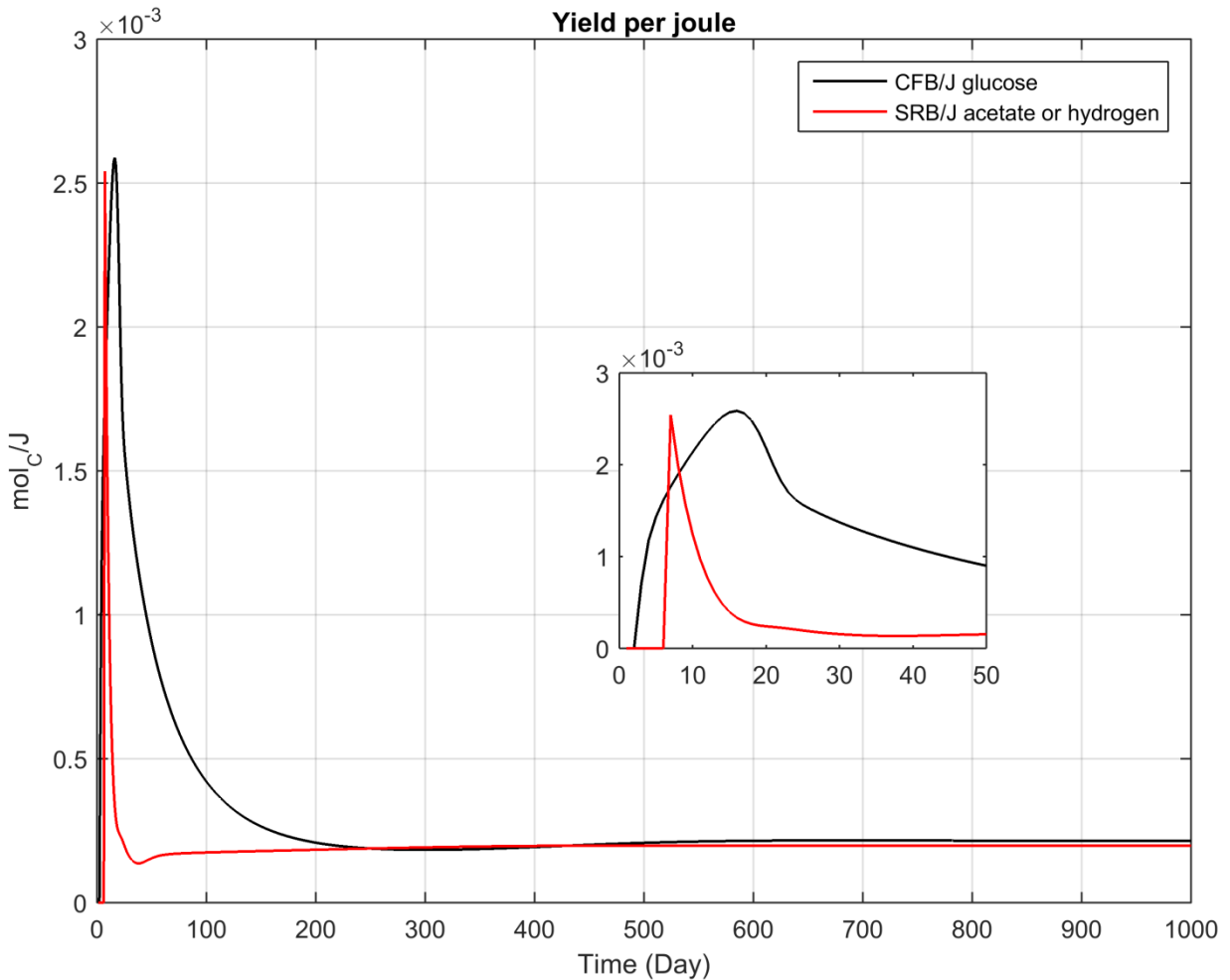


Figure 4.6: Bacterial yield (in mole-carbon per unit joule gained for acetate, glucose, and hydrogen)

In order to illustrate the advantages accounting for dynamic energy production, we run various simulations of the proposed model with identical parameters (as described in Table 4.1 and Table 4.2), except for the Gibbs energy calculation. We kept the Gibbs energy constant for three different scenarios where energy does not change according to the change of reaction quotient but only with respect to fermentation or respiration rates. These results are compared to our original model. The different scenarios are: (1) concentration-dependent, time-varying Gibbs energy (ΔG_o), which is the full and original model, (2) constant Gibbs energy calculated for the initial concentrations ($\Delta G_r^\circ_{\text{initial}}$), (3) constant standard Gibbs energy at 10° C ($\Delta G_r^\circ_{283K}$), and (4)

constant Gibbs energy at standard condition ($\Delta G_r^\circ_{298K}$). We observe very contrasting results in these simulations. The two models with $\Delta G_r^\circ_{298K}$ and $\Delta G_r^\circ_{283K}$ were unable to sustain any bacterial biomass over long time periods, leading to extinction of the biomasses (Figure 4.7). Only the models with $\Delta G_r^\circ_{initial}$ and ΔG_o reach non-zero steady-state concentrations. The total steady-state bacterial concentration in the proposed model (i.e., scenario 1, ΔG_o) is almost 9.5% lower than the total steady-state bacterial concentration using a constant Gibbs energy calculated for the initial concentrations (i.e., scenario 2, $\Delta G_r^\circ_{initial}$), implying that the energy gain decreases in the course of the experiment due to the change of the reaction quotient Q . The simulations also reveal that the concentrations of glucose, hydrolytic enzymes, and hydrogen differ by 11%, 7%, and 3% respectively in the model with $\Delta G_r^\circ_{initial}$ compared to the proposed model. Moreover, depending upon the initial concentration, the steady-state bacterial concentration in both cases may vary in term of magnitude.

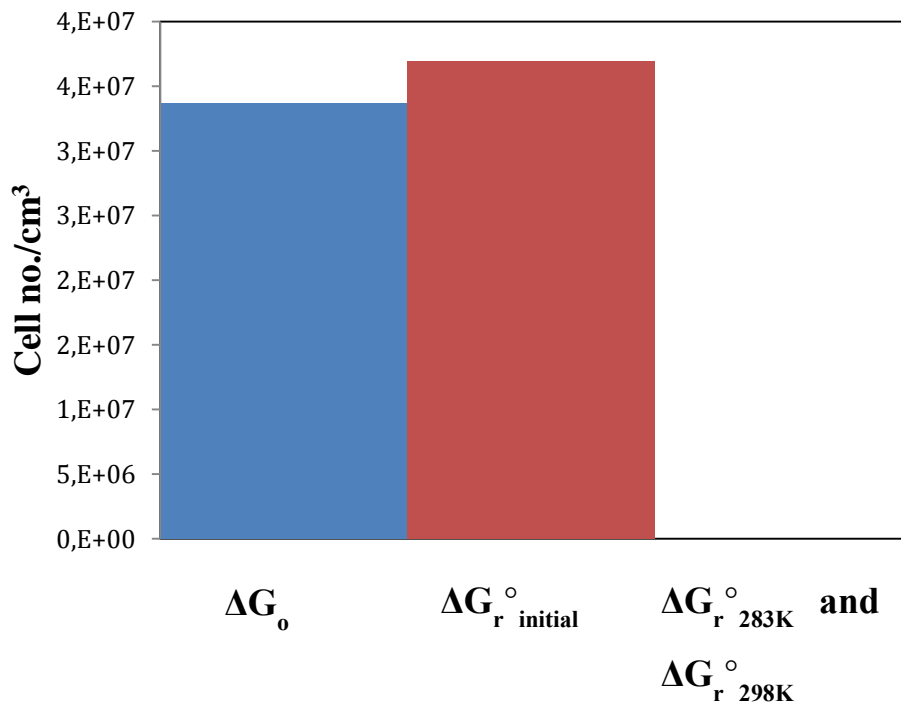


Figure 4.7: Comparison of Bacterial population at constant Gibbs energy with variable Gibbs energy (1) varying Gibbs energy (ΔG_o), (2) constant Gibbs energy calculated at initial concentration ($\Delta G_r^\circ_{initial}$), (3) constant Standard Gibbs energy at 10^0 C ($\Delta G_r^\circ_{283K}$), and (4) constant Gibbs energy at standard condition ($\Delta G_r^\circ_{298K}$).

4.4.3 Sulfate perturbation starting at steady-state

The groundwater is a dynamic system which is influenced by various environmental changes. A simple example of a perturbation is the seasonal variation of groundwater recharge, which can result in fluctuating positions of biogeochemical contrasts. As an example for a biogeochemical perturbation, we consider sudden change of the sulfate concentration from 4.68×10^{-5} M to 4.68×10^{-7} M at day 50 of a simulation that starts at the steady-state evaluated in the previous calculations. Figure 4.8 shows the resulting time series of simulated concentrations. As expected, the drop in sulfate leads to unfavorable condition for the SRB. The active SRB instantaneously start decaying or switch to dormancy (Figure 4.8 C). The dormant SRB quickly increases and then also decays. The total SRB population dies out completely within 150 days of simulation (Figure 4.8 C and D). Simultaneously, the acetate and hydrogen concentrations increase dramatically because they cannot be oxidized by sulfate anymore (Figure 4.8 A). The increased acetate and hydrogen concentrations hinder fermentation, by lowering the catabolic energy gains for CFB. Consecutively, the energy gain is not sufficient for the CFB which then start to decay. The total CFB will eventually die out due to low energy gain from accumulation of fermenting products (Figure 4.8 C and D). As the SRB start to die out, the fermenting product also being to level off. Concurrently, the glucose consumption (inset of Figure 4.8 A) and the HE concentration decrease (Figure 4.8 B). These results demonstrate that the decrease in sulfate, which is the terminal electron acceptor of the SRB only, also affects CRB population through lowering the catabolic energy, thereby affecting the whole ecosystem.

For comparison, we have run the same perturbation of sulfate concentration in the scenarios 2 defined in chapter 4.4.2 (constant Gibbs energy calculated at initial concentration). As before, the total SRB concentration dies out completely within 150 days (Figure 4.9 C and D). In contrast to our conceptual model, the CRB bacteria including HE, fermenting products and glucose concentration are not affected by the change due to decrease in sulfate concentration (Figure 4.9). The model with a static Gibbs energy of the reaction simply lacks the thermodynamic feedback of acetate/hydrogen consumption on fermentation.

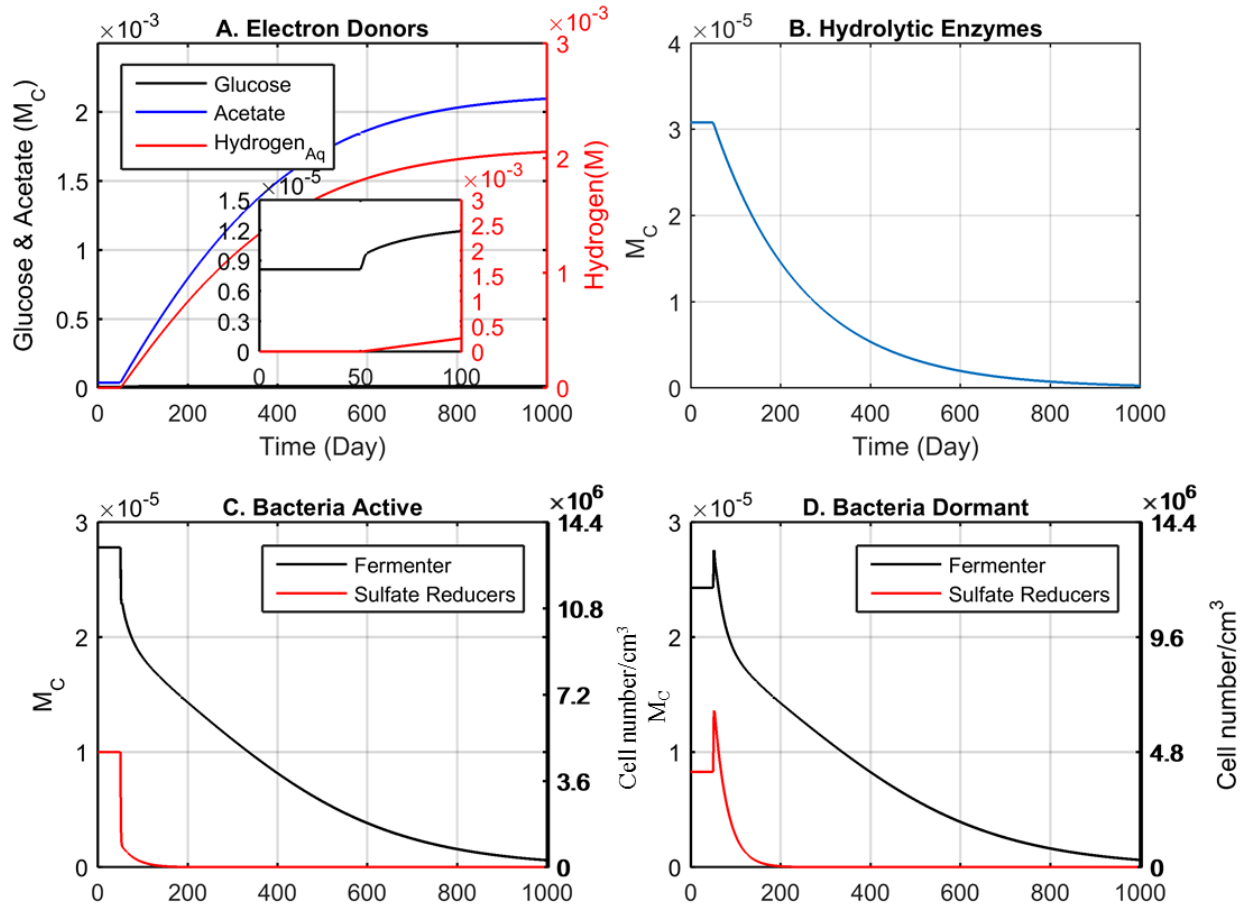


Figure 4.8: Concentration response to a change in sulfate concentration. A: the concentration of electron-donors, B: concentrations of hydrolytic enzymes, C: concentrations of active bacteria, D: concentrations of dormant bacteria. The inset figure in 'A' shows the first 100 days of simulation. All concentrations are in mass carbon per volume of water except hydrogen which is in mass per volume of water.

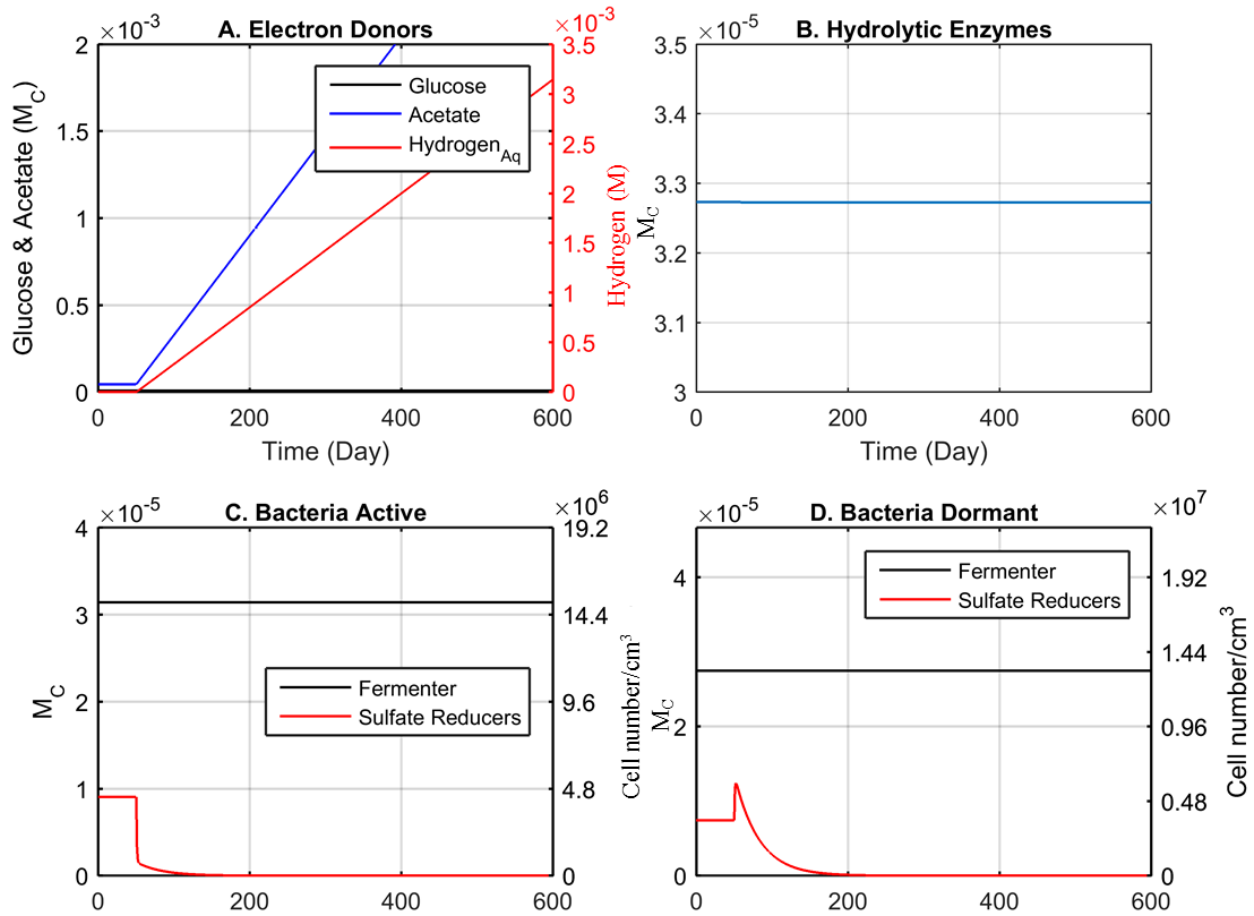


Figure 4.9: Concentration response to a change in sulfate concentration with static Gibbs energy calculated at initial concentration. A: the concentration of electron-donors, B: concentrations of hydrolytic enzymes, C: concentrations of active bacteria, D: concentrations of dormant bacteria. All concentrations are in mass carbon per volume of water except hydrogen which is in mass per volume of water.

4.5 Conclusions and future works

I have presented a bioenergetic framework to model microbial dynamics in energy-limited aquifers based on the distribution of catabolic energy to extracellular hydrolytic enzymes production, maintenance-energy requirement, and biomass growth. This framework forms the basis for a quantitative description of microbial activity under given environmental and thus

energetic conditions. Moreover, this model offers practical advantages over expensive and labor-intensive genomics-based modeling. While bioenergetics cannot explain all mechanistic details of microbial pathways, it can predict what activity is energetically beneficial. We illustrate that energy optimization is a likely driver of microbial behavior, at least under oligotrophic conditions, but we can of course not exclude that some microorganisms may catalyze reactions for which an energetic benefit is not obvious.

I have successfully used our conceptual model to simulate anaerobic cellulose degradation by a mixed culture of cellulolytic fermenting and sulfate-reducing bacteria. One of the main features of the model is the computation of catabolic Gibbs energy at every time step. Importance of a dynamic-based Gibbs energy approach is illustrated and compared with a static Gibbs energy model. As demonstrated, the results vary significantly and may lead to erroneous interpretation unless bioenergetics is properly implemented. The simulation of decreased sulfate concentrations illustrates the utility for modelling to model complex biogeochemical processes. The static model can't capture the change in thermodynamic efficiency that might be brought by perturbation of any component in the system (electron acceptor in our case). These concepts can further be modified to simulate different microbial species, different pathways of particulate-organic-matter degradation, or different activities excerpted by the same organisms considering the Gibbs energy of the considered reactions.

In the particular case of sulfate-perturbation's simulation (Figure 4.8), the increasing fermenting products lower the generated catabolic energy. When the energy gained is not sufficient for the CFB. This results in dying of CFB. The fermenting products start to plateau only when the CFB decrease significantly. However, if the concentrations of fermenting products increase tremendously due to external influences; this could lead to positive catabolic Gibbs energy. This should halt the fermentation rate at once. However, in the proposed model, the fermentation reaction will continue. Consecutively, the bacteria will go dormant and will die out slowly. An additional thermodynamic constraint (F_T) as mentioned in Eq. 2.3 (Chapter 2.2.4) will improve the model to portray these scenarios. Taking account of the thermodynamic term during the evaluation reaction rate (before the distribution of energy) will hinder the respiration/fermentation rate more quickly and the product accumulation will level off as soon as the Gibbs energy becomes zero or reached critical threshold energy (Jin and Bethke, 2005;

LaRowe et al., 2012). Several studies have been dedicated to find the accurate thermodynamic term (F_T). The search for appropriate F_T that will account the Gibbs free energy along with the reaction rate should be the future step for the proposed model.

Among the parameters required, the maximum hydrolysis rate and maintenance-energy (ME) requirement may be the most critical parameter for modelling population dynamics. Yet, maximum hydrolysis rates of POM in oligotrophic aquifers are one of the poorly constrained variables in the literature. Moreover, studies demonstrate that the ME requirements change with changing catabolic energy (Russell, 1986). We cannot be sure that the values we have chosen are correct, as there are no relevant measurements. Therefore, proper investigation of the aquifers is a must before assigning the values to these parameters.

Further studies are required to confirm and extend our hypothesis. Experiments under well-defined conditions could elucidate to which extent the principles set forward are valid. To address conditions of spatially variable and dynamic environments (Allison, 2005), the dependence of energetic and kinetic terms on physical and chemical conditions such as temperature, nutrients and pH should be accounted for (German et al., 2012). Furthermore, coupling of bioenergetics microbial dynamics to transport of the substrates on different scales could put biogeochemical zonation onto better thermodynamic grounds. The modeling framework can also be modified to simulate microbial dynamics in diverse environments in which carbon is not the limiting factor, as long as energetic constraints can be attached to the regulating process.

5. Soil organic matter degradation by microbes in fluctuating vs static redox condition

5.1 Introduction

Fluctuating redox conditions can occur naturally, e.g., in riparian floodplains, due to seiches in stratified lakes, within soils influenced by a fluctuating groundwater table, or in coastal environments. They can also be the result of anthropogenic influences, e.g., in paddy fields, or due to damming, recharging or discharging the water. Land-use changes can also lead to oscillating redox conditions. The fluctuating environment triggers biogeochemical changes that differ in comparison to strictly static oxic or anoxic conditions. Fluctuating redox conditions are important for predicting the degradation of soil organic matter (SOM), the emission of greenhouse gas (GHG) and microbial dynamics in general.

A few studies on the influence of fluctuating redox conditions have been conducted. Besides oscillating redox conditions, other factors might have affected the results in these studies. These factors include soil moisture (Blodau and Moore, 2003; Blodau, 2003; Butterly et al., 2009; Rezanezhad et al., 2014), the chemical gradient developed as a result of soil depth (Frindte et al., 2013), the quality and quantity of carbon content (Kristensen et al., 1995), the soil chemical composition (Hanke et al., 2013; Kristensen et al., 1995), among others. In addition, the period and direction (that is oxic to anoxic or vice versa) of redox oscillation also have an effect (Hanke et al. 2013). Some studies target specified effects of redox fluctuations; for example, Parsons et al., (2013) and Couture et al., (2015) focused mostly on contamination, while Thompson et al. (2006) concentrated their efforts on iron cycling. Teh et al. (2005) conducted an experiment in which they tried to maintain variable redox conditions by changing only the head-space gas; however, this could not prevent the formation of micro-anaerobic sites also under oxic conditions.

In static oxic or anoxic conditions the reactants fuelling important biogeochemical processes such as heterotrophic respiration become depleted and metabolic products build up decreasing

the energetic efficiency of important reactions. By contrast, an oscillating redox environment keeps the system far from thermodynamic equilibrium increasing the energetic efficiency (Parsons et al., 2013). This is the result of regenerating electron acceptors (EA) during the aerobic phase (Blodau and Moore, 2003; Knorr, 2013) and the variable pH associated with the adsorption of the organic matter (OM). The activity of hydrolase enzymes is higher under anaerobic than under aerobic conditions which results in high dissolved organic carbon (DOC) production (Chen et al., 2011). Additionally, mineralization of organic matter is less efficient under anaerobic conditions, resulting in the enrichment of water-soluble intermediate metabolites such as organic anions like acetate, formate, propionate, and lactate (Kögel-Knabner et al., 2010 and reference within). These labile substrates are an easy energy source for the aerobic bacteria. Moreover, these exoenzymes are activated after short term exposure to oxygen which can strongly increase carbon mineralization rates (Blodau and Moore, 2003). Some studies also suggest that alternating oxic and anoxic condition improve degradation of organic matter by enhancing chemical breakdown, recycling of biomass and reducing the accumulation of toxic intermediates (Aller, 1994; Blodau and Moore, 2003; Gerritse and Gottschal, 1992). Studies of fluctuating condition in estuaries have demonstrated enhanced degradation of particulate organic matter (Frindte et al., 2013 and reference within). Therefore, enhanced organic matter degradation seems plausible under these oscillating conditions. This also implies that there is a threat of carbon release from wetlands all over the world.

Microbial communities have been observed to change dramatically towards higher diversity under fluctuating redox conditions compared to static conditions (Pett-Ridge and Firestone, 2005; Rezanezhad et al., 2014). Microbes seem to adapt to continuous changes in water saturation and redox potential, and switch to other electron acceptors such as manganese and iron etc. (Grybos et al., 2009; Rezanezhad et al., 2014). Goodheart (2014) hypothesized that there could be potential synergy between aerobic and anaerobic bacteria which may be an important factor controlling the decomposition rates in wet forest soils. Microbes are also responsible for the emission of greenhouse gases (GHG). Their activities depend on redox conditions which would modulate the exchange of these gases with the atmosphere (Kögel-Knabner et al., 2010; Rezanezhad et al., 2014 and references within).

The cited studies demonstrate that oscillating redox conditions lead to deviating results compared to static conditions. However, current results regarding the carbon release and organic-matter mineralization are inconclusive. There is also contrasting evidence: carbon mineralization rates in incubated soil suspensions from different paddy and non-paddy soils decreased when the conditions changed regardless of whether the direction was from oxic to anoxic or vice versa (Hanke et al., 2013). This study also indicates that the repeated cycles of desorption followed by partial mineralization and re-adsorption could contribute to carbon accumulation under continuously alternating redox conditions. Some studies also suggest that a sudden change in redox conditions leads to an unusually high proportion of microbial cell lysis (Butterly et al., 2009; Sharma et al., 2013). Frindte et al., (2013) found that the bacterial concentration was the lowest under fluctuating condition, the highest under anoxic conditions, and in-between under oxic conditions. However, microbial activities under the anoxic conditions were found to be lower compared to oxic and variable conditions. The latter study illustrated that alternating redox conditions lead to similar chemical and microbial activities as those in oxic cores and which are significantly higher than those in anoxic cores.

These previous studies demonstrated the inconclusiveness with respect to biogeochemistry under oscillating conditions. Also, the effect on soil respiration is poorly known under fluctuating conditions (Rezanezhad et al., 2014). Therefore, an experimental approach with three bioreactors with peat material has been chosen in the present analysis. One reactor remained reducing, one oxic, and third underwent fluctuating redox conditions. By this, we want to study the influence of redox conditions on soil-organic-matter degradation excluding influences of other physical or chemical conditions. Peatlands play a vital role in the global carbon cycle. They form one of largest sinks for carbon in soils and can emit greenhouse gases (Blodau and Moore, 2003; Blodau, 2003). We want to compare carbon cycling processes under static and oscillating redox conditions, particularly organic-matter degradation rates, solid phase carbon transformations, greenhouse gas emission, and the interaction of heterotrophic metabolism and fermentation.

5.2 Materials and methods

5.2.1 Soil sampling and characterization

The soil used for the study was sampled from a marshy area, very close to a groundwater-fed small stream in the *rare* Charitable Research Reserve field site located in Cambridge, Ontario, Canada (3°22'34.42"N, 80°22'9.12"W). The soil was collected from a highly productive forested riparian wetland area which was an upwelling zone for nitrate contaminated groundwater. Naturally, the soil is anaerobic and contains an abundance of organic matter (acting as electron donor). The soils at the site are made of a combination of woody peat and incompletely decomposed organic matter. The organic-carbon content of the soil is 23% of dry weight. The soil was sampled from the top 20 cm of the soil surface. Large vegetative materials and root masses were manually removed to create a uniform mixture and the samples were thoroughly mixed and stored moist and airtight at 4°C until the start of the experiments. The soil moisture content was gravimetrically determined by drying approximately 30 g of fresh soil at 80°C for at least 48 h; its value was 60%. This was conducted in triplicates.

5.2.2 Experiment design and redox oscillation sequence

A set of three identical bioreactors (Applikon ®) based on the designs of Thompson et al., (2006) was set up. A homogenous soil suspension of 93 g/L was prepared with an artificial groundwater solution; the particle diameter was smaller than 500µm (See appendix A1 for details). Each bioreactor was filled with 1L soil suspension with a headspace of 250 ml. The bioreactors were subjected to three different redox conditions. The first bioreactor (O-reactor) and the second bioreactor (R-reactor) were continuously purged with air and nitrogen, respectively, resulting in static oxic and anoxic conditions. The third reactor (F-reactor) was subjected to anaerobic conditions for 6 days followed by 1 day under aerobic conditions by purging nitrogen and air, respectively. All suspensions were stirred at 500 rpm and maintained at 25±1°C and run simultaneously for 28 days (four full oscillating cycles). The values of temperature, pH, and Eh were continuously recorded throughout the experiment. A more detailed description of the sampling and analytical procedures is illustrated in appendix A2.

5.2.3 Aqueous chemistry analyses

All chemicals used in the experiment were analytical grade (Sigma-Aldrich and Anachemica). 18 M Ω cm⁻¹ water was used for preparing standards and reagents. The soil suspensions sampled from the reactors were centrifuged for 15 minutes at 3500 rpm and filtered through 0.2 μ m polyethersulfone sterile syringe filters prior to all aqueous analyses. All aqueous elemental concentrations were determined by ICP-OES after dilution and acidification (Thermo Scientific iCAP 6300). Chloride, nitrate, nitrite, sulfate, and phosphate concentrations were measured by ion chromatography using a Dionex ICS 5000 equipped with a capillary IonPac® AS18 hydroxide selective anion-exchange column. DOC, nitrogen, and DIC concentrations were determined on a TOC-LCPH/CPN analyzer (Shimadzu). All aqueous analyses were conducted in triplicate and the precision was less than 5% relative standard deviation (RSD). Organic acids (OA) were measured using a high capacity, high efficiency anion exchange column that provides an excellent resolution of organic acids (Thermo Scientific, Dionex IonPac AS11-HC). The measured organic acids were lactate, acetate, propionate, formate, isobutyrate, butyrate, succinate, sulfate, fumarate, and citrate.

5.2.4 Greenhouse gas analyses

The greenhouse gases (CH₄, N₂O, and CO₂) were sampled both in the aqueous and gaseous phase. Gas fluxes from the suspension to the headspace were calculated based on the increased concentration in the headspace over 15 minutes, during which sparging was stopped and gas outflow from the headspace was prevented. Samples were taken by a syringe. The sample volumes collected for gas and aqueous samples were 10 ml and 2 ml, respectively. The samples were analyzed on the same day using a GC-2014 Gas Chromatograph (Shimadzu). A correction of GHG fluxes was applied to account for increasing headspace volume caused by sampling of the soil suspension. The gas sample was directly injected in the GC and the mass of analyte in the gas sample was calculated. In case of an aqueous sample, 1ml of the sample was mixed with helium in the ratio of 1:9. When the greenhouse gases and helium equilibrated, the helium was injected into the GC. Then the mass of the analyte in both phases was calculated.

5.2.5 Specific ultra violet absorbance analysis

Specific ultra violet absorbance (SUVA₂₅₄) is defined as the UV absorbance at 254 nanometers measured in inverse meters (m⁻¹) that is normalized by the DOC concentration measured in milligrams per liter. SUVA is positively correlated with the percentage aromaticity in DOC (Weishaar and Aiken, 2001). Absorbance measurements were carried out on the day of sampling. The absorbance measurements were performed using a Thermo Scientific Evolution 260 Bio UV-visible Spectrophotometer. A 70 µl micro UV-Cuvette with a 10 mm path length was used for the analysis. All analyses were conducted in triplicate.

5.2.6 Solid analyses

The solid pellet resulting from centrifugation of the soil was used for solid analyses. Soil samples were collected to examine extracellular enzymes, microbial ecological analysis CHNS, and organic carbon. Organic carbon and carbonate fractions in the solid phase were determined by thermo-gravimetric analysis (TGA-Q500, TA Instruments Q500) based on the research by Pallasser et al., (2013). Microbial ecological analysis and extracellular enzymes have not been completed till the end of this thesis and will be continued in future work.

5.3 Results

Figure 5.1-5.4 show time series of all measured parameters and concentrations. In all experiments, the change in geochemistry is drastic during the first few days of the experiment, because the temperature higher than in the field, the water-to-soil ratio is larger, and mixing is enhanced by stirring and gas purging. Some data are inconsistent. For instance, the nitrogen species show unusual patterns and are therefore not considered in the following discussion. The precise reason behind this is not known. Potentially, there had been nitrate contaminated vials. Therefore, I have not shown NO₃⁻/NH₄⁺ ratios, nitrate, nitrous oxide etc. In addition, we also observed some anomalous results regarding CO₂ both in the aqueous and gaseous phases which is explained below. Data of major anions and cations that don't participate in redox cycling are

not shown in this report, since their results are not relevant for this study but would be used in future works.

5.3.1 pH and redox potential

The pH is highest in the R-reactor, followed by the F-reactor and the O-reactor. The pH-value in the O-reactor increases from 7.1 to 7.5 within three days (Figure 5.1 A). Then the pH keeps almost constant for two weeks. In the third week, the pH increases slightly up to 7.8 and then drops back to 7.5 by the end of the experiment. In the R-reactor, there is a steady increase of pH which stabilized at 8.1. In the F-reactor, the pH rises to approximately 7.8 during each anaerobic cycle and drops by roughly 0.15 units during each aerobic cycle.

The Eh maintains a high positive value 500 ± 20 mV during the experiment in the O-reactor, whereas it has a value of -270 mV in the R-reactor and continues decreasing (Figure 5.1 B). In the F-reactor, we observe oscillating behavior of Eh. The Eh increases sharply during the aerobic cycles up to 500 mV and decreases in the anaerobic cycle as low as -105 mV. The periodic change of Eh ranges from $+400$ to -100 mV. The values of both pH and Eh in the F-reactor are between the values of the R-reactor and O-reactor.

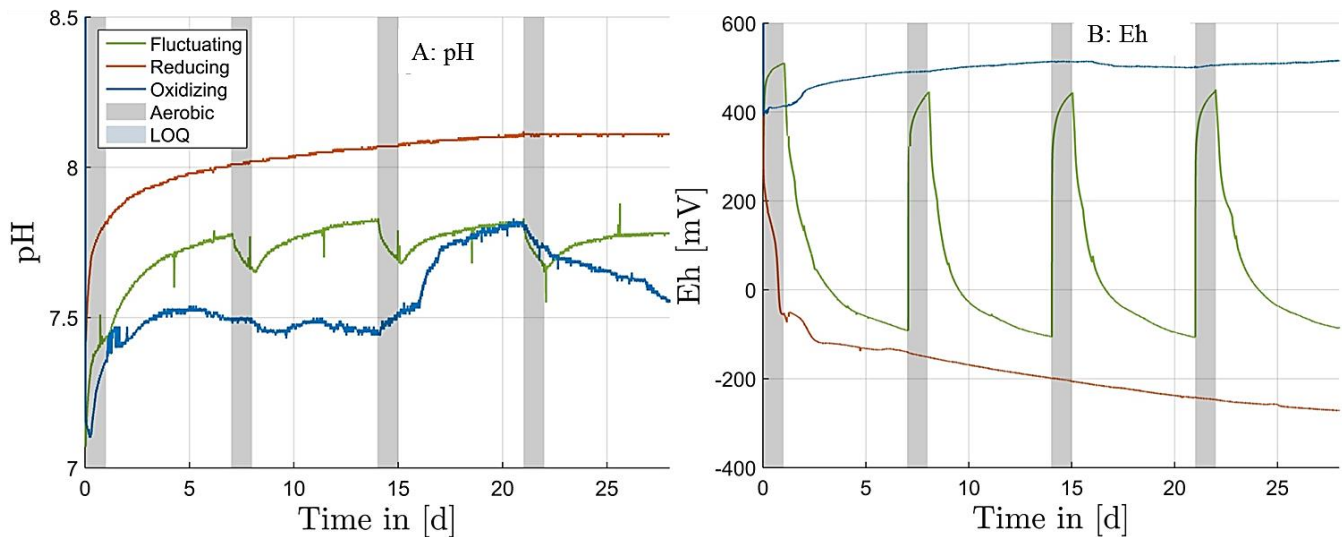


Figure 5.1: Time series of A: pH and B: Eh. The grey regions denote the one day oxidizing period in the fluctuating reactor and the Limit of quantification (LOQ) is marked by blue regions.

5.3.2 Carbon pool

The carbon is analyzed in all solid, aqueous and gaseous phases. SOM in the solid phase mostly consists of macromolecules that are initially degraded into monomers. These monomers are typically water soluble, but may undergo adsorption or desorption depending on pH and Eh. The monomers are further mineralized to carbon dioxide or methane gas with several byproducts.

5.3.2.1 Aqueous carbon pool

Dissolved organic carbon

DOC remains low throughout the entire experiment in the O-Reactor (Figure 5.2 A). DOC under anaerobic conditions increases rapidly and reaches a very high concentration of 70 mmol-C/L after 11 days. There is a sharp decrease in the next 4 days. After this period, DOC concentration is roughly constant with a final concentration of 13 mmol-C/L. In the F-reactor, DOC shows an interesting pattern: it increases at the beginning of each anoxic period but declines prior to the aerobic cycle. This degradation is enhanced during the aerobic cycle and reaches as low values as the concentration observed in the O-reactor. With each anaerobic cycle, the peak-value of DOC decreases. By the end of the experiment, the DOC concentration reaches 6.5 mmol-C/L, which is half the concentration of the R-reactor.

Unlike the DOC concentration, the fraction of aromatic DOC remains the highest in the aerobic reactor (Figure 5.2 D). By the end of the experiment, the aromaticity doubles from 12% to 24%, but the DOC concentration is very low. That is, the little DOC left in the oxic system is mainly recalcitrant aromatic DOC. By contrast, the aromaticity of DOC is very low in the R-reactor, but the DOC concentration is high. In the F-reactor, the aromaticity of DOC also shows a remarkable pattern. During the anaerobic cycle the aromaticity remains as low as that in the R-reactor and suddenly spikes to higher values comparable to those in the O-reactor within one day of the aerobic cycle.

Dissolved inorganic carbon (DIC)

The DIC in all bioreactors behaves almost similar. The concentration initially decreases within a week and remains approximately constant for the rest of the experiments (Figure 5.2 B). The

DIC concentration is highest for the O-reactor, followed by the F-reactor. The DIC concentration in the R-reactor is the lowest. The concentration decreases rapidly from 3.25 to 0.25 mmol-C/ L by the end of the experiments. We also observe a slight increase in the DIC concentration in the soil suspension during each aerobic cycle of the F-reactor.

Short-chain fatty acids

The measured short-chain fatty acids (SCFA) concentrations stay lowest in the O-reactor (Figure 5.2 C and Figure A3.1). In contrast, the SCFAs increase linearly in the R-reactor. Among the organic acids, only acetate, propionate, butyrate are observed during the analysis. The concentration of organic acids increases linearly, amounting to more than 35% of the total DOC by the end of the experiment. Acetate is the most abundant with a concentration of 3.9 mmol-C/L, followed by propionate with a final concentration of 0.72 mmol-C/L. Other SCFA concentrations are insignificant. The enrichment of these fermentation products starts a day later in the F-reactor as a result of the first aerobic cycle. In the first cycles, the SCFAs accumulate during the anaerobic cycle and are rapidly consumed during the following aerobic cycles. The accumulation of propionate, butyrate and formate plus isobutyrate can be clearly observed only in the first redox cycle. Acetate is the only fermentation product where the oscillations can be observed over several cycles. However, the increase of the acetate concentration is very small compared to that in the R-reactor and after every redox cycle, the acetate peak during the 6 days of anoxic period decreases. During each oxic cycle, the concentration of SCFAs in the F-reactor is as low as that in the O-reactor.

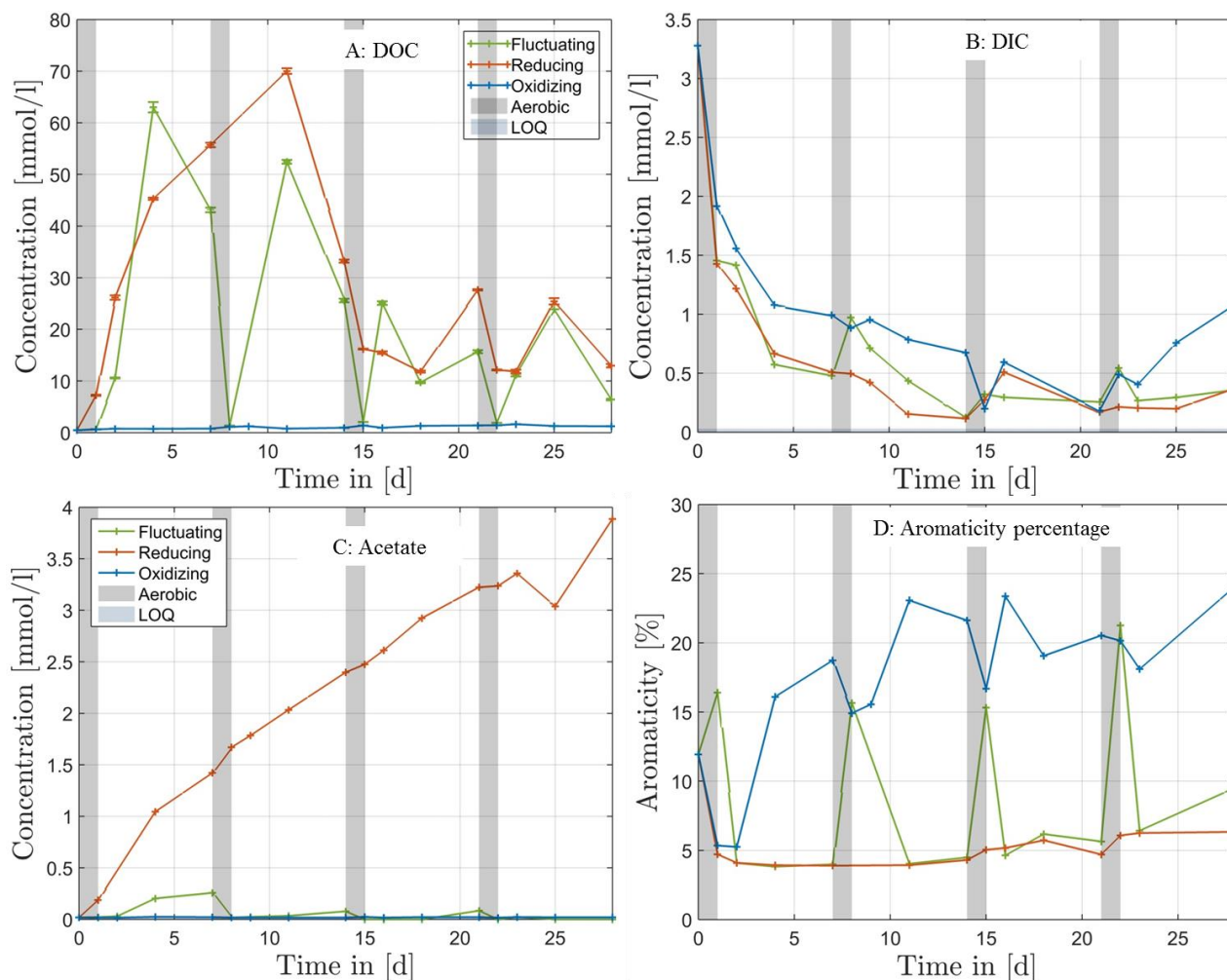


Figure 5.2: Dissolved carbons A: Dissolved organic carbon (DOC) B: Dissolved inorganic carbon (DIC) C: Acetate D: Aromaticity percentage of dissolved organic carbon. The grey regions denote the one day oxidizing period in the fluctuating reactor and the Limit of quantification (LOQ) is marked by blue regions. All concentrations are in mass carbon per volume of water.

5.3.2.2 Greenhouse gases

Greenhouse-gas concentrations were measured both in the aqueous and gaseous phase. Only data of CO_2 and CH_4 are discussed in this study (Figure 5.3 A and B). The aqueous-phase CO_2 concentration is approximately one order of magnitude higher than the headspace CO_2 converted

to dissolved CO₂ following Henry's law. The gas-phase concentrations were obtained after stopping the purging of the reactors for 15 minutes. Over this time, the equilibrium between the two phases has not been reached yet. Moreover, in some sampling of gas-phase CO₂ is also below the limit of detection (Figure not shown). Thus, the water-phase CO₂ concentrations are used as a proxy of the CO₂ release by the reactors.

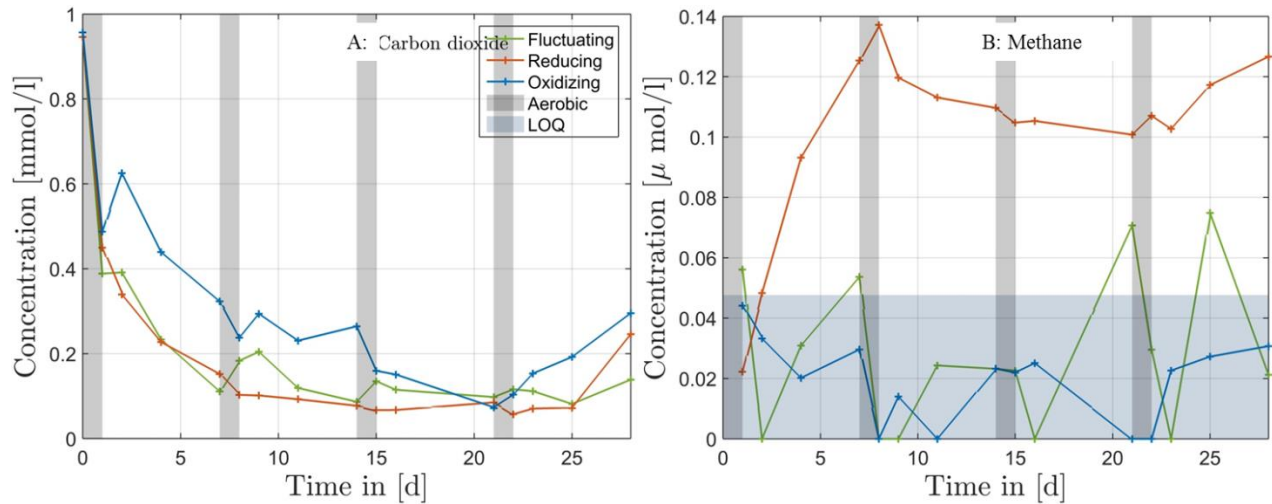


Figure 5.3: Greenhouse gases A: Carbon dioxide, and B: Methane. All concentrations are in mass carbon per volume of water

Flooding is known to cause complex patterns of CH₄ and CO₂ production (Blodau and Moore, 2003; Blodau, 2003). More cumulative CO₂ was produced under oxic conditions, followed by the fluctuating redox conditions and the anoxic conditions. The CO₂ concentration decreases in each bioreactor in the initial days in response to the change of environmental conditions. After the first week, the CO₂ is roughly constant in the R-reactor. The concentration of CO₂ is negatively correlated with pH, reflecting carbonate dissolution and precipitation. In the F-reactors, there is a small increase in the CO₂ concentration in the soil suspension during each aerobic cycle which gets smaller in each redox cycle. This decrease is probably due to depletion of the labile carbon in the F-reactor (Butterly et al., 2009; Rezanezhad et al., 2014).

Methane was not detected in the aqueous phase. Hence, only the methane collected in the gas phase is used for analysis. Methanogenesis is observed in the R-reactor within four days. There is also some methane production in the F-reactor during the anoxic cycles, particularly in the late

stage of the experiment. In the O-reactor, the methane concentration was lower than the limit of quantification throughout the whole experiment.

5.3.2.3 Solid organic carbon pool

Thermogravimetric analysis (TGA) performed on the soil samples shows a significant decrease of organic carbon in the O-reactor by 4.5% (Table 5.1). In the R-reactor, the decrease in organic-carbon content is 1.5%. Simultaneously an increase in carbonate is observed in the O- and R-reactors, respectively. By contrast, TGA results show a remarkable increase in solid phase organic carbon by 4.1% in the F-reactor; whereas carbonate decreases. CHNS analysis of the soil suspension does not show consistent data, however, it also indicates that there is an increase in organic carbon and total carbon but a decrease in inorganic carbon (Appendix Table A.2).

Table 5.1: Solid phase total organic carbon (%) measured using thermogravimetric analysis (TGA).

Bioreactor	Carbonate (%)			Organic Matter (%)		
	Day 1	Day 28	Difference	Day 1	Day 28	Difference
Oxidizing	10.3	12.89	2.59	21.3	16.7	-4.5
Reducing	10.37	13.44	3.07	19.9	18.4	-1.5
Fluctuating	11.39	8.67	-2.72	19.4	23.5	4.1

5.3.3 Electron acceptors

Among the different Terminal Electron Acceptors (TEAs), only dissolved oxygen (O₂), manganese (Mn) and sulfate (SO₄²⁻) were detected in the aqueous samples (Figure 5.4). Nitrate shows an anomalous behavior in all bioreactors which could not be interpreted (not shown). We observed that Fe(II) was mostly below the limit of quantification in all aqueous samples.

However, we observed low concentrations of Fe(II) in the F- and R-reactors at the end of the experiment (Figure not shown). Nevertheless, Fe cycling is considered as a vital process for DOC mineralization in the range of pH- and Eh-values observed in the F-reactor (Bishop et al., 2010). The measured redox potentials would allow Fe^{2+} reduction during the anoxic cycles. However, Fe^{2+} in the given pH-range of 7-8 is usually poorly soluble because it can adsorb to the sediment (Hanke et al., 2013 and references within). Ferrous iron may also precipitate in the form of FeS under reducing conditions. During oxidation, Fe is not observed since it may precipitate in the form of ferric iron hydroxyoxides (Konhauser, 2007). Manganese speciation was not measured, but only the reduced Mn^{2+} can exist as a free ion in the aqueous solution (Lutz Ehrlich and Newman, 2008). This concept is used to distinguish the Mn data.

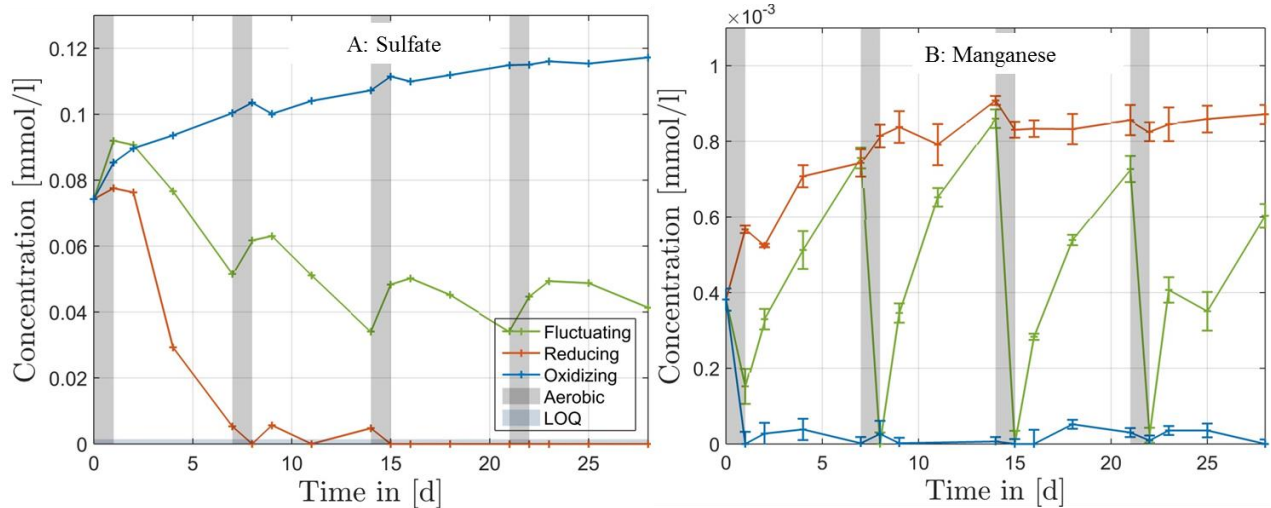


Figure 5.4: Electron Acceptors A: Sulfur concentration within sulfate, and B: Manganese.

In the O-reactor, an increase in the sulfate concentration can be observed, and Mn^{2+} becomes undetectable within one day, most likely due to oxidation to Mn^{4+} and precipitation as manganese oxide (Figure 5.4). As expected, oxygen is the only terminal electron acceptor being reduced in the O-reactor. On the contrary, manganese and sulfate reduction occurs within 1 and 2 days, respectively, in the R-reactor. The Mn^{2+} concentration increases to a constant value of $0.9 \mu\text{mol/L}$ until the end of the experiment, whereas sulfate vanishes below the detection limit within one week from the start of the experiment. In the F-reactor, the electron-acceptor concentrations (Mn^{4+} and sulfate) increase during aerobic cycles as the result of oxidation of Mn^{2+} and sulfide by oxygen. The anaerobic cycle is characterized by an increase in aqueous Mn^{2+} and a decrease

in the SO_4^{2-} concentrations. The Mn^{2+} increases rapidly at the first day of the anoxic cycles, which shows that manganese is the preferred electron acceptor at these times. The sulfate concentration starts to decrease only after the second day of the anaerobic cycles. Over the first two cycles, the concentration of sulfate decreases and approaches a dynamic steady state in the last two cycles. The increase in sulfate within each oxic cycle is also roughly similar.

5.4 Discussion

5.4.1 Dynamics of pH and Eh

The soil is naturally carbonate buffered. An artificial solution with a concentration of 1 mol/L bicarbonate was also added which also buffered the suspension. Despite that, there is slight pH increase in all bioreactors (Figure 5.1 A). This might be a result of continuously purging gas through the reactors which removes CO_2 . Additionally, water logging is also known to increase pH (Hanke et al., 2013, 2014). This is usually due to reductive dissolution of Mn- and Fe-oxyhydroxides (Grybos et al., 2009). The pH initially decreases in the O- and F-reactors because of oxidation of sulfides before it rises. After few hours, there is a steady rise in pH in these reactors. The redox conditions had significant effects on the pH of individual soils, because of H^+ consumption during reduction reactions (Grybos et al., 2009). Therefore, the largest change in pH is in the R-reactor, since it was only sparged by N_2 gas. In the F-reactor, the values of pH increased distinctly during the reducing periods, while they decreased during oxidation. The transition from oxic to anaerobic conditions results in a reduction in electron acceptors (e.g., Mn^{4+} and sulfate) which causes pH increase and vice versa (Knorr, 2013).

The redox potential indicates the capacity of the solution to provide electrons to the electrode. It may also give information about the terminal electron acceptor participating in the redox reactions and may be indicative of microbial respiration (DeLaune and Reddy, 2005). Nonetheless, Eh should be interpreted very carefully as many terminal electron acceptors may not fully contribute to the measured Eh. The Eh in the O-reactor remained at highly positive values whereas that in the R-reactor remained at strongly negative ones as expected for oxic and

anoxic conditions, respectively (Figure 5.1 B). In the F-reactor, we observe oscillating behavior of Eh in response to the purging with air and pure nitrogen. The change of Eh in the F-reactor indicates the major changes in the aqueous chemistry in the F-reactor (Figure 5.1 B). When the redox potential is higher than 400 mV, the suspension is considered aerobic and oxygen is used as the dominant terminal electron acceptor (DeLaune and Reddy, 2005; Tokarz and Urban, 2015). The range of Eh values also crossed the thermodynamic equilibria of several important redox pairs, namely $\text{Fe}(\text{OH})_3/\text{Fe}^{2+}$, $\text{MnO}_2/\text{Mn}^{2+}$, and $\text{SO}_4^{2-}/\text{HS}^-$. Similar changes in Eh are observed in redox-fluctuating natural systems such as periodically inundated wetlands.

5.4.2 Transformation of aqueous carbon

In wetlands, flooding causes mobilization of DOC from peat soils. Increase in DOC is usually related to microbial production of metabolites, desorption of organic matter due to pH changes, and reductive dissolution from Mn- and Fe- oxyhydroxides (Grybos et al., 2009). In a given field setting, it is difficult to assess the actual source, since these processes occur simultaneously. Studies performed by Grybos et al. (2009) and Hanke et al. (2013) illustrated that pH-changes were the main source of DOC release whereas Knorr (2013) considered reductive desorption as the main source.

In the O-reactor, we observed very low DOC concentrations because the aerobic microbes appear to be very efficient in consuming labile carbon under oxic system (Figure 5.2 A). In general, soil organic matter is considered to decompose more rapidly and completely under oxic conditions than that under anoxic ones (Hanke et al., 2013 and references within). We could not observe any accumulation of intermediate metabolites; and the concentration of single-chain fatty acids stayed low. High DOC decline is also associated with enhanced organic-matter mineralization (Grybos et al., 2009). This is also supported by the fact that CO_2 and DIC, which is the end product of carbon mineralization, were highest in the O-reactor.

In contrast, the DOC concentrations in the R- and F-reactors were initially high. However, the fatty-acid concentration were low at first, indicating that the microbes have little to do with the observed DOC increase (Figure 5.2 C and Figure A.1) Instead, the pH increase and reductive desorption could be the reason for the high DOC concentrations. In the R-reactor, the DOC increased quickly for ten days and then declined sharply. This was not associated with

concentration changes of CO₂, DIC, or methane. This observation is most likely caused by hydrochemical factors rather than biological ones (Kalbitz et al., 2000). In the R-reactor, the DOC concentration is the largest compared to those in the other reactors. This results from a combination of different effects: (1) Fermentation is a dominant process and the decomposition of organic matter is less efficient under anaerobic than under aerobic conditions. This results in accumulation of water-soluble intermediate metabolites such as organic anions like acetate, butyrate and propionate. (2) DOC processed under different conditions sorb differently to soil minerals; in particular, DOC resulting from anaerobic processing sorbs less than DOC from aerobic processing of organic matter (Hanke et al., 2014). (3) The high pH increases the solubility of humic compounds and results in enhanced desorption of organic matter from soil minerals and Fe oxides (Grybos et al., 2009; Hanke et al., 2013) and (4), the hydrolase enzyme activity is higher under anaerobic than under aerobic conditions, which results in high DOC production from soil organic matter (Chen et al., 2011).

In the F-reactor, the DOC declines at later times within the anaerobic cycles because of the respiration of heterotrophic bacteria including sulfate and manganese reducers prior to the aerobic period. However, this does not trigger CO₂ or methane emission or increase of DIC. We did not perceive any clear relationships between DOC and CO₂ or DIC production under the different redox conditions, which confirms findings of Yu et al. (2007). There are few speculations for potential explanations: (1) DOC might be transformed into calcium carbonate. The time scale of the sampling is too large to observe the precipitation or dissolution of carbonate. (2) The DOC transforms into solid carbon pools in the form of organic biomass (explained in chapter 4.5). Moreover, the DOC is consumed more rapidly in the oxic cycle, reaching values as low as those observed in the O-reactor. This confirms that the aerobic bacteria are efficient in consuming labile carbon. In the oxic cycle, we perceive a minor increase in CO₂ emission. This finding is in contrast with the previous study by Hanke et al. (2013) where the carbon mineralization decreased after every change in redox conditions. The increase of CO₂ during the aerobic phase is the result of carbonate dissolution and microbial respiration. This increase is smaller than the degraded DOC. Hence, it is difficult to predict the exact source of CO₂. By the end of the anaerobic cycle, DOC decreases in the F-reactor, while the fermentation

products (in particular acetate) appear to slightly increase, which suggests that the rate of respiration catches up with fermentation quickly and the aerobic bacteria are very efficient in consuming DOC. This also suggests that the microbial community in the redox-fluctuating system adapts over several cycles, leading to a declining accumulation of fermentation products with a larger number of repetitive redox cycles.

All these results confirm that soil-organic-matter mineralization is higher under oxic than under anoxic condition. This also holds true under fluctuating conditions where the mineralization of soil organic matter is larger compared to the R-reactor. The soil organic matter in the O-reactor gives the impression of a higher mineralization rate than in the F-reactor. However, low CO₂ production in F-reactor does not mean low organic-matter turnover. The carbon from the aqueous pool might go into a solid carbon pool (discussed in next section). The concentrations DOC and fatty acids under fluctuating conditions get lower after each progressive redox cycle in the F-reactor. The F-reactor is able to degrade as much DOC as the O-reactor. Over long time periods, the carbon mineralization rates in the F-reactor may be equal or even higher than in the O-reactor.

In the R-reactor, the methane concentration remains relatively constant after a week even when the fatty acids (mostly acetate) increases (Figure 5.3 B and Figure 5.2 C); indicating an inhibition of acetotrophic methanogenesis. This demonstrates that methane and fatty-acid production are not associated. The methane generation during the late stage under the fluctuating conditions suggests that methanogenesis was delayed but not inhibited by the oxic cycle (Blodau and Moore, 2003; Blodau, 2003; Goldhammer and Blodau, 2008).

5.4.3 DOC and aromaticity

The fermentation products accumulated in the R-reactor are non-aromatic (Figure 5.2 A and D). Thus the remaining low aromaticity of the DOC in the R-reactor mainly indicates that the non-aromatic compounds are not easily mineralized under strictly reducing conditions. The aromaticity of DOC in the F-reactor also reflects the behavior of the DOC concentration. When the DOC concentration is low, which is during the aerobic periods, the aromaticity of the remaining DOC is high, whereas the buildup of DOC in the anaerobic phases leads to a decrease in aromaticity because these intermediate compounds are predominantly non-aromatic. Our

results imply that the mineralization of non-aromatic compounds is significantly enhanced under aerobic conditions, whereas the degradation of aromatic compounds may be enhanced but to a much smaller extent. Moreover, the aromatic DOC of the F-reactor in the oxic cycle is similar to that in the O-reactor.

5.4.4 Electron acceptors, greenhouse gases and microbial activity

Oxygen is the only predominant electron acceptor in the O-reactor and there is no possibility of fermentation. The only process is aerobic respiration, and consequently the O-reactor produces more CO₂ than the other bioreactors. Whether the active bacteria are obligatory or facultative aerobes is not known. Strictly anaerobic bacteria, including fermenters, either die off or become dormant. The R-reactor is deprived of all energy-rich terminal electron acceptors within a week and promotes fermentation (Figure 5.4). The low CO₂ production is the result of incomplete degradation of soil organic matter, and the CO₂ produced may also have been utilized by methanogens (acetoclastic and hydrogenotrophic bacteria etc.) using hydrogen as an electron donor (Figure 5.3 A). Regarding the F-reactor, the six-days reducing cycle is characterized by an increase in aqueous Mn²⁺ and a decrease in SO₄²⁻ which indicates heterotrophic respiration of both electron acceptors. Sulfate usually regenerates even upon brief exposure to oxygen and also the sulfate reducing bacteria are known to recover instantly (Goldhammer and Blodau, 2008). The fluctuating redox conditions keep the system away from thermodynamic equilibrium by replenishing important pools of electron donors (e.g., acetate) and acceptors such as Mn⁴⁺ and sulfate. This may lead to larger carbon degradation. The fluctuating conditions may have the potential to degrade soil organic matter at similar rates as under strictly oxic condition. The microbes using oxygen for carbon mineralization may be able to switch to Mn(IV) and Fe(III) (Frindte et al., 2013). Additionally, various microbial processes such as fermentation, sulfate reduction, Mn⁴⁺ reduction etc. are all active in F-reactor. This illustrates that the microbes are acclimated to the oscillating condition (DeAngelis et al., 2010). The fluctuating redox condition most likely allows heterotrophic anaerobic, aerobic and fermenting microorganisms to co-exist.

Methanogenesis, a strict anaerobic process, is observed in only in R- and F-reactors. R-reactor, being under always anoxic condition, shows evidence of methanogenesis within a week (Figure

5.3 B). In previous studies, methane production was observed after few weeks only (Blodau and Moore, 2003; Blodau, 2003). However, in the cited studies, other electron acceptors, such as sulfate, inhibited the onset of methanogenesis. Such electron acceptors were absent in our R-reactor. Late methane production in the F-reactor suggests that the oxic cycles do not inhibit the methane production but only delay it. This also indicates that the methanogens co-exist along with other microorganism under the oscillating redox condition. The methane production in last two cycles is almost equal in magnitude indicating possible dynamic steady state. Moreover, the production of methane is less than R-reactor.

5.4.5 Solid carbon pool and microbial activity

The thermogravimetric analysis of the solid phase (Table 5.1) shows a decrease of solid-phase organic carbon in both the O- and R-reactors, whereas the F-reactor shows an apparent increase of organic carbon in the solid phase. In addition to that, there is also a decrease in carbonate under the fluctuating conditions. There is no precise explanation for this outcome. We hypothesize that biomass may have increased. Peatlands have been found to have higher rates of biomass formation than of organic-matter decomposition (Hugron et al., 2013). Autotrophs may exist in the F-reactor which converts CO₂ from calcite dissolution to new biomass. Heterotrophic respiration also could be the source of CO₂. Peat soils have a high reduction capacity (Leon and Lnicki, 2002). Some peat soils have very high sulfur contents (Andriessse, 1988). Sulfur may exist as polysulfides or elemental sulfur that can act as the electron donors needed for reduction of inorganic carbon to biomass. However, large amounts of reductants (that is, approximately 1.25 moles of electrons) would be required to form approximately 0.33 mol/L of carbon biomass (that is, 4% of organic matter) from carbonates. While the measurements of solid-phase inorganic and organic carbon are very reproducible, the representativeness of the samples may be questioned.

5.5 Conclusions and future works

With respect to carbon cycling, we observe an overall adaptation of the microbial community in the fluctuating reactor to the fluctuating redox conditions. In the first anaerobic phase, the

concentrations of DOC and fermentation products are the highest. During the oxic cycle, DOC rapidly declines. In this time Mn^{4+} , sulfate, and most likely ferric iron hydroxides are also replenished. These secondary electron acceptors are reduced in the following anaerobic cycle. There is also a replenishment important pools of electron donors in the anoxic cycles (e.g., acetate via fermentation). The externally driven redox variations, caused by oxygen fluctuations, keep the system always far from thermodynamic equilibrium, giving reducing and oxidizing microbial communities good conditions in alternating time periods. Obviously, the chosen frequency of redox fluctuations facilitates all types of microbial activities like fermentation, aerobic and anaerobic respiration including methanogenesis. Hence, fluctuating conditions maintain a more diverse microbial community than static conditions. There is the possibility that aerobic, anaerobic and fermenting bacteria work in concert. This results in efficient degradation of soil organic matter. In the F-reactor we can therefore perceive clear synergy between aerobic and anaerobic/fermenting processes to deplete the labile carbon at total rates that are definitely faster than those observed in the reducing reactor. We could not confirm that fluctuating condition will result into more carbon mineralization compared to aerobic conditions by this experiment. Nevertheless, the decline of DOC peaks after progressive redox cycles plus the concentration of DOC becoming similar to that of the oxidizing reactor indicates that the fluctuating conditions may have the potential for higher carbon mineralization in the long term than even the purely oxic system. Nevertheless, we found that the CO_2 production is higher under the continuously oxidizing than under the fluctuating conditions

The fraction of aromatic carbon increases predominantly in the F-reactor in the oxic cycles, when the total DOC decreases. This clearly indicates that the non-aromatic carbon is oxidized preferably under aerobic conditions. We also perceive a quite high fraction of aromatic organic carbon under aerobic conditions. However, we don't observe it under anaerobic conditions even when the total DOC is higher. By the end of the anaerobic cycle, DOC decreases in the F-reactor, while the fermentation products (in particular acetate) hardly increase which suggests that the rate of respiration quickly catches up with fermentation. Moreover, methanogenesis does not catch up with fermentation in the strictly reducing reactor, resulting in accumulation of acetate.

The most remarkable as well as unexplainable result is the increase in solid organic matter and dissolution of carbonate in the F-reactor which is in contrast to the O- and R-reactors. The exact reason behind this result could not be found in this study. One of the speculations is the formation of new autotrophic biomass. The tremendous amount of electron donors that needs to be oxidized for this conversion of inorganic to organic carbon make our hypothesis bit uncertain.

In future work, we will analyze all frozen samples in the lab for microbial analysis and extracellular enzymes. This will help us to understand how the microbial dynamics as well as genetic diversity of the microbial communities change. More TGA analysis of the samples collected during the experiment will also help us to confirm or disprove and understand the apparent increase of organic carbon in the F-reactor.

6. General conclusions and outlook

This dissertation focused on three research gaps that I identified and discussed in the introduction. To address the influence of environment, I developed two different models to represent microbial dynamics in two contrasting aquifers, and conducted an experiment to understand the organic matter degradation by microbial communities under static and fluctuating redox conditions.

6.1 Conclusions

This study demonstrated that the models developed of microbial dynamics in two different aquifers (that is, eutrophic and oligotrophic aquifers) require different assumptions for similar microbial activities. For example, the first-order decay term is used for the death of bacteria in the kinetic model representing eutrophic aquifers; however the same assumption can't be applied to oligotrophic aquifers. The bacterial growth is observed to be very slow in natural aquifers, which means that a constant first-order decay of bacteria will lead to total eradication of bacterial communities. Additionally, maintenance-energy can be neglected in eutrophic aquifers whereas maintenance-energy captures most of the energy generated by the bacteria in oligotrophic environments.

Chapter 3: Natural aquifers receiving constant supply of an energy/carbon substrate are well represented by reaction kinetics. The substrate consumption rate is defined by Monod kinetics. The bacterial transformation is calculated by a constant yield and substrate consumption rate. To the best of my knowledge, I developed the first one-dimensional bio-reactive transport model that depicts three hierarchal level interactions (substrate-bacteria-grazer) in groundwater. The dissolved substrate is advected with water flow whereas the biomasses of bacteria and grazers are considered essentially immobile. The one-dimensional reactive transport model also accounts for substrate dispersion and a random walk of grazers influenced by the bacterial concentration. These dispersive-diffusive terms affect the oscillations until steady state is reached, but hardly the steady-state value itself. The remarkable result is the steady-state concentration of the

bacteria. Both the analytical solution and numerical simulations illustrate that the maximum bacterial concentration is independent of the substrate inflow. Grazing, or infection by bacteriophages, is found to be a possible explanation of the maximum biomass concentration frequently needed in bio-reactive transport models. Its value depends on parameters related to the grazers or bacteriophages and is independent of bacterial growth parameters or substrate concentration, provided that there is enough substrate to sustain bacteria and grazers. The simulation results suggest that groundwater ecosystems could also be controlled top-down, which is in contradiction to the popular belief of a bottom-up control.

Chapter 4: In contrast, the bio-reactive model for an energy-limited aquifer contained more than kinetic equations. Resat et al. (2012) developed a comprehensive kinetic model to illustrate microbial dynamics which requires numerous parameters as well as mathematical formulations. Searching appropriate parameter values and solving all those equations can be painstaking. I developed a bioenergetics model and expressed kinetic rate laws in thermodynamic terms. The activity of microorganisms is based on efficient utilization of catabolic energy. A key point of the model is the distribution of energy, gained by catabolic reactions, between extracellular hydrolytic enzymes production, maintenance-energy requirement, and biomass growth. I hypothesized that the fraction of excess energy spent on extracellular hydrolytic enzyme production versus the fraction spent on growth is related to the fraction of free reactive centers of the extracellular hydrolytic enzymes breaking down the monomers generated by hydrolysis. I applied the model to simulate the anaerobic degradation of cellulose by a hypothetical microbial community consisting of cellulolytic fermenting bacteria and sulfate-reducing bacteria, under conditions representative of those encountered in oligotrophic aquifers. Inside the model, the catabolic Gibbs energy is computed at every time step. The simulation result is compared with a static Gibbs energy model. The results vary significantly and lead to serious discrepancies. The proposed model shows that lowering the sulfate concentration influences the thermodynamics of the whole system and affects whole microbial communities whereas, in the static bioenergetics model, only sulfate reducers is affected whereas the fermenter are not influenced because the model lacks thermodynamic feedbacks.

Chapter 5: To address contradicting results from previous studies about the effect of oscillating conditions on microbial dynamics, I conducted an experiment with three identical bioreactors. The soil suspensions were operated under static oxic, static anoxic, and fluctuating redox condition respectively. The oxic reactor emitted the highest CO₂ whereas the anoxic reactor emitted the highest CH₄. The microbial communities appeared to be flourishing within the fluctuating reactor where fermentation, aerobic/anaerobic respiration, and methanogenesis were observed. Under fluctuating conditions, the electron donors and acceptors were observed to be restored during the anoxic and oxic cycles, respectively. This propelled the environment away from thermodynamic equilibrium and soil organic matter could be transformed more quickly than under anoxic conditions. Fluctuating redox conditions showed the potential to facilitate higher transformation rates of soil organic carbon than oxic condition. An unsolved issue is the increase of solid organic matter in the fluctuating reactor. This may be as a result of increase in autotrophic microorganisms under the fluctuating conditions.

6.2 Outlook and future perspectives

Chapter 3: One dimensional reactive transport model developed, within this dissertation to illustrate three hierarchal level of biotic interaction, should not be perceived only as a concept but a new beginning to develop more complicated level of hierarchy. The model including different grazers and bacterial communities could be very interesting where either grazers or bacteria possess advantage against other competing species. This will deepen our knowledge on groundwater ecosystem. Furthermore, if “grazing” can explain maximum biomass, this will help to have better insight on the term carrying capacity and how it can be used in the modelling field. If relevant it may also be used while developing multi-dimensional model in larger scale. If a similar experiment is planned on the interactions discussed above, this model will also help to plan the time duration of the experiment, time-period for sampling and also to understand how the bacteria will fluctuate before it goes to steady-state condition.

Chapter 4: The bioenergetics model captures comprehensive microbial dynamics. This model coupled with transport will be able to represent the oligotrophic aquifer more closely. Knowledge of the dormancy triggered by energy can be used when modeling bio-reactive

transport with dynamic boundary conditions where the contaminant inflow varies with time. This concept is useful in reactive transport modelling to understand how a natural aquifer behaves if it is contaminated, or the contaminant comes along with groundwater recharge. Potential applications involve agricultural systems with seasonal variations in recharge and bank-filtration systems where the substrate and nutrient load changes during hydrological events.

If plausible representation of NOM within a particular aquifer can be presented; then bioenergetics combined into the microbial rate law will depict the microbial dynamics even in large scale ecosystems. Moreover, the model can be modified without lot of effort to incorporate more microbial dynamics. For e.g., if sulfate is reduced then, the system may switch to methanogenic-based system whereby there are now hydrogenotrophic and acetoclastic methanogens. It can also be changed to look at the relative impacts of limitations on nutrients (that is, P and N) versus limited energy or temperature etc. The current model only focuses on extracellular hydrolytic enzymes. With the current progress in biochemistry, there is the possibility of calculating energy required to form various biomolecules (Amend et al., 2013). Therefore, the model, modified according to these current or future progresses in biochemistry, can account several enzymes produced by the bacteria and will be able to represent in-depth microbial activities.

Chapter 5: The experiment was conducted on a peat soil, which is one of the largest reservoirs of carbon. There is a global threat of release of carbon from these peat soils (Tokarz and Urban, 2015). With the global climate change, the redox condition of the peatland may change drastically. The results may be used to understand the SOM degradation and GHG release from the peatland under different redox conditions. The possibility of increase of organic carbon under fluctuating condition might be also one of the interesting results which need to be verified. This may shed some insight on the current knowledge about peat soil.

Appendix to chapter 5

A1. Field site characterization

A1.1 Soil preparation:

The soil collected from the rare site was preserved in the temperature of 4°C for three days. The soil was kept in an anaerobic condition within an air-tight plastic container. The soil was transferred to another container to obtain the desired concentration of 100 gm/L to increase the workability. Artificial water was added to obtain target concentration after the moisture content were measured. The artificial water was made based on the groundwater composition (prepared with 18 MΩ cm⁻¹ water). Although the concentration of Na⁺ and K⁺ are relatively low in the natural groundwater, we added NaHCO₃ and KHCO₃ with a concentration of 0.5 mmol/L. Consequently the target of 1 mmol/L of HCO₃⁻ was achieved which is comparable to the groundwater. A comparison of artificial groundwater and real groundwater is shown in Supplementary Table A. 1. The soil suspension was made homogenous by continuous stirring for at least 10 minutes. The suspension was then passed through a sieve of 2 and 0.5 mm to segregate larger sediment fragments and solid organic material. The 2 mm sieve did not retain any of the material. The residues that retained in the 0.5 mm sieve were then grinded until the sediment was less in diameter than 0.5 mm. Therefore, we did not lose any materials which would result into more accurate interpretation. The minute soil particles (less than 0.5 mm) have less probability to clog the portal which might be used for sampling or purging of gas. A concentration of 93 g/L was achieved. This soil was let to stand in anaerobic condition for 6 more days before the main experiment in the bioreactor. The soil was again stirred to make it homogenous before transferring to the bioreactor. Soil sample was also taken for CHNS analysis.

A2. Experimental procedures

A2.1 Preliminary experiment

Soil samples were collected from four different sources; Beverly Swamp (BS), Commercial Peats (CP), rare Site (rare) and Laurel Creek (LC). Among these four, commercial peats were bought and other three were collected from the relative sites. The soil suspension were prepared aerobically using artificial water and left for three days. 30 mL soil suspensions (duplicates) were transferred to 40 mL amber glass vials and placed in the anaerobic chamber. Sampled were sacrificed anaerobically at 0, 1, 4 and 7 days respectively. It was observed that the rare soil had the lowest methanogenesis rate and high short chain fatty acid (SCFA) generation in 7 days period. This fulfils our goals to observe building up of organic acid during the anaerobic cycle in the bioreactor which will be consumed in the aerobic cycle. Low methanogenesis indicate that the bioavailable organic matter last longer. This allows us to run the experiment for sufficient redox cycle to observe better result.

A2.2 Reactors setup

A set of three identical air-tight borosilicate glass bioreactors (Applikon ®) with 1.2L working volumes and stainless steel head-plates were used. Each head-plate contained airtight ports for sampling, electrodes, gas sparging and mechanical agitation. Oxic or anoxic conditions were induced in the reactors by the sparging (30 mL min^{-1}) of either compressed air (oxic) or N_2 (anoxic) similar to the experiment set up in the study performed by Parsons et al., (2013). All the parts of the bioreactors were washed by $18 \text{ M}\Omega \text{ cm}^{-1}$ water initially followed by rinsing with 1M HCl. Subsequently, all bioreactors were stirred continuously filled with 0.1 M NaOH for half an hour. Finally, all bioreactors were soaked in $18 \text{ M}\Omega \text{ cm}^{-1}$ water for 24 hours before commencing the experiment. The first and second were labelled as static oxidizing bioreactor (O-reactor, continuous sparging with air), reducing bioreactor (R-reactor, continuous sparging with N_2) and third was oscillating or fluctuating reactor (F-reactor, alternating between N_2 and air). Eh, pH, temperature and dissolved oxygen (DO) were monitored continuously using a combined autoclavable Mettler Toledo InPro 3253i/SG open junction electrode and an AppliSens, Low drift polarographic sensor respectively, and logged every 8 minutes. The InPro system helps to

avoid interference between redox and pH electrodes in close proximity using a common reference electrode. Redox, pH and temperature data were converted to digital signals in the InPro electrode head to avoid degradation and transmitted to a Mettler Toledo M800 multi-parameter transmitter for temperature correction of the pH signal and adjustment of the redox signal to the standard hydrogen electrode (SHE) Eh values. The processed output of the M800 was transmitted to Applikon MyController systems before being recorded on a PC using BioXpert software. Dissolved oxygen (DO) value was continuously monitored only on F-reactor and R-reactor. The O reactor was considered saturated with oxygen at all times. The F-reactor was subjected to 6 days of anoxic conditions and 1 day of oxic conditions.

A total of four fluctuating cycles were conducted over a period of 28 days. The suspension was sampled four times a week (i.e. within one redox cycle). The sampling was carried out on both period when the air was turned on and off for F-reactor. One more sampling was conducted on the following day after the oxygen was shut off and the final sampling was collected after 1 day interval.

A2.3 Sampling procedure

18 ml of suspension was sampled through a connection on the top of the reactor by drawing on a 30 ml syringe connected to a soil sampling tube. Prior to these sampling the syringes was purged three times with either air or nitrogen corresponding to the reactors and redox cycle. The syringe was then capped. The anaerobic samples were transferred to an anaerobic atmosphere glove-box with less than 0.1 ppm oxygen. All the sample soil suspension was centrifuged at 3500 rpm for 15 minutes to isolate solid particles from the aqueous phase. The resulting supernatant was then filtered to 0.2 μm to confirm no large particles were present in the aqueous sample. The resulting aqueous sample is distributed for different analysis as shown in the Table A.3. For the solid analyses (extracellular enzymes, microbes), the segregated solid soil was mixed with 2 ml of aqueous sample to increase the workability and transferred to cryotube. The solid sample is frozen immediately in liquid nitrogen where it was stored until it was prepped for analysis. The sample preservation for the different analysis is also shown in the Table A.3. This table also includes total number of the samples, the variety of vial used for keeping the sample until the

analysis. The samples collected for DOC were also used for Specific Ultra-violet Absorbance (SUVA), being an indestructible sampling method. This analysis was usually performed on the same day as the experiment. After the SUVA, the DOC sample is acidified by HCl.

For the (Greenhouse gas) GHG samples for gaseous phase, the flow of the gas in the bioreactor is stopped for 15 minutes. The entire inlet and outlet valves are closed during this process. The gas is allowed to accumulate. 10 ml of the gas sample is collected via the gas tube on the top of the reactor by drawing from the syringe. For the GHG aqueous sampling, 2 ml of sample is also collected using syringe consequently after the aqueous sampling. The samples were also capped making sure that there is no gas in the sample.

A3. Figures

A3.1 Short chain fatty acids

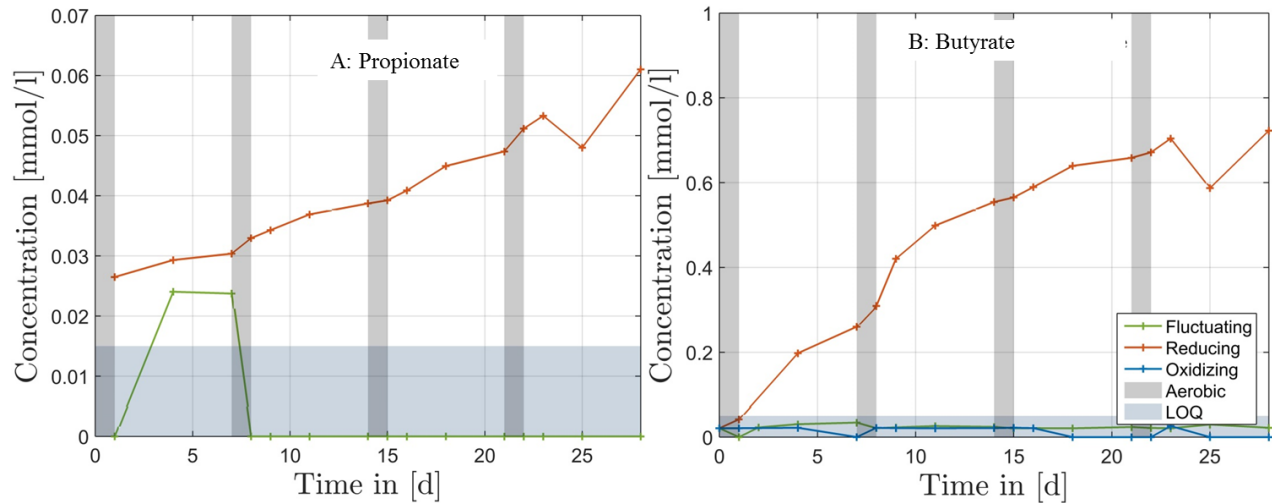


Figure A.1: Short chain fatty acids A: Propionate, and B: Butyrate. The grey regions denote the one day oxidizing period in the fluctuating reactor and the Limit of quantification (LOQ) is marked by blue regions. All concentrations are in mass carbon per volume of water

A4. Tables

Table A.1: Comparison of artificial and actual groundwater

Ion	Artificial solution(mmol/L)	Actual groundwater (mmol/L)
Na ⁺	0.5008338	0.3491
K ⁺	0.5000000	0.0172
Ca ²⁺	1	1.9610
Mg ²⁺	1	1.1467
HCO ³⁻	1	No data
CO ₃ ²⁻	0.0004169	
Cl ⁻	4	0.6699

Table A.2: CHNS analysis of soil suspension

Bioreactor	Total Carbon (%)			Inorganic carbon (%)			Organic carbon (%)		
	Day 0	Day 28	Difference	Day 0	Day 28	Difference	Day 0	Day 28	Difference
Oxidizing	23.7	22.2	1.5	1.56	1.81	-0.25	22.1	20.4	1.7
Reducing	23.7	24.9	-1.2	1.56	1.75	-0.19	22.1	23.2	-1.1
Fluctuating	23.7	30.3	-6.6	1.56	1.33	0.23	22.1	29.0	-6.9

Table A.3: Sampling Table

Sample	Technique	Analyte	Sample Preservation	Sample Vol (ml)	Vial	No of Sampling per week	Total no of sample
Water	ICP	Ca, Fe, S, K, Mg, Mn, Na, P	204 μ L HNO ₃ and temperature 4°C	2	HNO ₃ acid, Milli-Q rinsed, ICP tube (13 ml)	4	48
Water	IC	Cl-, NO ₃ -, NO ₂ -, SO ₄ -, PO ₄ -, Br-, F-	Freezing at -20°C	1	1.5 Eppendorf	4	48
Water	TOC	DOC	20 μ L HCl and temperature 4°C	1	HCl acid, Milli-Q rinsed, Glass tube	4	48
Water	TOC	DIC	20 μ L HCL and low temperature 4°C	1	HCl acid, Milli-Q rinsed, Glass tube	4	48
Water		Organic acid	20 μ l CrO ₄ , 500 ppm and low temperature 4°C	1	4 ml amber vial	4	48
Solid		Archive	Freezing at -80°C	1.5	Sterile cryptube	4	48
Solid		Enzyme	Freezing at -80°C	1.5	Sterile cryptube	4	48
Solid		Microbes	Freezing at -80°C	1.5	Sterile cryptube	4	48
Water	GC	GHG		2	Syringe (10 ml)	4	48
Gas	GC	GHG		10	Syringe (10 ml)	4	48
Solid	CHNS	TN/TC	Freeze @-80°C	5g solid		Start /End	4
Solid	SEM		Freezing at -20°C			Start /End	4
Solid	Extra Solid sample		Freezing at -20°C		MQ rinse, ICP tube (13ml)	4	48

7. Bibliography

- Acea, M.J., Alexander, M., 1988. Growth and survival of bacteria introduced into carbon-amended soil. *Soil Biol. Biochem.* 20, 703–709. doi:10.1016/0038-0717(88)90155-1
- Aller, R.C., 1994. Bioturbation and remineralization of sedimentary organic matter: effects of redox oscillation. *Chem. Geol.* 114, 331–345. doi:10.1016/0009-2541(94)90062-0
- Allison, S.D., 2005. Cheaters, diffusion and nutrients constrain decomposition by microbial enzymes in spatially structured environments. *Ecol. Lett.* 8, 626–635. doi:10.1111/j.1461-0248.2005.00756.x
- Amend, J.P., LaRowe, D.E., McCollom, T.M., Shock, E.L., 2013. The energetics of organic synthesis inside and outside the cell. *Philos. Trans. R. Soc. Lond. B. Biol. Sci.* 368, 20120255. doi:10.1098/rstb.2012.0255
- Anderson, T.H., Domsch, K.H., 1985. Determination of ecophysiological maintenance carbon requirements of soil microorganisms in a dormant state. *Biol. Fertil. Soils* 1, 81–89. doi:10.1007/BF00255134
- Andriessse, J.P. (Ed.), 1988. *Nature and Management of Tropical Peat Soils*. Food and Agriculture Organization of the United Nations.
- Anneser, B., Einsiedl, F., Meckenstock, R.U., Richters, L., Wisotzky, F., Griebler, C., 2008. High-resolution monitoring of biogeochemical gradients in a tar oil-contaminated aquifer. *Appl. Geochemistry* 23, 1715–1730. doi:10.1016/j.apgeochem.2008.02.003
- Anneser, B., Pilloni, G., Bayer, A., Lueders, T., Griebler, C., Einsiedl, F., Richters, L., 2010. High Resolution Analysis of Contaminated Aquifer Sediments and Groundwater—What Can be Learned in Terms of Natural Attenuation? *Geomicrobiol. J.* 27, 130–142. doi:10.1080/01490450903456723
- Ayuso, S.V., López-Archilla, A.I., Montes, C., Guerrero, M.D.C., 2010. Microbial Activities in a

- Coastal, Sandy Aquifer System (Doñana Natural Protected Area, SW Spain). *Geomicrobiol. J.* 27, 409–423. doi:10.1080/01490450903480277
- Azam, F., Fenchel, T., Field, J., 1983. The ecological role of water-column microbes in the sea. *Mar. Ecol. Prog. Ser.* 10, 257–263. doi:10.3354/meps010257
- Baath, E., 1998. Growth rates of bacterial communities in soils at varying pH: A comparison of the thymidine and leucine incorporation techniques. *Microb. Ecol.* 36, 316–327. doi:10.1007/s002489900118
- Bajracharya, B., Lu, C., Cirpka, O.A., 2014. Modeling substrate-bacteria-grazer interactions coupled to substrate transport in groundwater. *Water Resour. Res.* 50, 4149–4162. doi:10.1002/2013WR015173.
- Bales, R., Li, S., Maguire, K., 1995. Virus and bacteria transport in a sandy aquifer, Cape Cod, MA. *Ground Water* 33, 653–661. doi:10.1111/j.1745-6584.1995.tb00321.x
- Bär, M., Von Hardenberg, J., Meron, E., Provenzale, A., 2002. Modelling the survival of bacteria in drylands: the advantage of being dormant. *Proc. Biol. Sci.* 269, 937–42. doi:10.1098/rspb.2002.1958
- Barry, D.A., Prommer, H., Miller, C.T., Engesgaard, P., Brun, A., Zheng, C., 2002. Modelling the fate of oxidisable organic contaminants in groundwater. *Adv. Water Resour.* 25, 945–983. doi:10.1016/S0309-1708(02)00044-1
- Battin, T.J., Sloan, W.T., Kjelleberg, S., Daims, H., Head, I.M., Curtis, T.P., Eberl, L., 2007. Microbial landscapes: new paths to biofilm research. *Nat. Rev. Microbiol.* 5, 76–81. doi:10.1038/nrmicro1556
- Béguin, P., Aubert, J.P., 1994. The biological degradation of cellulose. *FEMS Microbiol. Rev.* 13, 25–58. doi:10.1111/j.1574-6976.1994.tb00033.x
- Bezerra, R.M.F., Dias, A.A., 2004. Discrimination among eight modified michaelis-menten kinetics models of cellulose hydrolysis with a large range of substrate/enzyme ratios: inhibition by cellobiose. *Appl. Biochem. Biotechnol.* 112, 173–184.

doi:10.1385/ABAB:112:3:173

Billen, G., Joiris, C., Wijnant, J., Gillain, G., 1980. Concentration and microbiological utilization of small organic molecules in the Scheldt estuary, the Belgian coastal zone of the North Sea and the English Channel. *Estuar. Coast. Mar.* ... 11, 279–294. doi:10.1016/S0302-3524(80)80084-3

Bishop, M.E., Jaisi, D.P., Dong, H., Kukkadapu, R.K., Ji, J., 2010. Bioavailability of Fe(III) in loess sediments: An important source of electron acceptors. *Clays Clay Miner.* 58, 542–557. doi:10.1346/CCMN.2010.0580409

Blodau, C., 2003. Micro-scale CO₂ and CH₄ dynamics in a peat soil during a water fluctuation and sulfate pulse. *Soil Biol. Biochem.* 35, 535–547. doi:10.1016/S0038-0717(03)00008-7

Blodau, C., Moore, T.R., 2003. Experimental response of peatland carbon dynamics to a water table fluctuation. *Aquat. Sci.* 65, 47–62. doi:10.1007/s000270300004

Boras, J.A., Sala, M.M., Vázquez-Domínguez, E., Weinbauer, M.G., Vaqué, D., 2009. Annual changes of bacterial mortality due to viruses and protists in an oligotrophic coastal environment (NW Mediterranean). *Environ. Microbiol.* 11, 1181–93. doi:10.1111/j.1462-2920.2008.01849.x

Botheju, D., Lie, B., Bakke, R., 2010. Oxygen effects in anaerobic digestion - II. Model. *Identif. Control* 31, 55–65. doi:10.4173/mic.2010.2.2

Boyd, E.S., Cummings, D.E., Geesey, G.G., 2007. Mineralogy influences structure and diversity of bacterial communities associated with geological substrata in a pristine aquifer. *Microb. Ecol.* 54, 170–182. doi:10.1007/s00248-006-9187-9

Brown, R.M., 1996. the biosynthesis of cellulose. *J. Macromol. Sci.* 10, 466–474. doi:10.1016/S0268-005X(87)80024-3

Butler, G., Hsu, S., Waltman, P., 1983. Coexistence of competing predators in a chemostat. *J. Math. Biol.* 133–151.

- Butterly, C.R., Bünemann, E.K., McNeill, A.M., Baldock, J.A., Marschner, P., 2009. Carbon pulses but not phosphorus pulses are related to decreases in microbial biomass during repeated drying and rewetting of soils. *Soil Biol. Biochem.* 41, 1406–1416. doi:10.1016/j.soilbio.2009.03.018
- Calbet, A., Landry, M., Nunnery, S., 2001. Bacteria-flagellate interactions in the microbial food web of the oligotrophic subtropical North Pacific. *Aquat. Microb. Ecol.* 23, 283–292. doi:10.3354/ame023283
- Canfield, D.E., Kristensen, E., Thamdrup, B., 2005. 2 Structure and Growth of Microbial Populations, *Aquatic Geochemistry*.
- Cao, J., Fussmann, G.F., Ramsay, J.O., 2008. Estimating a predator-prey dynamical model with the parameter cascades method. *Biometrics* 64, 959–67. doi:10.1111/j.1541-0420.2007.00942.x
- Carter, M.R., Angers, D.A., Gregorich, E.G., Bolinder, M.A., 2003. Characterizing organic matter retention for surface soils in eastern Canada using density and particle size fractions. *Can. J. Soil Sci.* 83, 11–23. doi:10.4141/S01-087
- Chapelle, F.H., 2000. *Ground-Water Microbiology and Geochemistry*, 2nd ed. John Wiley and Sons, New York.
- Chen, Y., Wen, Y., Cheng, J., Xue, C., Yang, D., Zhou, Q., 2011. Effects of dissolved oxygen on extracellular enzymes activities and transformation of carbon sources from plant biomass: Implications for denitrification in constructed wetlands. *Bioresour. Technol.* 102, 2433–2440. doi:10.1016/j.biortech.2010.10.122
- Christensen, T.H., Bjerg, P.L., Banwart, S.A., Jakobsen, R., Heron, G., Albrechtsen, H.J., 2000. Characterization of redox conditions in groundwater contaminant plumes. *J. Contam. Hydrol.* 45, 165–241. doi:10.1016/S0169-7722(00)00109-1
- Cirpka, O.A., 2010. Simplified simulation of steady state bioreactive transport with kinetic solute uptake by the biomass. *Water Resour. Res.* 46. doi:10.1029/2009WR008977

- Cirpka, O.A., Olsson, Å., Ju, Q., Rahman, M.A., Grathwohl, P., 2006. Determination of transverse dispersion coefficients from reactive plume lengths. *Ground Water* 44, 212–221. doi:10.1111/j.1745-6584.2005.00124.x
- Cirpka, O.A., Valocchi, A.J., 2007. Two-dimensional concentration distribution for mixing-controlled bioreactive transport in steady state. *Adv. Water Resour.* 30, 1668–1679. doi:10.1016/j.advwatres.2006.05.022
- Classen, A.T., Sundqvist, M.K., Henning, J.A., Newman, G.S., Moore, J.A.M., Cregger, M.A., Moorhead, L.C., Patterson, C.M., 2015. Direct and indirect effects of climate change on soil microbial and soil microbial-plant interactions: What lies ahead? *Ecosphere* 6, art130. doi:10.1890/ES15-00217.1
- Corapcioglu, M.Y., Haridas, A., 1985. Microbial transport in soils and groundwater: A numerical model. *Adv. Water Resour.* 8, 188–200.
- Coughlan, M., 1991. Mechanisms of cellulose degradation by fungi and bacteria. *Anim. Feed Sci. Technol.* 32, 77–100. doi:10.1016/0377-8401(91)90012-H
- Couture, R.M., Charlet, L., Markelova, E., Madé, B., Parsons, C.T., 2015. On–Off Mobilization of Contaminants in Soils during Redox Oscillations. *Environ. Sci. Technol.* 150210141728007. doi:10.1021/es5061879
- Cueto-Rojas, H.F., Van Maris, A.J.A., Wahl, S.A., Heijnen, J.J., 2015. Thermodynamics-based design of microbial cell factories for anaerobic product formation. *Trends Biotechnol.* 33, 534–546. doi:10.1016/j.tibtech.2015.06.010
- Dale, A., Regnier, P., Van Cappellen, P., 2006. Bioenergetic controls on anaerobic oxidation of methane (AOM) in coastal marine sediments: A theoretical analysis. *Am. J. Sci.* 306, 246–294. doi:10.2475/04.2006.0246
- Davis, P.G., Sieburth, J.M., 1984. Estuarine and oceanic microflagellate predation of actively growing bacteria : estimation frequency dividing-divided bacteria. *Mar. Ecol. Prog. Ser.* 19, 237–246.

- De Vries, F.T., Shade, A., 2013. Controls on soil microbial community stability under climate change. *Front. Microbiol.* 4, 1–16. doi:10.3389/fmicb.2013.00265
- DeAngelis, K.M., Silver, W.L., Thompson, A.W., Firestone, M.K., 2010. Microbial communities acclimate to recurring changes in soil redox potential status. *Environ. Microbiol.* 12, 3137–3149. doi:10.1111/j.1462-2920.2010.02286.x
- Del Giorgio, P., Cole, J.J., 1998. Bacterial Growth Efficiency in Natural Aquatic Systems. *Annu. Rev. Ecol. Syst.* 29, 503–541.
- del Monte-Luna, P., Brook, B.W., Zetina-Rejon, M.J., Cruz-Escalona, V.H., 2004. The carrying capacity of ecosystems. *Glob. Ecol. Biogeogr.* 13, 485–495. doi:10.1111/j.1466-822X.2004.00131.x
- DeLaune, R., Reddy, K., 2005. Redox potential, in: *Encyclopedia of Soils in the Environment*. Elsevier, pp. 366–371. doi:10.1016/B0-12-348530-4/00212-5
- Demirel, Y., Sandler, S.I., 2002. Thermodynamics and bioenergetics. *Biophys. Chem.* 97, 87–111.
- Demoling, F., Figueroa, D., Bååth, E., 2007. Comparison of factors limiting bacterial growth in different soils. *Soil Biol. Biochem.* 39, 2485–2495. doi:10.1016/j.soilbio.2007.05.002
- Desvaux, M., Guedon, E., Desvaux, L., Petitdemange, H., 2001. Kinetics and Metabolism of Cellulose Degradation at High Substrate Concentrations in Steady-State Continuous Cultures of *Clostridium cellulolyticum* on a Chemically Defined Medium Kinetics and Metabolism of Cellulose Degradation at High Substrate Concentra. *Appl. Environ. Microbiol.* 67, 3837–3845. doi:10.1128/AEM.67.9.3837-3845.2001
- Detmers, J., Schulte, U., Strauss, H., Kuever, J., 2001. Sulfate Reduction at a Lignite Seam: Microbial Abundance and Activity. *Microb. Ecol.* 42, 238–247. doi:10.1007/s00248-001-1014-8
- Doussan, C., Poitevin, G., Ledoux, E., Delay, M., 1997. River bank filtration: Modelling of the changes in water chemistry with emphasis on nitrogen species. *J. Contam. Hydrol.* 25, 129–

156. doi:10.1016/S0169-7722(96)00024-1

Eastman, J.A., Ferguson, J.F., 1981. Solubilization of particulate organic carbon during the acid phase of anaerobic digestion. *J. Water Pollut. Control Fed.* 53, 352–366.

Egli, T., 2010. How to live at very low substrate concentration. *Water Res.* 44, 4826–37.
doi:10.1016/j.watres.2010.07.023

Falkowski, P.G., Fenchel, T., Delong, E.F., 2008. The Microbial Engines That Drive Earth's Biogeochemical Cycles. *Science.* 320, 1034–1039. doi:10.1126/science.1153213

Faust, K., Raes, J., 2012. Microbial interactions: from networks to models. *Nat. Rev. Microbiol.* 10, 538–550. doi:10.1038/nrmicro2832

Fenchel, T., 1982. Ecology of Heterotrophic Microflagellates. II. Bioenergetics and Growth. *Mar. Ecol. Prog. Ser.* 8, 225–231.

Fenchel, T., 2004. Orientation in two dimensions: chemosensory motile behaviour of *Euplotes vannus*. *Eur. J. Protistol.* 40, 49–55. doi:10.1016/j.ejop.2003.09.001

Fenchel, T., Blackburn, N., 1999. Motile chemosensory behaviour of phagotrophic protists: mechanisms for and efficiency in congregating at food patches. *Protist* 150, 325–36.
doi:10.1016/S1434-4610(99)70033-7

Figueiredo, C.C.D., Resck, D.V.S., Carneiro, M.A.C., 2010. Labile and stable fractions of soil organic matter under management systems and native cerrado. *Rev. Bras. Ciência do Solo* 34, 907–916. doi:10.1590/S0100-06832010000300032

Foulquier, A., Malard, F., Mermillod-Blondin, F., Montuelle, B., Dolédec, S., Volat, B., Gibert, J., 2011. Surface Water Linkages Regulate Trophic Interactions in a Groundwater Food Web. *Ecosystems* 14, 1339–1353. doi:10.1007/s10021-011-9484-0

Fraser, M., Barker, J.F., Butler, B., Blaine, F., Joseph, S., Cooke, C., 2008. Natural attenuation of a plume from an emplaced coal tar creosote source over 14 years. *J. Contam. Hydrol.* 100, 101–115. doi:10.1016/j.jconhyd.2008.06.001

- Frindte, K., Eckert, W., Attermeyer, K., Grossart, H.P., 2013. Internal wave-induced redox shifts affect biogeochemistry and microbial activity in sediments: a simulation experiment. *Biogeochemistry* 113, 423–434. doi:10.1007/s10533-012-9769-1
- Gasol, J., 1994. A framework for the assessment of top-down vs bottom-up control of heterotrophic nanoflagellate abundance. *Mar. Ecol. Prog. Ser.* 113, 291–300.
- Gauze, G.F., 1934. *The struggle for existence*. Waverly Press, Baltimore, p. 192.
doi:10.1016/B978-008045046-Baltimore,The Williams & Wilkins company9.01641-7
- German, D.P., Marcelo, K.R.B., Stone, M.M., Allison, S.D., 2012. The Michaelis-Menten kinetics of soil extracellular enzymes in response to temperature: a cross-latitudinal study. *Glob. Chang. Biol.* 18, 1468–1479. doi:10.1111/j.1365-2486.2011.02615.x
- Gerritse, J., Gottschal, J.C., 1992. Co-culture of anaerobic and aerobic bacteria Mineralization of the herbicide 2,3,6-trichlorobenzoic acid by a co-culture of anaerobic and aerobic bacteria. *FEMS Microbiol. Ecol.* 101, 89–98. doi:10.1016/0378-1097(92)90830-H
- Gerritse, J., Schut, F., Gottschal, J.C., 1990. Mixed chemostat cultures of obligately aerobic and fermentative or methanogenic bacteria under oxygen-limiting conditions. *FEMS Microbiol. Lett.* 66, 87–94. doi:10.1016/0378-1097(90)90263-P
- Goldhammer, T., Blodau, C., 2008. Desiccation and product accumulation constrain heterotrophic anaerobic respiration in peats of an ombrotrophic temperate bog. *Soil Biol. Biochem.* 40, 2007–2015. doi:10.1016/j.soilbio.2008.03.005
- González-Cabaleiro, R., Lema, J.M., Rodríguez, J., 2015. Metabolic energy-based modelling explains product yielding in anaerobic mixed culture fermentations. *PLoS One* 10, 1–17. doi:10.1371/journal.pone.0126739
- Goodheart, D.B., 2014. *Influence of Physical and Biological Factors on Methane Emissions and Organic Carbon Mineralization in a Wet, Tropical Forest Soil*. University of California, Berkeley.
- Griebler, C., Lueders, T., 2009. Microbial biodiversity in groundwater ecosystems. *Freshw. Biol.*

54, 649–677. doi:10.1111/j.1365-2427.2008.02013.x

Griebler, C., Mindl, B., 2002. Distribution patterns of attached and suspended bacteria in pristine and contaminated shallow aquifers studied with an in situ sediment exposure microcosm. *Aquat. Microb. Ecol.* 28, 117–129.

Griebler, C., Mindl, B., Slezak, D., 2001. Combining DAPI and SYBR Green II for the enumeration of total bacterial numbers in aquatic sediments. *Int. Rev. ...* 86, 453–466. doi:10.1002/1522-2632(200107)86:4/5<453::AID-IROH453>3.3.CO;2-C

Griebler, C., Slezak, D., 2001. Microbial activity in aquatic environments measured by dimethyl sulfoxide reduction and intercomparison with commonly used methods. *Appl. Environ. Microbiol.* 67, 100–109. doi:10.1128/AEM.67.1.100

Grünheid, S., Amy, G., Jekel, M., 2005. Removal of bulk dissolved organic carbon (DOC) and trace organic compounds by bank filtration and artificial recharge. *Water Res.* 39, 3219–3228. doi:10.1016/j.watres.2005.05.030

Grybos, M., Davranche, M., Gruau, G., Petitjean, P., Pédrot, M., 2009. Increasing pH drives organic matter solubilization from wetland soils under reducing conditions. *Geoderma* 154, 13–19. doi:10.1016/j.geoderma.2009.09.001

Haandel, A. V., Lubbe, J. Van der, 2012. *Handbook Biological Wastewater Treatment - Design and optimization of Activated Sludge Systems.* IWA Publishing of Alliance House, London-UK ISBN.

Habte, M., Alexander, M., 1977. Further Evidence for the Regulation of Bacterial Populations in Soil by Protozoa. *Arch. Microbiol.* 133, 181–183. doi:10.1007/BF00492022

Hall, S.J., Treffkorn, J., Silver, W.L., 2014. Breaking the enzymatic latch: Impacts of reducing conditions on hydrolytic enzyme activity in tropical forest soils. *Ecol. Soc. Am.* 95, 2964–2973. doi:10.1890/13-2151.1

Handayani, I.P., Coyne, M.S., Tokosh, R.S., 2010. Soil organic matter fractions and aggregate

- distribution in response to tall fescue stands. *Int. J. Soil Sci.* 5, 1–10.
doi:10.3923/ijss.2010.1.10
- Hanke, A., Cerli, C., Muhr, J., Borken, W., Kalbitz, K., 2013. Redox control on carbon mineralization and dissolved organic matter along a chronosequence of paddy soils. *Eur. J. Soil Sci.* 64, 476–487. doi:10.1111/ejss.12042
- Hanke, A., Sauerwein, M., Kaiser, K., Kalbitz, K., 2014. Does anoxic processing of dissolved organic matter affect organic-mineral interactions in paddy soils? *Geoderma* 228-229, 62–66. doi:10.1016/j.geoderma.2013.12.006
- Harder, J., 1997. Species-independent maintenance energy and natural population sizes. *FEMS Microbiol. Ecol.* doi:10.1016/S0168-6496(97)00011-1
- Hardin, G., 1968. The tragedy of commons. *Science.* 162, 1243–1248.
doi:10.1126/science.162.3859.1243
- Harvey, R.W., Harms, H., Landkamer, L., 2002. Transport of microorganisms in the terrestrial subsurface: In situ and laboratory methods, 2nd ed, *Manual of environmental Microbiology.* Washington, ASM Press.
- Harvey, R.W., Kinner, N.E., Bunn, A., Macdonald, D., Metge, D., 1995. Transport behavior of groundwater protozoa and protozoan-sized microspheres in sandy aquifer sediments. *Appl. Environ. Microbiol.* 61, 209–217.
- Haughney, H.A., Nauman, E.B., 1990. A Bioenergetic Model of a Mixed Production Fermentation. *Biotechnol. Bioeng.* 36, 143–148.
- Heijnen, J.J., Dijken, J.P., 1992. In search of a thermodynamic description of biomass yields for the chemotrophic growth of microorganisms. *Biotechnol. Bioengineering* 39, 833–852.
- Hernandez, E., Johnson, M.J., 1967. Energy supply and cell yield in aerobically growth microorganisms. *J. Bacteriol.* 94, 996–1001.
- Hibbing, M.E., Fuqua, C., Parsek, M.R., Peterson, S.B., 2010. Bacterial competition: surviving and thriving in the microbial jungle. *Nat. Rev. Microbiol.* 8, 15–25.

doi:10.1038/nrmicro2259

- Hill, N.A., Häder, D.P., 1997. A Biased Random Walk Model for the Trajectories of Swimming Micro-organisms. *J. Theor. Biol.* 186, 503–526.
- Hoehler, T.M., 2004. Biological energy requirements as quantitative boundary conditions for life in the subsurface. *Geobiology* 2, 205–215. doi:10.1111/j.1472-4677.2004.00033.x
- Hoehler, T.M., Alperin, M.J., Albert, D.B., Martens, C.S., 1998. Thermodynamic control on hydrogen concentrations in anoxic sediments. *Geochim. Cosmochim. Acta* 62, 1745–1756. doi:10.1016/S0016-7037(98)00106-9
- Hoehler, T.M., Jørgensen, B.B., 2013. Microbial life under extreme energy limitation. *Nat. Rev. Microbiol.* 11, 83–94. doi:10.1038/nrmicro2939
- Horiuchi, J.I., Shimizu, T., Tada, K., Kanno, T., Kobayashi, M., 2002. Selective production of organic acids in anaerobic acid reactor by pH control. *Bioresour. Technol.* 82, 209–213. doi:10.1016/S0960-8524(01)00195-X
- Hugron, S., Bussi eres, J., Rochefort, L., 2013. Tree plantations within the context of ecological restoration of peatlands: practical guide.
- Hyndman, D.W., Dybas, M.J., Forley, L., Heine, R., Mayotte, T., Phanikumar, M.S., Tatara, G., Tiedje, J., Voice, T., Wallace, R., Wiggert, D., Zhao, X., Criddle, C.S., 2000. Hydraulic characterization of biocurtain. *Ground Water* 38, 462–474. doi:10.1111/j.1745-6584.2000.tb00233.x
- Jin, Q., Bethke, C., 2002. Kinetics of electron transfer through the respiratory chain. *Biophys. J.* 83, 1797–808. doi:10.1016/S0006-3495(02)73945-3
- Jin, Q., Bethke, C.M., 2003. A New Rate Law Describing Microbial Respiration A New Rate Law Describing Microbial Respiration. *Appl. Environ. Microbiol.* 69, 2340–2348. doi:10.1128/AEM.69.4.2340
- Jin, Q., Bethke, C.M., 2005. Predicting the rate of microbial respiration in geochemical

- environments. *Geochim. Cosmochim. Acta* 69, 1133–1143. doi:10.1016/j.gca.2004.08.010
- Jin, Q., Roden, E.E., 2011. Microbial physiology-based model of ethanol metabolism in subsurface sediments. *J. Contam. Hydrol.* 125, 1–12. doi:10.1016/j.jconhyd.2011.04.002
- Joergensen, R.G., Brookes, P.C., Jenkinson, D.S., 1990. Survival of the soil microbial biomass at elevated temperatures. *Soil Biol. Biochem.* 22, 1129–1136. doi:10.1016/0038-0717(90)90039-3
- Jones, S.E., Lennon, J.T., 2010. Dormancy contributes to the maintenance of microbial diversity. *Proc. Natl. Acad. Sci. U. S. A.* 107, 5881–5886. doi:10.1073/pnas.0912765107
- Jürgens, K., Massana, R., Kirchman, D., 2008. Protist grazing on marine bacterioplankton, 2nd ed, *Microbial ecology of the oceans*. John Wiley & Sons, Hoboken, NJ. doi:10.1002/9780470281840.ch11
- Jurtshuk, P., 1996. Bacterial Metabolism, in: Baron, S. (Ed.), *Medical Microbiology*. Galveston (TX): University of Texas Medical Branch at Galveston.
- Kalbitz, K.; Solinger, S.; Park, J. H.; Michalzik, B.; Matzner, E., 2000. Controls on the dynamics of dissolved organic carbon and nitrogen in a Central European deciduous forest. *SOIL Sci.* 165, 277–304. doi:10.1097/00010694-200004000-00001
- Kaplan, L.A., Newbold, J.D., 1995. Measurement of Stream Biodegradable Dissolved Organic Carbon with a Plug-flow Reactor. *Water Res.* 29, 2696–2706. doi:10.1016/0043-1354(95)00135-8
- Karp, G., 2009. *Cell and Molecular Biology: Concepts and Experiments*, 7th ed. NY:John Wiley & Sons, Inc.
- Keymer, J.E., Galajda, P., Muldoon, C., Park, S., Austin, R.H., 2006. Bacterial metapopulations in nanofabricated landscapes. *Proc. Natl. Acad. Sci. U. S. A.* 103, 17290–17295. doi:10.1073/pnas.0607971103
- Khatri, B.S., Free, A., Allen, R.J., 2012. Oscillating microbial dynamics driven by small populations, limited nutrient supply and high death rates. *J. Theor. Biol.* 314, 120–9.

doi:10.1016/j.jtbi.2012.08.013

Khosrovi, B., Macpherson, R., Miller, J.D., 1971. Some observations on growth and hydrogen uptake by *Desulfovibrio vulgaris*. *Arch. Mikrobiol.* 80, 324–337.

Kjørboe, T., Grossart, H., Ploug, H., Tang, K., Auer, B., 2004. Particle-associated flagellates: swimming patterns, colonization rates, and grazing on attached bacteria. *Aquat. Microb. Ecol.* 35, 141–152. doi:10.3354/ame035141

Kleman, G., Strohl, W., 1994. Metabolism by *Escherichia coli* in High-Cell-Density Fermentation. *Appl. Environ. Microbiol.* 60, 3952–3958.

Knorr, K.H., 2013. DOC-dynamics in a small headwater catchment as driven by redox fluctuations and hydrological flow paths – are DOC exports mediated by iron reduction/oxidation cycles? *Biogeosciences* 10, 891–904. doi:10.5194/bg-10-891-2013

Kögel-Knabner, I., Amelung, W., Cao, Z., Fiedler, S., Frenzel, P., Jahn, R., Kalbitz, K., Kölbl, A., Schloter, M., 2010. Biogeochemistry of paddy soils. *Geoderma* 157, 1–14. doi:10.1016/j.geoderma.2010.03.009

Konhauser, K., 2007. Introduction to geomicrobiology, *European Journal of Soil Science*. doi:10.1111/j.1365-2389.2007.00943_4.x

Konopka, A., 2000. Theoretical Analysis of the Starvation Response under Substrate Pulses. *Microb. Ecol.* 38, 321–329. doi:10.1007/s002489900178

Kristensen, E., Ahmed, S.I., Devol, A.H., 1995. Aerobic and anaerobic decomposition of organic matter in marine sediment : Which is fastest ? *Water* 40, 1430–1437. doi:10.4319/lo.1995.40.8.1430

LaRowe, D., Cappellen, P. Van, 2011. Degradation of natural organic matter: A thermodynamic analysis. *Geochim. Cosmochim. Acta* 75, 2030–2042. doi:10.1016/j.gca.2011.01.020

LaRowe, D.E., Amend, J.P., 2014. Microbial Life of the Deep Biosphere, in: Kallmeyer, J., Dirk, W. (Eds.), *Microbial Life of Deep Biosphere*. Walter De Gruyter GMBH, Berlin, pp. 279–

302. doi:10.1515/9783110300130

- LaRowe, D.E., Amend, J.P., 2015a. Power limits for microbial life. *Front. Microbiol.* 6, 1–11. doi:10.3389/fmicb.2015.00718
- LaRowe, D.E., Amend, J.P., 2015b. Catabolic rates, population sizes and doubling/replacement times of microorganisms in natural settings. *Am. J. Sci.* 315, 167–203. doi:10.2475/03.2015.01
- LaRowe, D.E., Dale, A.W., Amend, J.P., Van Cappellen, P., 2012. Thermodynamic limitations on microbially catalyzed reaction rates. *Geochim. Cosmochim. Acta* 90, 96–109. doi:10.1016/j.gca.2012.05.011
- Lennon, J.T., Jones, S.E., 2011. Microbial seed banks: the ecological and evolutionary implications of dormancy. *Nat. Rev. Microbiol.* 9, 119–130. doi:10.1038/nrmicro2504
- Leon, E.P., Lnicki, P. (Eds.), 2002. *Organic Soils and Peat Materials for Sustainable Agriculture*, New York. Taylor & Francis, 2002.
- Leschine, S.B., 1995. Cellulose degradation in anaerobic environments. *Annu. Rev. Microbiol.* 49, 399–426. doi:10.1146/annurev.mi.49.100195.002151
- Lodish, H., Berk, A., Zipursky, S.L., Matsudaira, P., Baltimore, D., Darnell, J., 2000. *Molecular Cell Biology*, 4th ed. New York.
- Lovley, D.R., Chapelle, F.H., 1995. Deep subsurface microbial processes. *Rev. Geophys.* 33, 365–381. doi:10.1016/S0168-6445(97)00013-2
- Lovley, D.R., Phillips, E.J.P., 1989. Requirement for a microbial consortium to completely oxidize glucose in Fe(III)-reducing sediments. *Appl. Environ. Microbiol.* 55, 3234–3236.
- Luna, G.M., Dell’Anno, A., Corinaldesi, C., Armeni, M., Danovaro, R., 2009. Diversity and spatial distribution of metalreducing bacterial assemblages in groundwaters of different redox conditions. *Int. Microbiol.* 153–159. doi:10.2436/20.1501.01.93
- Lutz Ehrlich, H., Newman, D., 2008. *Geomicrobiology*, 5th ed. CRC Press, Cambridge.

doi:10.1201/9780849379079

Lynd, L.R., Weimer, P.J., Zyl, W.H. Van, Isak, S., 2002. Microbial Cellulose Utilization :
Fundamentals and Biotechnology. *Microbiol. Mol. Biol. Rev.* 66, 506–577.

doi:10.1128/MMBR.66.3.506

Machemer, H., 2001. The swimming cell and its world: Structures and mechanisms of
orientation in protists. *Eur. J. Protistol.* 37, 3–14. doi:10.1078/0932-4739-00816

Madsen, E.L., 2011. Microorganisms and their roles in fundamental biogeochemical cycles.
Curr. Opin. Biotechnol. 22, 456–464. doi:10.1016/j.copbio.2011.01.008

Mailloux, B.J., Fuller, M.E., 2003. Determination of In Situ Bacterial Growth Rates in Aquifers
and Aquifer Sediments 69, 3798–3808. doi:10.1128/AEM.69.7.3798

Marvin-Sikkema, F.D., Richardson, A.J., Stewart, C.S., Gottschal, J.C., Prins, R.A., 1990.
Influence of hydrogen-consuming bacteria on cellulose degradation by anaerobic fungi.
Appl. Environ. Microbiol. 56, 3793–3797.

Marzadri, A., Tonina, D., Bellin, A., 2012. Morphodynamic controls on redox conditions and on
nitrogen dynamics within the hyporheic zone: Application to gravel bed rivers with
alternate-bar morphology. *J. Geophys. Res. Biogeosciences* 117, 1–14.
doi:10.1029/2012JG001966

McArthur, J.V. (Ed.), 2006. *Microbial Ecology: An Evolutionary Approach*. Academic Press,
Amsterdam.

Mccarty, P.L., Goltz, M.N., Hopkins, G.D., Dolan, M.E., Allan, J.P., Kawakami, B.T.,
Carrothers, T.J., 1998. Full-scale evaluation of in situ cometabolic degradation of
trichloroethylene in groundwater through toluene injection. *Environ. Sci. Technol.* 32, 88–
100. doi:10.1021/es970322b

Mellage, A., Eckert, D., Grösbacher, M., Inan, A.Z., Cirpka, O.A., Griebl, C., 2015. Dynamics
of Suspended and Attached Aerobic Toluene Degradation in Small-Scale Flow-through

- Sediment Systems under Growth and Starvation Conditions. *Environ. Sci. Technol.* 49, 7161–7169. doi:10.1021/es5058538
- Mempin, R., Tran, H., Chen, C., Gong, H., Kim Ho, K., Lu, S., 2013. Release of extracellular ATP by bacteria during growth. *BMC Microbiol.* 13, 301. doi:10.1186/1471-2180-13-301
- Mittal, M., Rockne, K.J., 2012. Dynamic models of multi-trophic interactions in microbial food webs. *J. Environ. Sci. Health. A. Tox. Hazard. Subst. Environ. Eng.* 47, 1391–406. doi:10.1080/10934529.2012.672316
- Moorhead, D.L., Rinkes, Z.L., Sinsabaugh, R.L., Weintraub, M.N., 2013. Dynamic relationships between microbial biomass, respiration, inorganic nutrients and enzyme activities: informing enzyme-based decomposition models. *Front. Microbiol.* 4, 223. doi:10.3389/fmicb.2013.00223
- Morita, R.Y., 1988. Bioavailability of energy and its relationship to growth and starvation survival in nature. *Can. J. Microbiol.* 34, 436–441.
- Morita, R.Y., 1990. The starvation-survival state of microorganisms in nature and its relationship to the bioavailable energy. *Experientia* 46, 813–817. doi:10.1007/BF01935530
- Murray, A., Jackson, G., 1992. Viral dynamics: a model of the effects of size, shape, motion and abundance of single-celled planktonic organisms and other particles. *Mar. Ecol. Prog. Ser.* ... 89, 103–116.
- Muyinda, 2014. Finite Volume Method of Modelling Transient Groundwater Flow. *J. Math. Stat.* 10, 92–110. doi:10.3844/jmssp.2014.92.110
- Novelli, P.C., Michelson, A.R., Scranton, M., Banta, G., Hobbie, J., Howarth, R., 1988. Hydrogen and acetate cycling in two sulfate-reducing sediments: Buzzards Bay and Town Cove, Mass. *Geochim. Cosmochim. Acta* 52, 2477–2486. doi:10.1016/0016-7037(88)90306-7
- Oehmen, A., Lemos, P.C., Carvalho, G., Yuan, Z., Keller, J., Blackall, L.L., Reis, M.A.M., 2007. Advances in enhanced biological phosphorus removal: From micro to macro scale. *Water*

Res. 41, 2271–2300. doi:10.1016/j.watres.2007.02.030

Owens, J., Legan, J., 1987. Determination of the Monod substrate saturation constant for microbial growth. *FEMS Microbiol. Lett.* 46, 419–432.

Pallasser, R., Minasny, B., McBratney, A.B., 2013. Soil carbon determination by thermogravimetrics. *PeerJ* 1, e6. doi:10.7717/peerj.6

Pallud, C., Van Cappellen, P., 2006. Kinetics of microbial sulfate reduction in estuarine sediments. *Geochim. Cosmochim. Acta* 70, 1148–1162. doi:10.1016/j.gca.2005.11.002

Parsons, C.T., Couture, R.M., Omoregie, E.O., Bardelli, F., Greneche, J.M., Roman-Ross, G., Charlet, L., 2013. The impact of oscillating redox conditions: Arsenic immobilisation in contaminated calcareous floodplain soils. *Environ. Pollut.* 178, 254–263. doi:10.1016/j.envpol.2013.02.028

Payn, R.A., Helton, A.M., Poole, G.C., Izurieta, C., Burgin, A.J., Bernhardt, E.S., 2014. A generalized optimization model of microbially driven aquatic biogeochemistry based on thermodynamic, kinetic, and stoichiometric ecological theory. *Ecol. Modell.* 294, 1–18. doi:10.1016/j.ecolmodel.2014.09.003

Pedersen, K., Ekendahl, S., 1990. Distribution and activity of bacteria in deep granitic groundwaters of southeastern sweden. *Microb. Ecol.* 20, 37–52. doi:10.1007/BF02543865

Pérez, J., Muñoz-Dorado, J., De La Rubia, T., Martínez, J., 2002. Biodegradation and biological treatments of cellulose, hemicellulose and lignin: An overview. *Int. Microbiol.* 5, 53–63. doi:10.1007/s10123-002-0062-3

Peter, S., Koetzsch, S., Traber, J., Bernasconi, S.M., Wehri, B., Durisch-Kaiser, E., 2012. Intensified organic carbon dynamics in the ground water of a restored riparian zone. *Freshw. Biol.* 57, 1603–1616. doi:10.1111/j.1365-2427.2012.02821.x

Pett-Ridge, J., Firestone, M.K., 2005. Redox Fluctuation Structures Microbial Communities in a Wet Tropical Soil. *Appl. Environ. Microbiol.* 71, 6998–7007. doi:10.1128/AEM.71.11.6998

- Phanikumar, M.S., Hyndman, D.W., Zhao, X., Dybas, M.J., 2005. A three-dimensional model of microbial transport and biodegradation at the Schoolcraft, Michigan, site. *Water Resour. Res.* 41, 1–17. doi:10.1029/2004WR003376
- Phelps, T.J., Murphy, E.M., Pfiffner, S.M., White, D.C., 1994. Comparison between geochemical and biological estimates of subsurface microbial activities. *Microb. Ecol.* doi:10.1007/BF00662027
- Plugge, C.M., Zhang, W., Scholten, J.C.M., Stams, A.J.M., 2011. Metabolic Flexibility of Sulfate-Reducing Bacteria. *Front. Microbiol.* 2, 1–8. doi:10.3389/fmicb.2011.00081
- Prommer, H., Anneser, B., Rolle, M., Einsiedl, F., Griebler, C., 2009. Biogeochemical and isotopic gradients in a BTEX/PAH contaminant plume: Model-based interpretation of a high-resolution field data set. *Environ. Sci. Technol.* 43, 8206–8212. doi:10.1021/es901142a
- Reardon, K.F., Mosteller, D.C., Rogers, J.B., DuTeau, N.M., Kim, K.H., 2002. Biodegradation kinetics of aromatic hydrocarbon mixtures by pure and mixed bacterial cultures. *Environ. Health Perspect.* 110 Suppl, 1005–11.
- Regnier, P., Dale, A., Pallud, C., 2005. Incorporating geomicrobial processes in reactive transport models of subsurface environments, in: Nützmann, G., Viotti, P., Aagaard, P. (Eds.), *Reactive Transport in Soil and Groundwater: Processes and Models*. Springer Berlin Heidelberg, pp. 109–125. doi:10.1007/3-540-26746-8_8
- Reis, M.A., Almeida, J.S., Lemos, P.C., Carrondo, M.J., 1992. Effect of hydrogen sulfide on growth of sulfate reducing bacteria. *Biotechnol. Bioeng.* 40, 593–600. doi:10.1002/bit.260400506
- Remus-Emsermann, M.N.P., Tecon, R., Kowalchuk, G.A., Leveau, J.H.J., 2012. Variation in local carrying capacity and the individual fate of bacterial colonizers in the phyllosphere. *ISME J.* 6, 756–765. doi:10.1038/ismej.2011.209
- Resat, H., Bailey, V., McCue, L.A., Konopka, A., 2012. Modeling microbial dynamics in heterogeneous environments: growth on soil carbon sources. *Microb. Ecol.* 63, 883–97.

doi:10.1007/s00248-011-9965-x

- Rezanezhad, F., Couture, R.M., Kovac, R., O'Connell, D., Van Cappellen, P., 2014. Water table fluctuations and soil biogeochemistry: An experimental approach using an automated soil column system. *J. Hydrol.* 509, 245–256. doi:10.1016/j.jhydrol.2013.11.036
- Rickard, A.H., Gilbert, P., High, N.J., Kolenbrander, P.E., Handley, P.S., 2003. Bacterial coaggregation: An integral process in the development of multi-species biofilms. *Trends Microbiol.* 11, 94–100. doi:10.1016/S0966-842X(02)00034-3
- Rickard, D., Luther, G.W., 1997. Kinetics of pyrite formation by the H₂S oxidation of iron (II) monosulfide in aqueous solutions between 25 and 125°C: The mechanism. *Geochim. Cosmochim. Acta* 61, 135–147. doi:10.1016/S0016-7037(96)00322-5
- Rivers, D.B., Emert, G.H., 1988. Factors affecting the enzymatic hydrolysis of municipal-solid-waste components. *Biotechnol. Bioeng.* 31, 278–281. doi:10.1002/bit.260310314
- Roden, E.E., 2008. Microbiological Controls on Geochemical Kinetics 1 : Fundamentals and Case Study on Microbial Fe (III) Oxide Reduction, in: Brantley, S.L., Kubicki, J.D., White, A.F. (Eds.), *Kinetics of Water-Rock Interactions*. Springer New York, pp. 335–415. doi:10.1007/978-0-387-73563-4_8
- Roden, E.E., Jin, Q., 2011. Thermodynamics of microbial growth coupled to metabolism of glucose, ethanol, short-chain organic acids, and hydrogen. *Appl. Environ. Microbiol.* 77, 1907–1909. doi:10.1128/AEM.02425-10
- Roden, E.E., Wetzal, R.G., 2002. Kinetics of microbial Fe(III) oxide reduction in freshwater wetland sediments. *Limnol. Oceanogr.* 47, 198–211. doi:10.4319/lo.2002.47.1.0198
- Rodriguez-Martinez, J.M., Pascual, A., 2006. Antimicrobial resistance in bacterial biofilms. *Rev. Med. Microbiol.* 17, 65–75. doi:10.1097/01.revmedmi.0000259645.20603.63
- Rotter, B.E., Barry, D.A., Gerhard, J.I., Small, J.S., 2008. Parameter and process significance in mechanistic modeling of cellulose hydrolysis. *Bioresour. Technol.* 99, 5738–48.

doi:10.1016/j.biortech.2007.10.020

- Russell, J., Cook, G., 1995. Energetics of bacterial growth: balance of anabolic and catabolic reactions. *Microbiol. Rev.* 59, 48–62.
- Russell, J.B., 1986. Heat production by ruminal bacteria in continuous culture and its relationship to maintenance energy. *J. Bacteriol.* 168, 694–701.
- Schäfer, W., Therrien, R., 1995. Simulating transport and removal of xylene during remediation of a sandy aquifer. *J. Contam. Hydrol.* 19, 205–236. doi:10.1016/0169-7722(95)00018-Q
- Scheibe, T.D., Mahadevan, R., Fang, Y., Garg, S., Long, P.E., Lovley, D.R., 2009. Coupling a genome-scale metabolic model with a reactive transport model to describe in situ uranium bioremediation. *Microb. Biotechnol.* 2, 274–286. doi:10.1111/j.1751-7915.2009.00087.x
- Schmidt, M.W.I., Torn, M.S., Abiven, S., Dittmar, T., Guggenberger, G., Janssens, I.A., Kleber, M., Kögel-Knabner, I., Lehmann, J., Manning, D.A.C., Nannipieri, P., Rasse, D.P., Weiner, S., Trumbore, S.E., 2011. Persistence of soil organic matter as an ecosystem property. *Nature* 478, 49–56. doi:10.1038/nature10386
- Sharma, S.B., Sayyed, R.Z., Trivedi, M.H., Gobi, T.A., 2013. Phosphate solubilizing microbes: sustainable approach for managing phosphorus deficiency in agricultural soils. *Springerplus* 2, 587. doi:10.1186/2193-1801-2-587
- Simmons, C.S., Ginn, T.R., Wood, B.D., 1995. Stochastic-Convective Transport with Nonlinear Reaction: Mathematical Framework. *Water Resour. Res.* 31, 2675–2688. doi:10.1029/95WR02178
- Sinsabaugh, R.L., Follstad Shah, J.J., 2012. Ecoenzymatic Stoichiometry and Ecological Theory. *Annu. Rev. Ecol. Evol. Syst.* 43, 313–343. doi:10.1146/annurev-ecolsys-071112-124414
- Sinsabaugh, R.L., Lauber, C.L., Weintraub, M.N., Ahmed, B., Allison, S.D., Crenshaw, C., Contosta, A.R., Cusack, D., Frey, S., Gallo, M.E., Gartner, T.B., Hobbie, S.E., Holland, K., Keeler, B.L., Powers, J.S., Stursova, M., Takacs-Vesbach, C., Waldrop, M.P., Wallenstein, M.D., Zak, D.R., Zeglin, L.H., 2008. Stoichiometry of soil enzyme activity at global scale.

Ecol. Lett. 11, 1252–1264. doi:10.1111/j.1461-0248.2008.01245.x

Small, J., Nykyri, M., Helin, M., Hovi, U., Sarlin, T., Itävaara, M., 2008. Experimental and modelling investigations of the biogeochemistry of gas production from low and intermediate level radioactive waste. *Appl. Geochemistry* 23, 1383–1418.
doi:10.1016/j.apgeochem.2007.11.020

Smith, P., Smith, J.U., Powlson, D.S., McGill, W.B., Arah, J.R.M., Chertov, O.G., Coleman, K., Franko, U., Frolking, S., Jenkinson, D.S., Jensen, L.S., Kelly, R.H., Klein-Gunnewiek, H., Komarov, A.S., Li, C., Molina, J.A.E., Mueller, T., Parton, W.J., Thornley, J.H.M., Whitmore, A.P., 1997. A comparison of the performance of nine soil organic matter models using datasets from seven long-term experiments. *Geoderma* 81, 153–225.
doi:10.1016/S0016-7061(97)00087-6

Sowerby, A., Emmett, B., Beier, C., Tietema, A., Penuelas, J., Estiarte, M., Van Meeteren, M.J.M., Hughes, S., Freeman, C., 2005. Microbial community changes in heathland soil communities along a geographical gradient: Interaction with climate change manipulations. *Soil Biol. Biochem.* 37, 1805–1813. doi:10.1016/j.soilbio.2005.02.023

Stark, J., Firestone, M.K., 1995. Mechanisms for soil moisture effects on activity of nitrifying bacteria. *Appl. Environ. Microbiol.* 61, 218–221.

Steinweg, J.M., Dukes, J.S., Paul, E.A., Wallenstein, M.D., 2013. Microbial responses to multi-factor climate change: Effects on soil enzymes. *Front. Microbiol.* 4, 1–11.
doi:10.3389/fmicb.2013.00146

Stolpovsky, K., Gharasoo, M.G., Thullner, M., 2012. Spatio-temporal variations of microbial metabolic activity caused by pore scale heterogeneity of porous media. *SOIL Sci.* 177, 98–110. doi:10.1097/SS.0b013e318241105d

Stolpovsky, K., Martinez-Lavanchy, P., Heipieper, H.J., Van Cappellen, P., Thullner, M., 2011. Incorporating dormancy in dynamic microbial community models. *Ecol. Modell.* 222, 3092–3102. doi:10.1016/j.ecolmodel.2011.07.006

- Stouthamer, A.H., Bettenhausen, C., 1973. Utilization of energy for growth and maintenance in continuous and batch cultures of microorganisms. *Biochim. Biophys. Acta* 301, 53–70. doi:10.1016/0304-4173(73)90012-8
- Teh, Y.A., Silver, W.L., Conrad, M.E., 2005. Oxygen effects on methane production and oxidation in humid tropical forest soils. *Glob. Chang. Biol.* 11, 1283–1297. doi:10.1111/j.1365-2486.2005.00983.x
- Thompson, A., Chadwick, O.A., Rancourt, D.G., Chorover, J., 2006. Iron-oxide crystallinity increases during soil redox oscillations. *Geochim. Cosmochim. Acta* 70, 1710–1727. doi:10.1016/j.gca.2005.12.005
- Thornton, S.F., Quigley, S., Spence, M.J., Banwart, S.A., Bottrell, S., Lerner, D.N., 2001. Processes controlling the distribution and natural attenuation of dissolved phenolic compounds in a deep sandstone aquifer. *J. Contam. Hydrol.* 53, 233–267. doi:10.1016/S0169-7722(01)00168-1
- Thurman, E.M., 1985. *Organic Geochemistry of Natural Waters*. Springer Science & Business Media. doi:10.1007/978-94-009-5095-5
- Tiehm, A., Nickel, K., Neis, U., 1997. The use of ultrasound to accelerate the anaerobic digestion of sewage sludge, in: *Water Science and Technology*. pp. 121–128. doi:10.1016/S0273-1223(97)00676-8
- Tijhuis, L., Van Loosdrecht, M.C., Heijnen, J.J., 1993. A thermodynamically based correlation for maintenance gibbs energy requirements in aerobic and anaerobic chemotrophic growth. *Biotechnol. Bioeng.* 42, 509–519. doi:10.1002/bit.260420415
- Tokarz, E., Urban, D., 2015. Soil Redox Potential and Its Impact on Microorganisms and Plants of Wetlands. *J. Ecol. Eng.* 16, 20–30. doi:10.12911/22998993/2801
- Trasar-Cepeda, C., Gil-Sotres, F., Leiros, M.C., 2007. Thermodynamic parameters of enzymes in grassland soils from Galicia, NW Spain. *Soil Biol. Biochem.* 39, 311–319. doi:10.1016/j.soilbio.2006.08.002

- Tufenkji, N., 2007. Modeling microbial transport in porous media: Traditional approaches and recent developments. *Adv. Water Resour.* 30, 1455–1469.
doi:10.1016/j.advwatres.2006.05.014
- Vallino, J., Hopkinson, C., Hobbie, J., 1996. Modeling bacterial utilization of dissolved organic matter: optimization replaces Monod growth kinetics. *Limnol. Oceanogr.* 41, 1591–1609.
- Van Bodegom, P., 2007. Microbial maintenance: a critical review on its quantification. *Microb. Ecol.* 53, 513–23. doi:10.1007/s00248-006-9049-5
- Van Walsum, G.P., Lynd, L.R., 1998. Allocation of ATP to synthesis of cells and hydrolytic enzymes in cellulolytic fermentative microorganisms: Bioenergetics, kinetics, and bioprocessing. *Biotechnol. Bioeng.* 58, 316–320. doi:10.1002/(SICI)1097-0290(19980420)58:2/3<316::AID-BIT31>3.0.CO;2-7
- VanBriesen, J.M., 2002. Evaluation of methods to predict bacterial yield using thermodynamics. *Biodegradation* 13, 171–90.
- Vargas, R., Hattori, T., 1986. Protozoan predation of bacterial cells in soil aggregates. *FEMS Microbiol. Lett.* 38, 233–242. doi:10.1016/0378-1097(86)90031-5
- Vavilin, V.A., Fernandez, B., Palatsi, J., Flotats, X., 2008. Hydrolysis kinetics in anaerobic degradation of particulate organic material: an overview. *Waste Manag.* 28, 939–51.
doi:10.1016/j.wasman.2007.03.028
- von Stockar, U., Maskow, T., Liu, J., Marison, I.W., Patiño, R., 2006. Thermodynamics of microbial growth and metabolism: an analysis of the current situation. *J. Biotechnol.* 121, 517–33. doi:10.1016/j.jbiotec.2005.08.012
- Waksman, S.A., Gerretsen, F.C., 1931. Influence of temperature and moisture upon the nature and extent of decomposition of plant residues by microorganism. *Ecology* 12, 33–60.
doi:10.2307/1932933
- Wallenstein, M.D., Weintraub, M.N., 2008. Emerging tools for measuring and modeling the in

- situ activity of soil extracellular enzymes. *Soil Biol. Biochem.* 40, 2098–2106.
doi:10.1016/j.soilbio.2008.01.024
- Wang, G., Post, W., Mayes, M., 2013. Development of microbial-enzyme-mediated decomposition model parameters through steady-state and dynamic analyses. *Ecol. Appl.* 23, 255–272.
- Watson, I.A., Oswald, S.E., Banwart, S.A., Crouch, R.S., Thornton, S.F., 2005. Modeling the dynamics of fermentation and respiratory processes in a groundwater plume of phenolic contaminants interpreted from laboratory- to field-scale. *Environ. Sci. Technol.* 39, 8829–8839. doi:10.1021/es0507970
- Weishaar, J., Aiken, G., 2001. Evaluation of specific ultra-violet absorbance as an indicator of the chemical content of dissolved organic carbon. *Environ. Chem.* 41, 843–845.
- Whitbread, A., 1995. Soil organic matter: its fractionation and role in soil structure. *Soil Org. Matter Manag. Sustain.*
- Whitman, W.B., Coleman, D.C., Wiebe, W.J., 1998. Prokaryotes: the unseen majority. *Proc Natl Acad Sci U S A* 95, 6578–6583. doi:10.1073/pnas.95.12.6578
- Wilson, D.B., 2008. Three microbial strategies for plant cell wall degradation. *Ann. N. Y. Acad. Sci.* 1125, 289–297. doi:10.1196/annals.1419.026
- Wilson, D.B., 2009. Cellulases and biofuels. *Curr. Opin. Biotechnol.* 20, 295–299.
doi:10.1016/j.copbio.2009.05.007
- Wilson, D.B., 2011. Microbial diversity of cellulose hydrolysis. *Curr. Opin. Microbiol.* 14, 259–63. doi:10.1016/j.mib.2011.04.004
- Woyke, T., Teeling, H., Ivanova, N.N., Huntemann, M., Richter, M., Gloeckner, F.O., Boffelli, D., Anderson, I.J., Barry, K.W., Shapiro, H.J., others, 2006. Symbiosis insights through metagenomic analysis of a microbial consortium. *Nature* 443, 950–955.
doi:10.1038/nature05192
- Wright, D.A., Killham, K., Glover, L.A., Prosser, J.I., 1995. Role of Pore-Size Location in

Determining Bacterial-Activity During Predation by Protozoa in Soil. *Appl. Environ. Microbiol.* 61, 3537–3543.

Wright, R.T., 1988. A model for short-term control of the bacterioplankton by substrate and grazing. *Hydrobiologia* 159, 111–117. doi:10.1007/BF00007372

Wrighton, K.C., Castelle, C.J., Wilkins, M.J., Hug, L.A., Sharon, I., Thomas, B.C., Handley, K.M., Mullin, S.W., Nicora, C.D., Singh, A., Lipton, M.S., Long, P.E., Williams, K.H., Banfield, J.F., 2014. Metabolic interdependencies between phylogenetically novel fermenters and respiratory organisms in an unconfined aquifer. *ISME J.* 8, 1452–63. doi:10.1038/ismej.2013.249

Yu, K., Böhme, F., Rinklebe, J., Neue, H.U., DeLaune, R.D., 2007. Major Biogeochemical Processes in Soils-A Microcosm Incubation from Reducing to Oxidizing Conditions. *Soil Sci. Soc. Am. J.* 71, 1406. doi:10.2136/sssaj2006.0155

Yukalov, V., Yukalova, E., Sornette, D., 2012. Modeling symbiosis by interactions through species carrying capacities. *Phys. D Nonlinear Phenom.* 7.

Zhou, Y., Kellermann, C., Griebler, C., 2012. Spatio-temporal patterns of microbial communities in a hydrologically dynamic pristine aquifer. *FEMS Microbiol. Ecol.* 81, 230–42. doi:10.1111/j.1574-6941.2012.01371.x

Zysset, A., Stauffer, F., Dracos, T., 1994. Modeling of reactive groundwater transport governed by biodegradation. *Water Resour. Res.* 30, 2423–2434. doi:10.1109/TAC.1967.1098633